FEBRUARY 2004

SOURCES OF SALINITY IN THE RIO GRANDE AND MESILLA BASIN GROUNDWATER

WRRI Technical Completion Report No. 330

James C. Witcher
J. Phillip King
John W. Hawley
John F. Kennedy
Jerry Williams
Michael Cleary
Lawrence R. Bothern

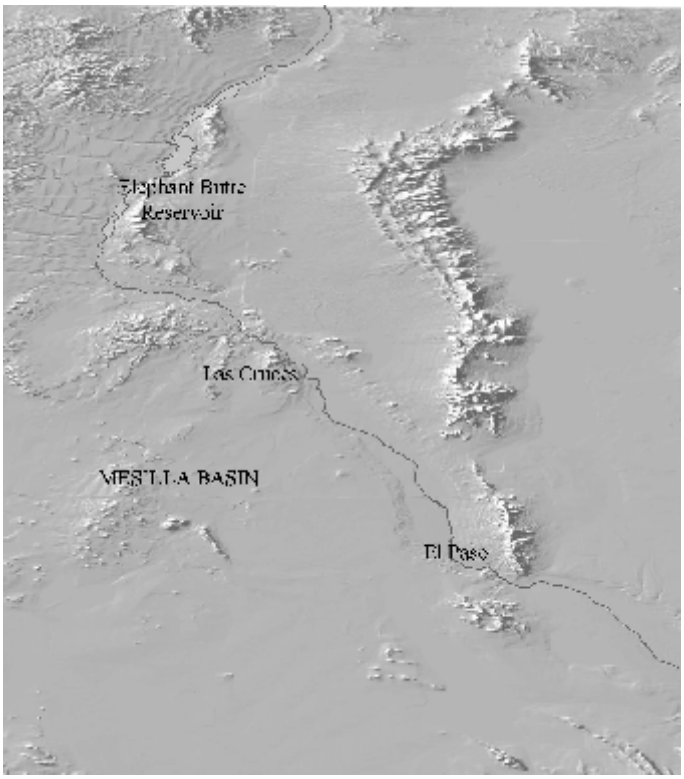

NEW MEXICO WATER RESOURCES RESEARCH INSTITUTE
New Mexico State University
MSC 3167
Box 30001
Las Cruces, New Mexico 88003-0001
Telephone (505) 646-4337 FAX (505) 646-6418
email: nmwrri@wrri.nmsu.edu

SOURCES OF SALINITY IN THE RIO GRANDE AND MESILLA BASIN GROUNDWATER

By

James C. Witcher
Southwest Technology Development Institute
New Mexico State University

J. Phillip King
Department of Civil and Geological Engineering
New Mexico State University

John W. Hawley
New Mexico Water Resources Research Institute
New Mexico State University

John F. Kennedy
New Mexico Water Resources Research Institute
New Mexico State University

Jerry Williams
Department of Civil and Geological Engineering
New Mexico State University

Michael Cleary
New Mexico Water Resources Research Institute
New Mexico State University

and

Lawrence R. Bothern
Department of Geological Sciences
New Mexico State University

TECHNICAL COMPLETION REPORT

Account Number 01423960B

February 2004

New Mexico Water Resources Research Institute
In cooperation with the
New Mexico Interstate Stream Commission

The research on which this report is based was financed in part by the U.S. Department of the Interior, Geological Survey, and the New Mexico Interstate Stream Commission through the New Mexico Water Resources Research Institute.

DISCLAIMER

The purpose of the Water Resources Research Institute technical reports is to provide a timely outlet for research results obtained on projects supported in whole or in part by the institute. Through these reports, we are promoting the free exchange of information and ideas, and hope to stimulate thoughtful discussions and actions that may lead to resolution of water problems. The WRRI, through peer review of draft reports, attempts to substantiate the accuracy of information contained in its reports, but the views expressed are those of the authors and do not necessarily reflect those of the WRRI or its reviewers. Contents of this publication do not necessarily reflect the views and policies of the Department of the Interior, nor does the mention of trade names or commercial products constitute their endorsement by the United States government.

ACKNOWLEDGEMENTS

This study was supported by the New Mexico Water Resources Research Institute at New Mexico State University and the New Mexico Interstate Stream Commission. Special thanks are due to Rob Bowman, Tom Cliett, Lee Gile, Barry Hibbs, Mike Kernodle, Bill King, Rick Lozinsky, Greg Mack, Suzanne Mills, Bob Myers, Fred Phillips, Bill Seager, Ken Stevens, Francis West and the late Frank Kottlowski and Clyde Wilson for their contributions over the past four decades to our “underground view” of the Mesilla Basin. Interpretations presented in this paper, however, are solely our own. Assistance in editing and preparation of tables by Cathy Ortega Klett, Darlene Reeves, and Michelle Del Rio is greatly appreciated.

ABSTRACT

An integrated geologic and geochemical investigation of groundwater, coupled with a study of temporal changes in surface water chemical balances for basins along the Rio Grande from San Marcial to Ft Quitman, is used to investigate salinity in the Mesilla Basin of southcentral New Mexico and West Texas. A conceptual hydrogeologic framework delineates the major geologic influences on flow, storage characteristics, and chemical evolution of groundwater in the basin. The conceptual framework is integrated into a GIS and is general enough to be used in adjacent basins and with groundwater flow models. Three basic hydrogeologic features are detailed: 1) lithofacies assemblages (LFAs), 2) hydrostratigraphic units (HSUs), 3) and bedrock and structural boundaries. LFAs are the basic building blocks for the HSUs. The LFAs are primarily defined by grain size, mineralogy, depositional environment, and diagenetic modifications. LFAs may have distinct geochemical and hydrologic characteristics and can be recognized by diagnostic borehole geophysical responses. HSUs are mappable and informal basin-fill designations with hydrologic attributes that overlap formalized lithostratigraphic and chronostratigraphic basin-fill units. The primary purpose of a HSU is to highlight and classify an overall hydrogeologic and geochemical behavior of a basin-fill package.

This investigation of salinity sources uses a combined interpretation of groundwater isotopic signatures and major cation and anion compositions. Because aquifer salinity can involve dissolution, non-reversible chemical reactions, ion exchange, near-surface evaporation or evapotranspiration, and various anthropogenic processes, special emphasis is given to fingerprinting processes, mixing, and flow paths. Isotopes such as δD, $\delta^{18}0$, and $^{87}Sr/^{86}Sr$ and conservative anions such as Cl and Br are especially useful. In particular, the systematics of the Cl/Br, δD, $\delta^{18}O$ provide useful insight into mixing and evaporative salinity processes. The isotopic systems of $^{87}Sr/^{86}Sr$, $\delta^{13}C$, and $\delta^{34}S$ show groundwater flow paths or water chemistry provenance. Saline and brackish water from deeper HSUs and geothermal water have Cl/Br ratios greater than 600 to 800, $^{87}Sr/^{86}Sr$ ratios greater than 0.710, heaver δD and $\delta^{18}O$ than upper HSUs non-thermal water. However, the

deeper HSU and geothermal water is lighter than the δD and $\delta^{18}O$ of water from the Rio Grande.

The salinity balance in the Rio Grande during the last 40 years for the Mesilla Basin is positive, meaning that more salts are entering the basin than are transported by the Rio Grande out of the basin at El Paso. Higher salinity in shallow groundwater and the Rio Grande in the southern and southeastern Mesilla Basin is probably dominated by structurally forced upwelling of brackish and saline water from deep HSUs and by upflow of geothermal water from shallow bedrock structures and bedrock boundaries.

TABLE OF CONTENTS

APPENDICES (contained on CD)

TABLES

LIST OF TABLES

LIST OF FIGURES

LIST OF PLATES (contained on CD)

1.0 INTRODUCTION

1.1 PURPOSE

Irrigation has been a significant hydrologic component in New Mexico's Mesilla and Rincon valleys since the 1820s, and a dominant one since the construction of the Rio Grande Project in 1917 (Ackerly et al. 1992). Crop production from the area shows no indication of salinization of land in the Elephant Butte Irrigation District (EBID), but the irrigation district to the south faces serious salt management problems. Salinization of agricultural lands is a problem in much of the United States, where 20 to 25% of all irrigated cropland is impaired by salt (Postel 1993). Understanding the sources of salt in EBID is critical to assuring continued productivity, managing changes in water use from agricultural to municipal applications, and for assessing potential responsibilities to downstream water users.

Chemical quality of surface and groundwater in the Mesilla Basin generally degrades southward prior to discharge from the basin at the Paso Del Norte narrows in El Paso (Frenzel and Kaehler 1992, see section by Anderholm; Gates et al. 1978; Leggat et al. 1962, and Wilson et al. 1981). Chemical quality of groundwater and surface water drains also deteriorates significantly on the eastern margins from Las Cruces southward adjacent to Interstate 10 (Frenzel and Kaehler 1992, see section by Anderholm; and Wilson et al. 1981). In general, water quality is also lower in the far western and northwestern margins of the basin (Wilson et al. 1981). A zone of poor quality water overlies good quality in the shallow aquifer system beneath the Mesilla Valley floodplain (Wilson et al. 1981).

Impacts to water quality can occur from hydrogeologic components that are frequently not simulated in numerical models and hydrologic budget studies of the basin. To fully appreciate the saline sources and the relative strength of salinity additions, all hydrogeologic components operating in the basin must be considered. Because subsurface structure and stratigraphy control hydraulic properties and may dominate the evolution of chemical quality, a general groundwater framework must be studied and viewed in terms of a complete

compilation of subsurface geology, aquifer properties, and flow paths (Hawley 1984).

Several recent studies concluded that the salinity in the shallow aquifers and in the Rio Grande is largely the result of agricultural practices (Fisher and Mullican 1997; Hibbs 1999; Walton et al. 1999). However, the information points to mixing of geothermal waters with shallow groundwater to increase salinities (Frenzel and Kaehler 1992, see section by Anderholm; Swanberg 1975). Vertical leakage from deep-seated regional groundwater flow systems, which includes geothermal systems, may also be a significant source for salinity increases in the shallow aquifers and Rio Grande as the basin outlet is approached south of Anthony.

This study characterizes the salt balance in the EBID area with surface water data. Data of questionable quality must be evaluated and, where possible, corrected or calibrated. A negative balance, where salt in flow is greater than salt out flow, would indicate that salt is accumulating within the district. A positive salt balance would indicate that either salt is being depleted within the district, or that salt from sources other than annual inflows from the river are contributing to the balance. In any case, intelligent planning for salt management requires a clear understanding of the status of the salt balance. The surface water data analysis cannot differentiate between salt sources, and so the second task will investigate groundwater salinity sources, processes, and contributions.

1.2 GEOGRAPHIC SETTING

The part of the Rio Grande basin covered in this report (Fig. 1-1) is located in the Mexican Highland section of the Basin and Range physiographic province (Fenneman 1931; Hawley 1986), and in the southern part of the Rio Grande rift tectonic province of south-central New Mexico, western Trans-Pecos Texas, and northern Chihuahua, Mexico (Hawley 1978; Keller and Cather 1994). As a distinct geographic and hydrologic feature (Conover 1954; King et al. 1971; Wilson et al. 1981), this area includes parts of Sierra and Doña Ana Counties, New Mexico, the Mesilla and El Paso Valley sections of El Paso County, Texas, and part of Hudspeth County, Texas (Fig. 1-2). The area extends from Elephant

Butte Reservoir just upstream from Truth or Consequences, at the northern end of the Palomas Basin, to the southern end of the Hueco Bolson, near Fort Quitman, TX. Major river-valley segments, originally named by W.T. Lee (1907), comprise 1) the Rincon Valley between Caballo Dam (central Palomas Basin) and Leasburg Dam at the lower end of Selden Canyon, 2) the Mesilla Valley between Selden Canyon and "El Paso del Norte" or El Paso Narrows, and 3) the El Paso Valley, located in the southern Hueco Bolson.

The primary surface-water source is the Rio Grande, which in many places includes a network of canals, laterals and drainage ditches that receive, distribute, and contribute water to the surface and shallow subsurface flow systems. The watershed of the basin above Elephant Butte Dam is about 26,500 mi^2 (excluding the *closed* part of the San Luis Valley of Colorado, Ortiz et al. 2001). The river channel has remained in approximately the same position since the Civil War; however, it has been straightened and diked (canalized) since initiation of the Elephant Butte Irrigation Project in 1915. The gradient of the pre-1865 meandering channel was as low as 1.4 ft/mi, and maximum-channel sinuosity (length/meander-wave length) was about 2.5 (U.S. Reclamation Service 1914). Measured peak discharges during the great floods of 1904 and 1905 in the San Marcial to El Paso reach (Water Resources Division 1965) ranged from about 50,000 cfs at San Marcial on 10/11/04 (upper end of Elephant Butte Reservoir) to 24,000 cfs (El Paso on 6/12/05). Since 1917, measured releases from Elephant Butte Reservoir show a mean annual flow for the 1917-1998 period of about 1,000 cfs, with a minimum of 253 cfs in 1964 and a maximum of 2,512 cfs in 1942. Peak discharge since closure of Caballo Dam (1/1938) is less than 8,000 cfs and average discharges at Caballo Dam and El Paso are about 850 cfs and 500 cfs, respectively (IBWC 1939—2000; Ortiz et al. 2001).

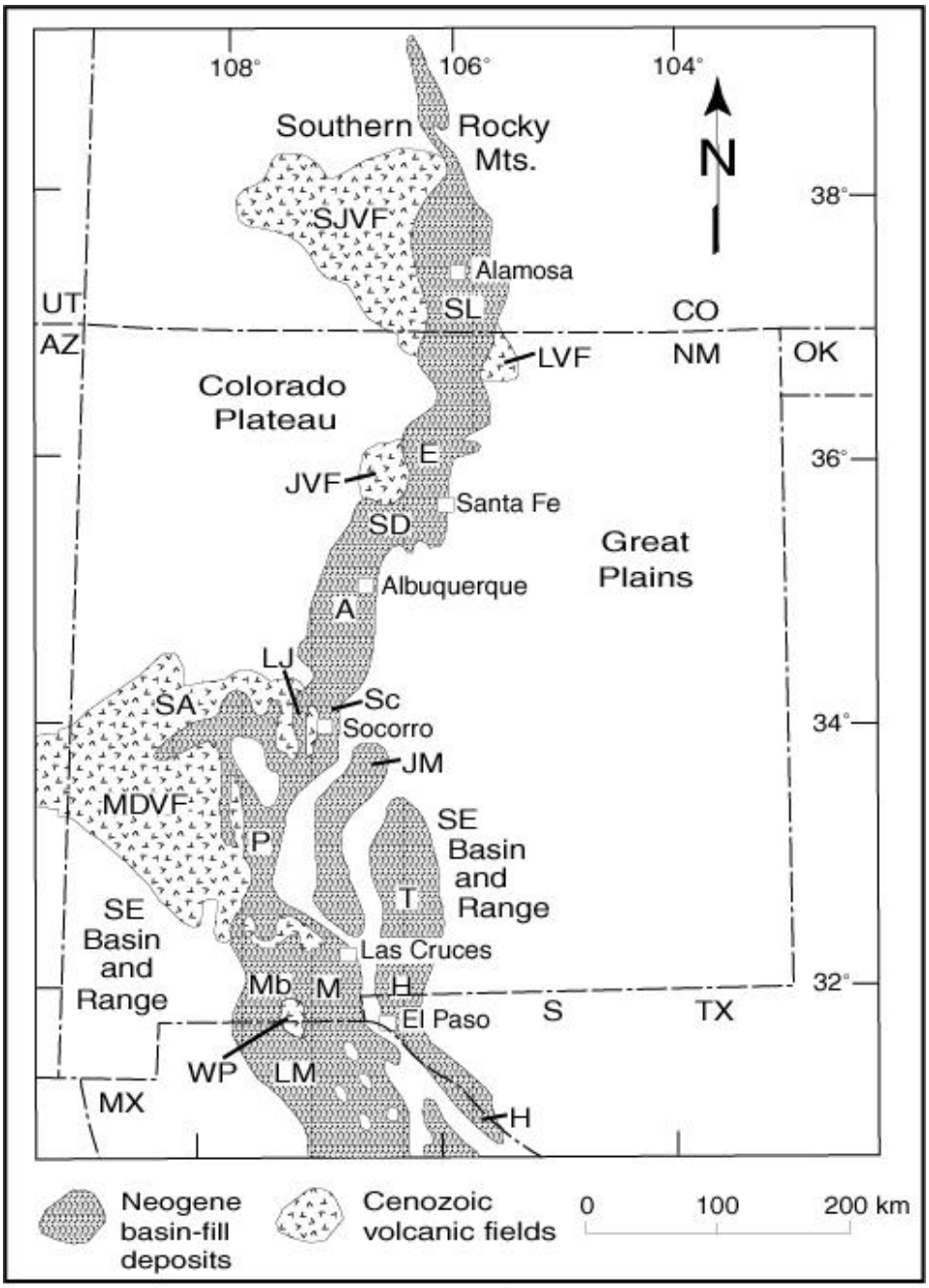

Figure 1-1. Index map showing location of the Mesilla Basin in the context of other basins and volcanic fields within the Rio Grande rift structural province. Basin abbreviations from north to south: San Luis (SL), Española (E), Santo Domingo (SD), Albuquerque (A), Socorro (Sc), La Jencia (LJ), San Agustin (SA), Jornada del Muerto (JM), Palomas-Rincon (P), Tularosa (T), Mimbres (Mb), Mesilla (M), Los Muertos (LM), Hueco (H), and Salt (S). Cenozoic volcanic fields: San Juan (SJVF), Latir (LVF), Jemez (JVF), Mogollon-Datil (MDVF), and West Potrillo (WP). Modified from Keller and Cather (1994).

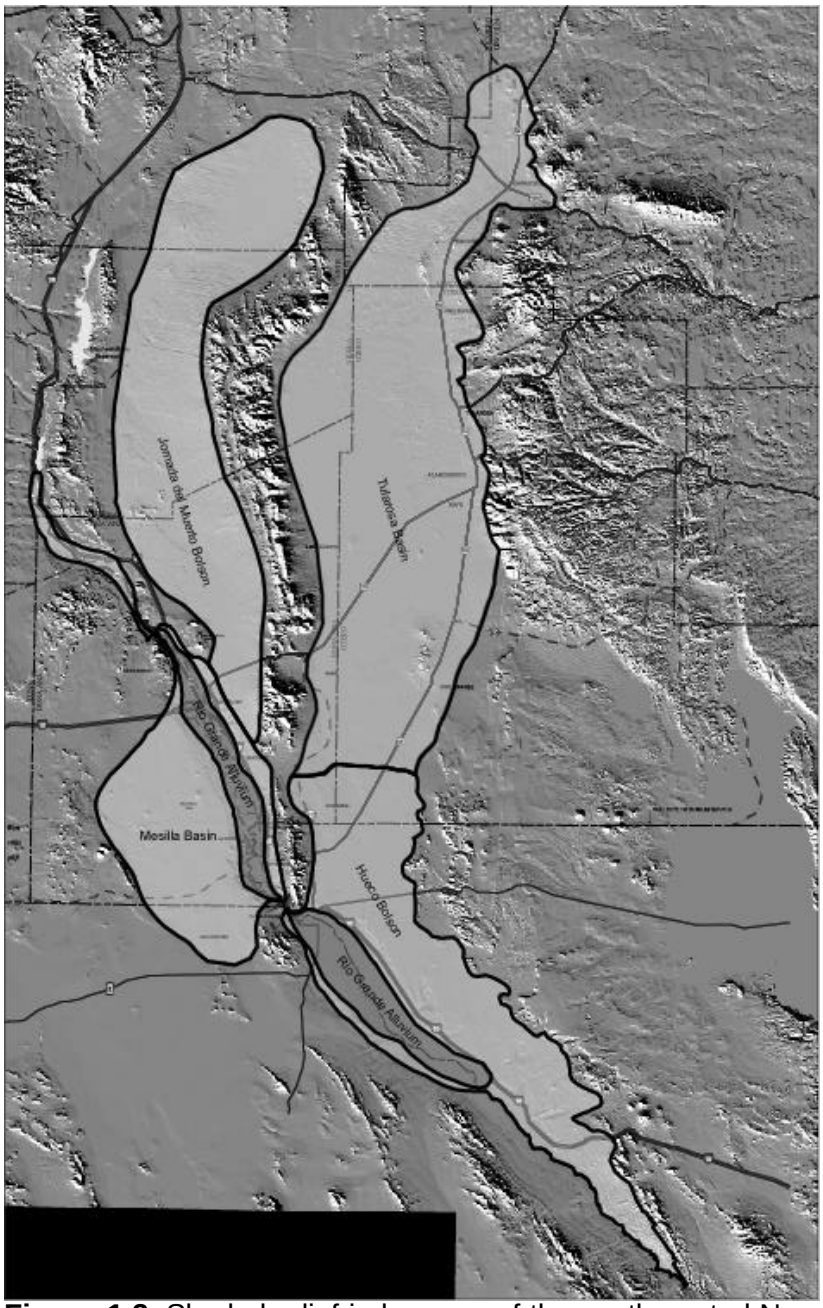

Figure 1-2. Shaded-relief index map of the south-central New Mexico border region, including adjacent parts of Trans-Pecos Texas and Chihuahua, Mexico. The major aquifer systems shown extend along the Rio Grande from Elephant Butte Reservoir to the southern part of Hueco Bolson, near Fort Quitman, Texas. They include 1) the shallow-alluvial systems in the Rincon, Mesilla and El Paso valleys of the Rio Grande, and 2) the intermediate and deep basin-fill (Santa Fe Gp) aquifers of the Palomas-Rincon, Jornada del Muerto, Mesilla, and Hueco basins. Shaded relief from latest available U.S. Geological Survey DEM database.

In the entire Rio Grande basin region (extending from the northern San Luis Basin to the southeastern Hueco Bolson Fig. 1-1) the major aquifer systems comprise 1) Upper Quaternary alluvium of the inner Rio Grande Valley (valley-fill aquifer system), and 2) poorly consolidated sedimentary fill of Rio Grande rift basins (basin-fill aquifer system). The Santa Fe Group forms the bulk of the latter unit. The hydrogeologic framework formed by the hydrostratigraphic subdivisions of these two aquifer systems and associated Basin and Range structures has a profound influence on groundwater and surface-water flow and quality in the entire study area. This topic is covered in detail in the following two sections, with emphasis on hydrogeologic-framework elements in Section 2 and groundwater chemistry and associated geothermal components in Section 3. Finally, the central theme of Section 4 concerns the salt balance in the surface-flow system of the entire Rio Grande Project area.

1.3 PARTICIPANTS

The New Mexico Water Resources Research Institute (NMWRRI) at New Mexico State University (NMSU) is the lead organization in this cooperative effort. Besides the NMWRRI, this cooperative effort includes the NMSU Southwest Technology Development Institute (SWTDI), the NMSU Civil and Geological Engineering Department (CAGE), the NMSU Geological Sciences Department (GSD), and the U.S. Geological Survey, Water-Resources Division (USGS-WRD). The New Mexico Interstate-Stream Commission (NMISC) is the major source of non-federal project funding. In addition, much of the baseline information on geologic framework and geophysical properties of basin-fill deposits (only partly published) has been compiled from data collected by the U.S. Soil [Natural Resource] Conservation Service, Soil Survey Investigations Division (SCS-SSI) and the New Mexico Bureau of Mines and Mineral Resources (NMBMMR) between 1962 and 1993. The NMWRRI, USGS-WRD, New Mexico Office of the State Engineer (NMOSE), State Agricultural Experiment Station at NMSU, and El Paso Water Utilities (EPWU) also gave substantial logistical and technical support for these early investigations.

2.0 HYDROGEOLOGY

2.1 INTRODUCTION

This report section on Mesilla Basin hydrogeology is part of a larger document that presents the results of a multidisciplinary research program on sources of salinity in both groundwater and surface water in the Rio Grande basin between Elephant Butte Reservoir and the El Paso Valley (Figs. 1-1, 1-2; Sections 3.0 and 4.0). As a distinct hydrogeologic and geohydrologic entity (King et al. 1971; Hawley et al. 2001), the Mesilla Basin includes much of southern Doña Ana County, New Mexico and the Mesilla Valley section of El Paso County, Texas; and the study area extends a short distance into the State of Chihuahua, Mexico (Fig. 2-1). An important aspect of this phase of the "sources of salinity" project has been development of GIS approaches that allow syntheses and new interpretations of large amounts of surface and subsurface hydrogeologic information on aquifer systems of the Mesilla Basin region. The resulting synoptic product(s) can then be used in future numerical models of groundwater-flow and geochemical systems (e.g., Hibbs, Boghici et al. 1998; Hawley and Kernodle 2000; Hawley et al. 2000; Kennedy et al. 2000).

2.1.1 Purpose and Scope

Emphasis of this section is on 1) the hydrogeologic framework of intermontane-basin (bolson) and river-valley fills, which collectively form the Mesilla Basin aquifer system; and 2) the major hydrogeologic factors that influence groundwater flow and chemistry within this complex of poorly consolidated basin deposits and bedrock-boundary units. Past conceptual and physical models of basin hydrogeology were primarily designed for use in numerical models of groundwater-flow systems, with little attention given to their equally important, geochemical/geothermal components. Therefore, an important

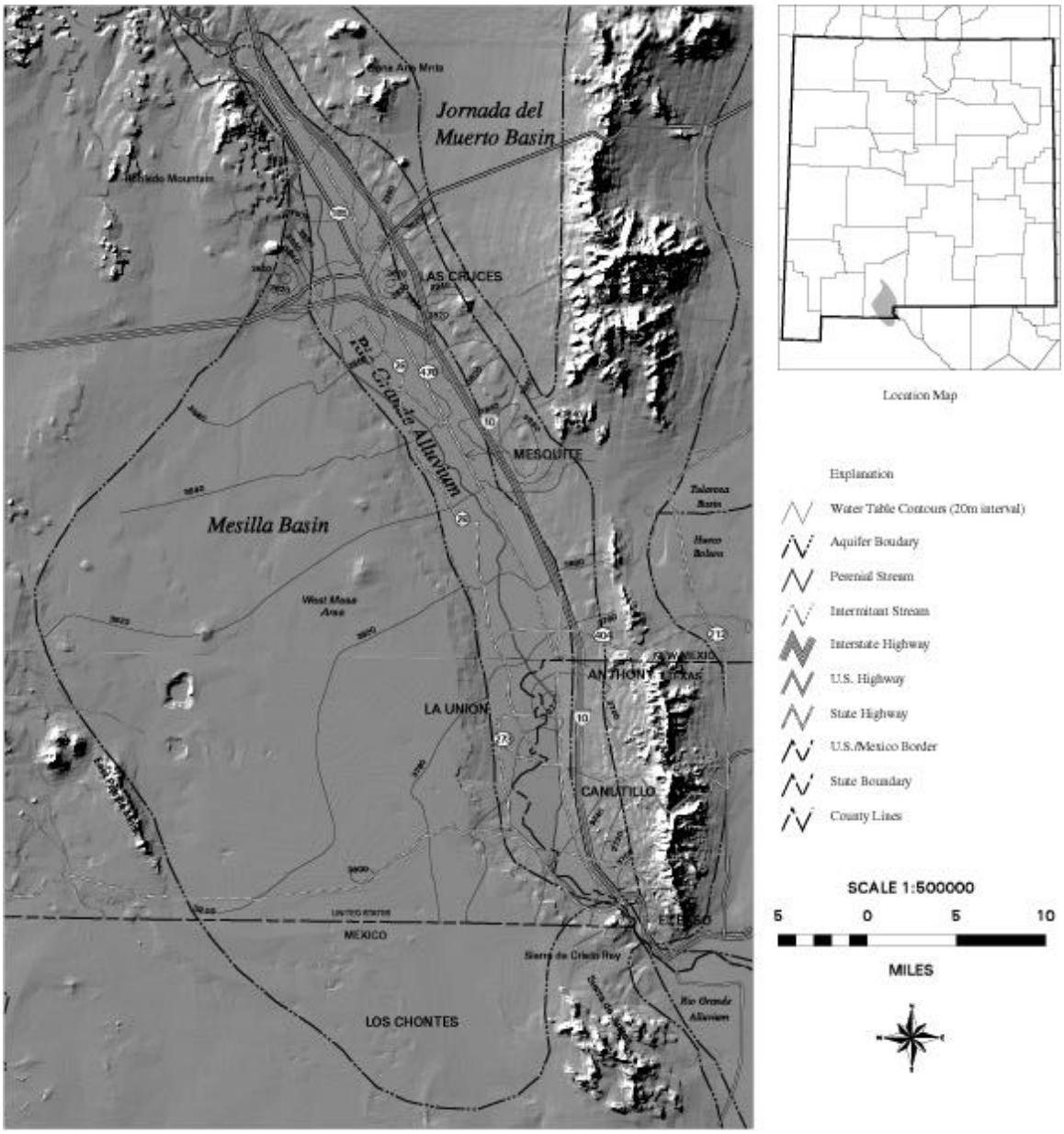

Figure 2-1. Shaded-relief index map of the Mesilla Basin area of southern New Mexico and adjacent parts of Texas and Chihuahua. The extent of major basin-fill (Santa Fe Group) and Mesilla Valley (Rio Grande alluvium) aquifer systems is shown; and the general water-table configuration and groundwater-flow direction in the basin's upper aquifer units are also illustrated. Adapted from Hibbs and others (1997), with shaded relief from latest available U.S. Geological Survey DEM database.

part of this study has been the development of a GIS-based, hydrogeologic classification scheme that integrates basic geologic-framework components (e.g., lithology, stratigraphy and structure) that influence the chemical and thermal properties of both shallow and deep parts of the flow system (e.g., Kennedy 1998; Hibbs 1999; Hibbs et al. 1999, 2000; Hawley et al. 2000). The (3-D) schematic model of the Basin's hydrogeologic framework that has been developed for this report has a combined surface-map—fence-diagram format (Plates 1, 8, 9; map-scale 1:100,000; 10x vertical exaggeration, base elev. 1,000 ft asl). Base-line information for 60 "key wells" in six reference sections (Plates 2 to 7) includes: digitized borehole geophysical logs, water chemical data, static-water levels, and interpretations of the major lithofacies, hydrostratigraphic and structural components of the basin's hydrogeologic framework.

Appendix A**,** which supplements Sections 2 and 3, includes 1) a synopsis of hydrogeologic work completed prior to 1981, 2) a description of research methods, and 3) an expanded explanation of the many salient features illustrated on the plates that we cannot adequately cover in the following discussion of hydrogeologic controls on groundwater flow and salinity. Appendix A, Tables 1 and 2 contain much of the essential base-line information that was used in developing the conceptual framework model (Plates 2 to 9). Most of this material was originally compiled and interpreted by Hawley (1984) and Hawley and Lozinsky (1992) as part of earlier cooperative efforts in groundwater-flow modeling involving NM Tech, NMWRRI, NMOSE, EPWU and USGS-WRD. Major advances have been made during the past decade, however, primarily in GIS capability, and an expanded geological-geophysical-geochemical information base. Therefore, updating of some hydrogeologic concepts used in numerical modeling of groundwater-flow and geothermal systems is merited. In addition, there is a definite need for a consistent, GIS-based model that integrates best-available hydrogeologic information for the entire Mesilla—southern Jornada del Muerto basin system. The information on aquifer systems presented here (Sections 2, 3, and supporting documentation in Appendix A) represents the first stage in preparation of a more comprehensive NMWRRI research report on the hydrogeologic framework of that larger area.

2.1.2 Physiographic Setting

The Mesilla Basin (bolson) is located in the Mexican Highland section of the Basin and Range physiographic province (Fenneman 1931; Hawley 1969, 1986) and it is one of the larger structural depressions of the southern Rio Grande rift tectonic province (Fig. 1-1; Hawley 1978; Keller and Cather 1994). From a bio-geographic and regional-climate perspective, the basin is also located in the north-central Chihuahuan Desert (Schmidt 1986; Van Devender 1990). The distinctive geomorphic characteristic of this part of the Basin and Range province is the large extent of basin-floor areas relative to the flanking piedmont slopes and mountain uplifts (Fig. 2-1, Plate 1). Most ranges are narrow and low-lying (most less than 8,000 ft elev.) in comparison with highlands of the northern and central Rio Grande rift (Hawley 1975).

The Mesilla Basin is bounded on the east by the Organ-Franklin-Juarez mountain chain and on the west by fault-block and volcanic uplands, which extend northward from the East Potrillo Mountains (near the International Boundary) to the Aden and Sleeping Lady Hills. Organ Needle (elev. 9,012 ft) in the central Organ uplift is the highest point on the basin's perimeter. The Robledo and Doña Ana Mountains form the respective western and eastern boundaries in the northern section of the basin. Between the Doña Ana-Goat Mountain uplift and Tortugas Mountain in the eastern Las Cruces area, the northeastern Mesilla Basin border is transitional (in terms of both surface and subsurface flow) with the Jornada del Muerto Basin (Figs. 1-2, 2-1; Plate 1; King et al. 1971; Frenzel and Kaehler 1992; Woodward and Myers 1997).

The Mesilla Basin extends southward about 60 mi from the upper end of the Mesilla Valley, at the mouth of Selden Canyon (Leasburg Dam site), to a poorly defined groundwater divide located about 15 mi south of the International Boundary and southwest of Sierra Juárez (Figs. 1-2, 2-1). This part of the topographic basin merges southward with the floor of Bolson de Los Muertos in north-central Chihuahua (Córdoba et al. 1969; Hawley 1969; Morrison 1969; Reeves 1969; Hawley et al. 2000). Basin width varies from about 5 mi at its northern end to about 25 mi (40 km) in its central part. The extensive,

undissected plain west of the Mesilla Valley is locally designated the West Mesa or “La Mesa”. The former name is used in this report, following USGS-WRD practice (e.g., Wilson et al. 1981; Nickerson and Myers 1993), and “La Mesa” is used only in reference to the relict fluvial plain of the ancestral Rio Grande (i.e., the Plio-Pleistocene La Mesa geomorphic surface of Gile, Hawley et al. 1995).

The entrenched Mesilla Valley segment occupies much of the eastern part of the Mesilla Basin and includes the Las Cruces metro-area. The northwestern El Paso-Ciudad Juárez metro-area extends through the El Paso Narrows (El Paso del Norte) into the southern end of the valley. The valley-floor geohydrologic unit (Rio Grande floodplain), with a length of about 60 mi, extends southward from Leasburg Dam to the upper end of the Narrows near the NM-TX-Mexico boundary point. The area of the valley floor is about 215 mi^2 (135,000 acres); and the river’s drainage basin above Leasburg Dam occupies about 28,000 mi^2 of New Mexico and southern Colorado (excluding the *closed* part of the San Luis Basin, Ortiz et al. 2001).

The major components of the Mesilla Basin aquifer system occur in 1) Upper Quaternary alluvium of the inner Rio Grande Valley (valley-fill aquifer), and 2) poorly consolidated sedimentary deposits of the Santa Fe Group (basin-fill aquifer). The surface-water supply is derived from the Rio Grande, a few large tributary arroyo systems, and a network of canals, laterals and drainage ditches that discharge to the river. The watershed of the Mesilla Basin, including an area of as much as 250 mi^2 west of Sierra Juárez in Chihuahua, Mexico, covers approximately 1,600 mi^2. The Mesilla Basin watershed area north of the International Boundary is about 1,350 mi^2 (excluding the ~30,000 mi^2 upstream river-basin component).

2.2 PREVIOUS W0RK

An exhaustive review of the many relevant studies that predate the current (post-1980) generation of hydrogeologic and hydrologic investigations is beyond the scope of this report section. However, a synopsis of previous work is presented in Appendix A.

2.2.1 Hydrogeologic-Model Development Since 1980

Accelerated emphasis on geological and geophysical investigations in the Mesilla Basin area since 1980 has resulted in a very large body of published information, much of which is directly applicable to the development of the present generation of hydrogeologic models. The following reports and maps, many of which include cross-section views of basin deposits and structures, served as the primary baseline-information sources used in this study: Gile and others (1981), Seager (1981, 1995), Wilson and others (1981), Gross and Icerman (1983), Wilson and White (1984), Hawley (1984), Seager and others (1982, 1984, 1987), Hawley and Lozinsky (1992), Nickerson and Myers (1993), Mack and others (1993, 1997), Wade and Reiter (1994a and b), Kennedy (1998), Keller and others (1998), Collins and Raney (2000), and Hawley and others (2000, 2001). Our syntheses and interpretations of information from the above-cited source are presented in Sections 2.6 to 2.9. Hydrogeologic controls on the complex groundwater-flow regimes associated with the major geothermal systems of the Mesilla Basin area are described in Sections 2.4, 2.6.1, 2.7 to 2.9; and Appendix A**.** This topic (Witcher 1988; Ross and Witcher 1998) is covered in detail in Section 3 discussions of the interrelations between groundwater chemistry and salinity, and geothermal-flow components.

2.2.2 Groundwater-Flow Modeling Since 1980

Substantial progress has been made since 1981 in the development of basin-scale numerical models of groundwater-flow systems in the Mesilla Basin area (e.g., Peterson et al. 1984; Frenzel and Kaehler 1992; Nickerson and Myers 1993; Shomaker and Finch 1996; Balleau 1999). The Frenzel and Kaehler (1992)

report also includes an excellent synthesis of then available information on groundwater chemistry by Scott Anderholm (see Sections 2.9 and 3). Much current emphasis of numerical modeling has been on the well-integrated, surface-water and shallow groundwater systems of the irrigated-valley area of the Rio Grande Project (e.g., Hamilton and Maddock 1993), and it is important to note that recent studies also involve much-needed assessments of the complex geochemical interrelationships between surface-water and shallow groundwater throughout the basin (e.g., Anderholm et al. 1995; Healy 1996; see Section 4).

Detailed review of groundwater-flow modeling is beyond the scope of this investigation, but an overview is presented in Appendix A. The essential point made here is that all groundwater-flow models must meet the hydrogeologic constraints placed on flow regimes by lithofacies, stratigraphic, structural-boundary and geochemical conditions that are either well documented or reasonably inferred (Hawley and Kernodle 2000).

2.3 WELL NUMBERING SYSTEMS

Wells in New Mexico are identified by a location-number system based on the township-range system of subdividing public lands. The location number consists of four segments separated by periods, corresponding to the township, range, section, and tract within a section (Fig. 2-2a). The townships and ranges are numbered according to their location relative to the New Mexico base line and the New Mexico principal meridian. The smallest division, represented by the third digit of the final sequent, is a 10-acre (4 ha) tract. If a well has not been located precisely enough to be placed within a particular section or tract, a zero is used for that part of the location number.

Wells in Texas are officially given a well number consisting of five parts (Fig. 2-2b). The first part is a two-letter prefix used to identify the county, with El Paso County being represented by JL. The second part of the number has two digits indicating the 1-degree quadrangle. Each 1-degree quadrangle is divided into 64 7½-minute quadrangles. This is the third part of the well number. The first digit of the fourth part indicates the 2½-minute quadrangle, and the last two digits

2a

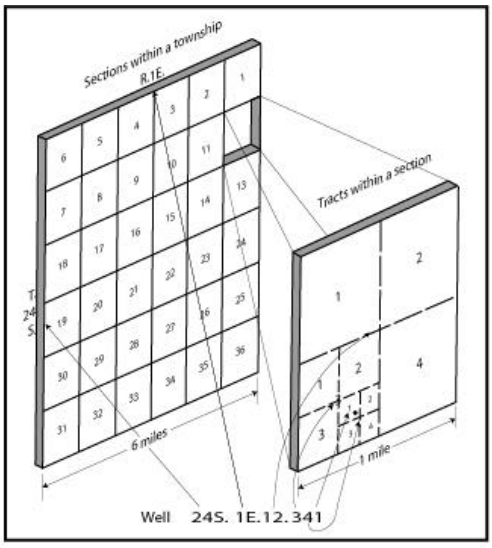

2b

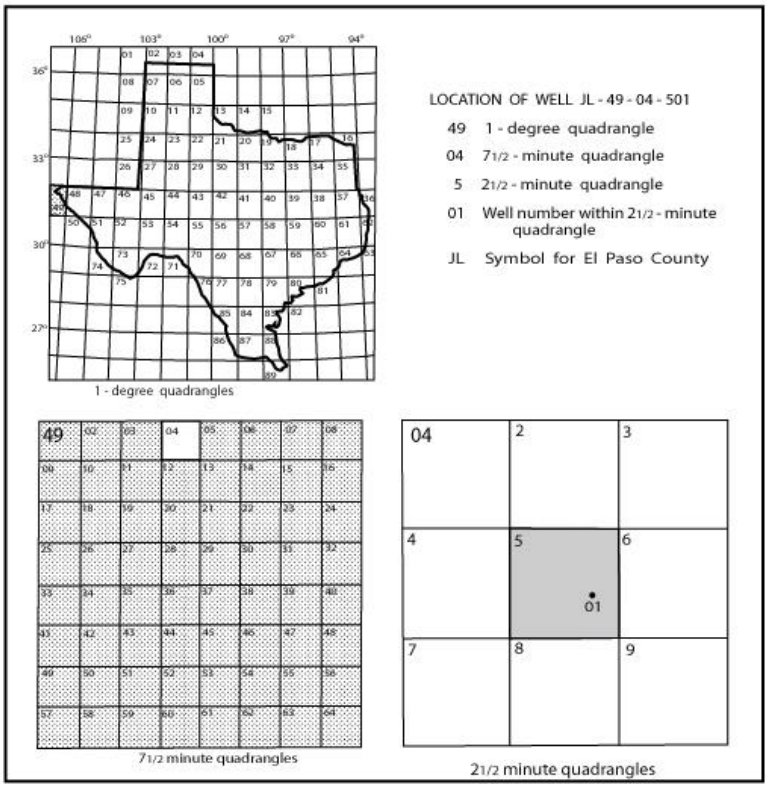

Figure 2-2. Well numbering systems: a. New Mexico; b. Texas

comprise a sequence number that identifies the well from others in the same 2½-minute quadrangle. As an example (Fig. 2-2b), well JL-49-04-501 is in El Paso County (JL), in 1-degree quadrangle 49, in 7½-minute quadrangle 04, in 2½-minute quadrangle 5, and was the first well inventoried in this 2½-minute quadrangle.

2.4 BASIC HYDROGEOLOGIC AND GEOHYDROLOGIC CONCEPTS

The primary groundwater reservoirs in the Basin and Range province are in the poorly consolidated sediments that have accumulated in the intermontane structural basins (bolsons, semibolsons). While they are commonly referred to as "alluvial basins" (Wilkins 1986, 1998), their fills are not entirely of alluvial origin because they also include lesser amounts of lacustrine, eolian and colluvial deposits (Hawley et al. 1969, 2000, 2001; Seager 1995; Seager et al. 1987). Fractured volcanic rocks (basalts, andesites, and tuffs), which immediately underlie or are locally interlayered with the Santa Fe Group, form important aquifers in only a few places (Hawley et al. 2000). Groundwater production from most consolidated rocks of the region, however, is limited to mostly low-yield fracture zones, which occur in a wide variety of bedrock types including sedimentary, volcanic, intrusive-igneous, and metamorphic.

Bedrock terranes of structural highlands are the ultimate source areas for the basin fill, and they usually form effective boundaries for basin-fill aquifer systems. Unlike some parts of the Basin and Range province (e.g., southern Nevada and Trans-Pecos Texas), there are no extensive bodies of carbonate rock that provide conduits for regional, inter-basin groundwater flow (Maxey 1968; Winograd and Thordarson 1975; Hibbs et al. 1998; Sharp 2001). As noted in Sections 2.6.3, 2.8.3 and 3, however, local bedrock terranes dominated by dissolution-prone carbonate and gypsiferous sedimentary units may play a significant role in intrabasin, geothermal-flow systems and as sources of saline groundwater. Inter-basin and intrabasin boundary structures, such as faults and flexures, are also part of the group of tectonic and volcanic features that play a major role in groundwater-flow dynamics.

As adapted from Eakin and others (1976), Figure 2-3 illustrates the general model of hydrogeologic framework and groundwater flow that is applicable throughout the Basin and Range province.

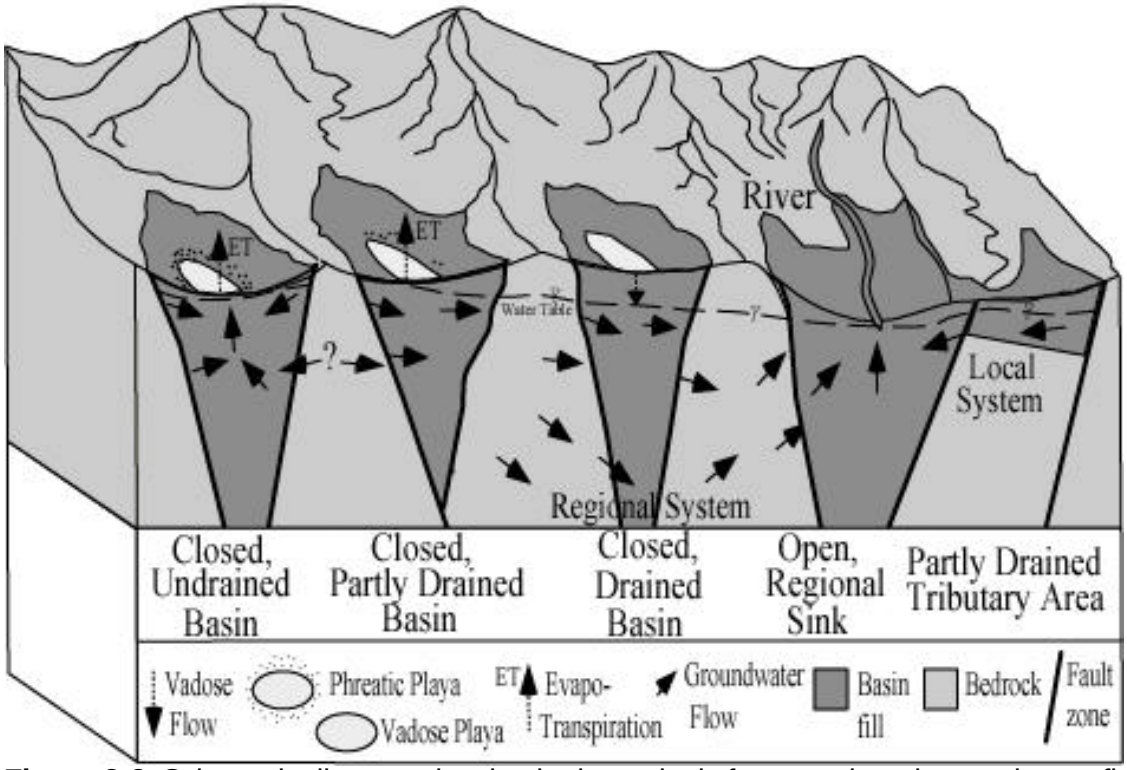

Figure 2-3. Schematic diagram showing hydrogeologic framework and groundwater-flow system in interconnected group of closed and open; undrained, partly drained, and drained intermontane basins. Modified from Eakin and others (1976) and Hibbs and others (1998).

This block diagram also incorporates information from other studies in the Basin and Range Province-Great Basin section (e.g., Mifflin 1968, 1988), and the West Texas--Chihuahua region (Hibbs et al. 1998; Sharp 2001). Note that the topographic terms *closed* and *open* are here used only in reference to the surface flow into, through, and from intermontane basins; whereas the terms *undrained*, *partly drained*, and *drained* designate basin types with groundwater-flow regimes involving intrabasin and/or inter-basin movement. *Phreatic* and *vadose*, respectively, indicate saturated and unsaturated subsurface conditions. *Phreatic playas* (with springs and seeps) are restricted to floors of *closed* basins (*bolsons, bolsones*) that are *undrained* or *partly drained;* while *vadose playas*

occur in both *closed* and *open*, *drained* basins. *Cienegas* are a special wetland class located in places where the zone of saturation intersects an undissected valley-floor surface. Few intermontane basins (*bolsons* and *semibolsons*) of the southern Basin and Range province are truly *undrained* in terms of groundwater discharge, whether or not they are topographically *closed* or *open*. In the Mesilla Basin region, the (intermediate) *partly drained* basin type, which is also "incompletely" *open*, represents the major geohydrologic system.

Under predevelopment conditions, groundwater discharge in the region occurred mainly through 1) interbasin subsurface leakage, 2) contributions to gaining reaches of perennial or intermittent streams, 3) flow from seeps and springs, 4) evapotranspiration from basin- and valley-floor wetlands (including *phreatic playas, bosques* and *cienegas*), and 5) evaporation from open-water bodies. Most recharge to basin-fill aquifers occurs by two mechanisms: "mountain front," where some precipitation falling on bedrock highlands contributes to the groundwater reservoir along basin margins (Fig. 2-4); and "tributary," where the reservoir is replenished and along losing reaches of larger intra-basin streams (Section 2.8; Hearne and Dewey 1988; Nickerson and Myers 1993; Anderholm 1994, 2000; Wasiolek 1995; Scanlon et al. 2001).

We must also emphasize that short- and long-term climatic changes have significant impacts on all water-resource concerns in this arid to semi-arid region (Sections 2.8.3 and 2.8.4). Therefore, while very large quantities (millions of ac-ft) of fresh to slightly saline water are stored in the basin-fill aquifer system, much of it is not being effectively recharged under the warm-dry environmental conditions of the past 5 to 10 thousand years. Current research in the region indicates that most groundwater in storage is thousands to tens of thousands of years old and was recharged during cooler and wetter parts of Quaternary glacial-pluvial cycles (Plummer et al. 2000; Scanlon et al. 2001).

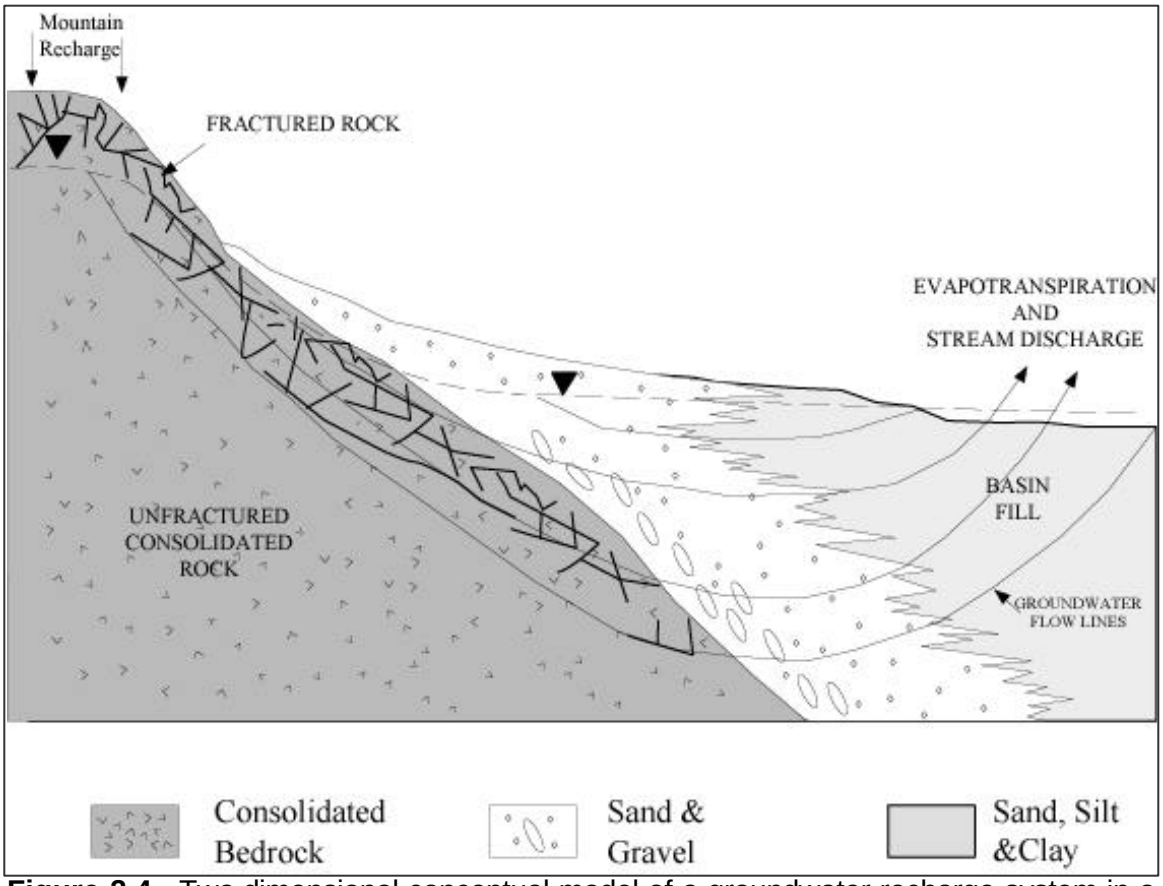

Figure 2-4. Two-dimensional conceptual model of a groundwater recharge system in a Basin and Range by hydrogeologic setting (from Wasiolek 1995, modified from Feth 1964, and Mifflin 1968).

2.5 CONCEPTUAL HYDROGEOLOGIC-FRAMEWORK MODEL

The conceptual hydrogeologic framework of basin-fill aquifers in the Rio Grande rift region, with special emphasis on features related to groundwater flow and quality, is best characterized in terms of three basic building blocks: lithofacies assemblages (LFAs), hydrostratigraphic units (HSUs), and bedrock and structural-boundary conditions (Hawley and Haase 1992; Hawley and Lozinsky 1992; Hawley et al. 1995). Our current conceptual hydrogeologic model of an interconnected shallow valley-fill/basin-fill and deep-basin aquifer system was initially developed for use in groundwater-flow models of the Mesilla and Albuquerque basins (Appendix A; Peterson et al. 1984; Thorn et al. 1993; Kernodle et al. 1995). However, basic design of the conceptual model is flexible enough to allow it to be modified for use in other basins of the Rio Grande rift and

adjacent parts of the southeastern Basin and Range province (e.g., Hawley and Kernodle 2000; Hawley et al. 2000).

Hydrogeologic models of this type are simply qualitative to semi-quantitative descriptions (graphical, numerical, and verbal) of how a given geohydrologic system is influenced by 1) bedrock-boundary conditions, 2) internal-basin structure, and 3) lithofacies characteristics of various basin-fill stratigraphic units. They provide a mechanism for systematically organizing a large amount of relevant hydrogeologic information of widely varying quality and scale (from very general drillers observations to detailed bore-hole logs and water-quality data). Model elements can then be graphically displayed in combined map and cross-section (GIS) formats so that basic information and inferences on geohydrologic attributes (e.g., hydraulic conductivity, transmiss-ivity, anisotropy, and general patterns of unit distribution) may be transferred to basin-scale, three-dimensional numerical models of groundwater-flow systems. As emphasized by Hawley and Kernodle (2000), however, this scheme of data presentation and interpretation is normally not designed for site-specific groundwater investigations.

2.5.1 Lithofacies Assemblages

Lithofacies assemblages (LFAs) are the basic building blocks of the hydrogeologic model (Fig. 2-5, Table 2-1) and the primary components of the hydrostratigraphic units (HSUs) discussed below. These sedimentary-facies classes are defined primarily on the basis of grain-size distribution, mineralogy, sedimentary structures, and degree of post-depositional alteration. Inferred depositional environments provide a secondary basis for definition. LFAs have distinctive geophysical, geochemical and hydrologic attributes, and they provide a mechanism for showing distribution patterns of major aquifers and confining units in hydrogeologic sections. Basin and valley fills are subdivided into thirteen major LFAs that are ranked in decreasing order of aquifer potential (Tables 2-1 to 2-3; LFAs *1-10, a-c*). Figure 2-5 is a schematic illustration of the distribution pattern of major facies assemblages in the basins of the Rio Grande rift region.

Lithofacies properties that influence groundwater flow and production potential are summarized in Tables 2-2 and 2-3. *Roman numeral* notations (I to X) used in earlier versions of this classification scheme (Hawley and Lozinsky 1992; Hawley et al. 1995) are changed to *Arabic* style to facilitate development of alphanumeric attribute codes that are more appropriate for GIS applications and numerical modeling.

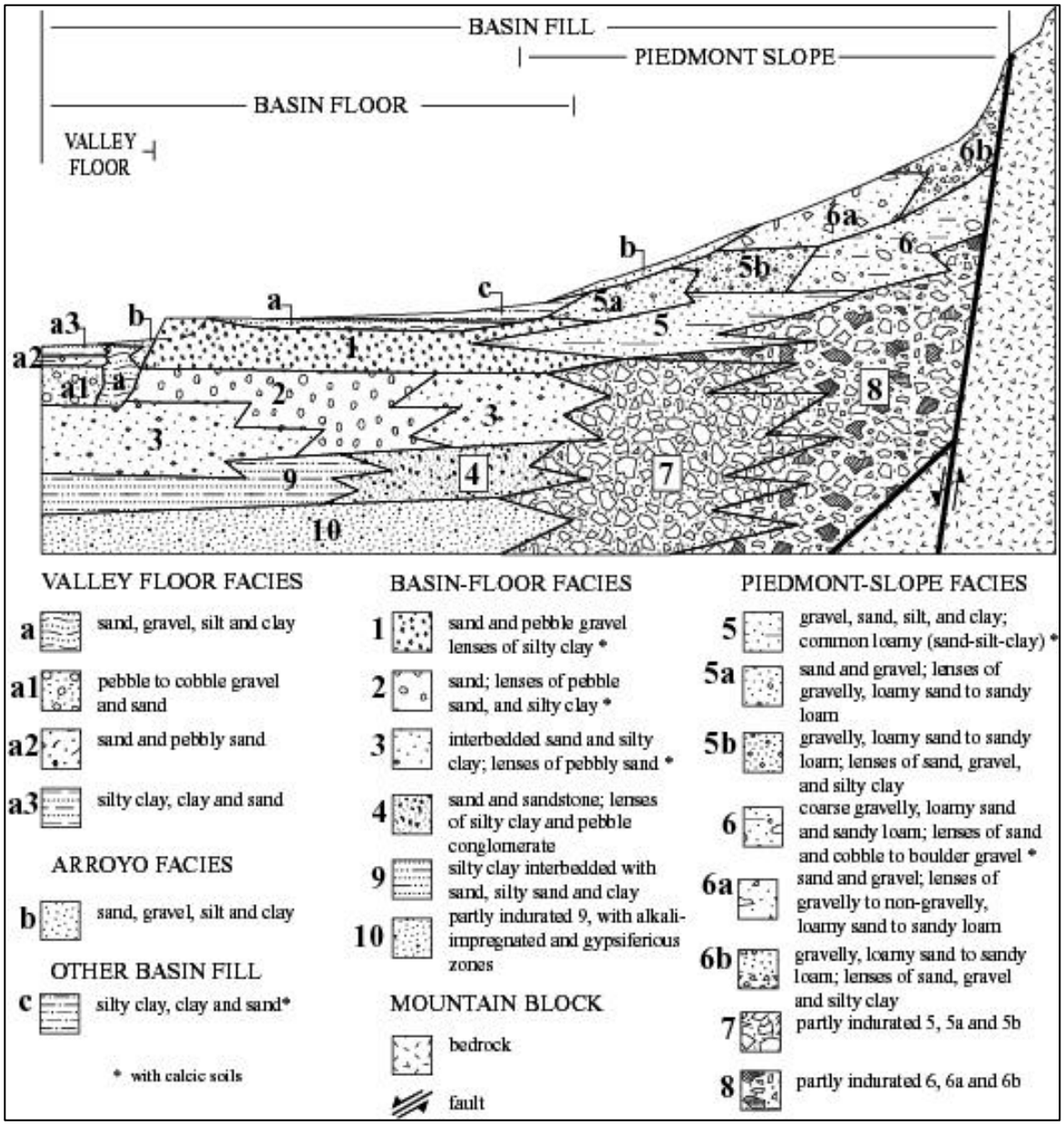

Figure 2-5. Schematic distribution pattern of major lithofacies assemblages (Tables 2-1 to 2-3) in basin and valley fills of the Rio Grande rift region (from Hawley et al. 2000).

Table 2-1. Summary of lithofacies – assemblage depositional settings and dominant textures for Santa Fe Group (1-10) and post-Santa Fe (a, b, c) basin and valley fills in the Mesilla Basin area (Modified from Hawley and Haase 1992, Table III-2)

Lithofacies		Dominant depositional settings and process	Dominant textural classes
1		Basin-floor fluvial plain	Sand and pebble gravel, lenses of silty clay
2		Basin-floor fluvial, locally eolian	Sand; lenses of pebble sand, and silty clay
3		Basin-floor, fluvial-overbank, fluvial-deltaic and playa-lake; Locally eolian	Interbedded sand and silty clay; lenses of pebbly sand
4		Eolian, basin-floor alluvial	Sand and sandstone; lenses of silty sand to clay
5		Distal to medial piedmont-slope; coalescent alluvial fan and alluvial slope	Gravel, sand, silt, and clay; common loamy (sand-silt-clay)
	5a	Associated with large watersheds; sub-parallel and distributary-channel (primary), sheet-flood and debris-flow (secondary)	Sand and gravel; lenses of gravelly, loamy sand to sandy loam
	5b	Associated with small steep watersheds; sheet-flood, debris-flow, and distributary-channel	Gravelly, loamy sand to sandy loam; lenses of sand, gravel, and silty clay
6		Proximal to medial piedmont-slope, alluvial-fan	Coarse gravelly, loamy sand and sandy loam; with lenses of sand, and cobble to boulder gravel
	6a	Like 5a	Sand and gravel; lenses of gravelly to non-gravelly, loamy sand to sandy loam
	6b	Like 5b; debris flow (dominant)	Gravelly, loamy sand to sandy loam; lenses of sand, gravel, and silty clay
7		Like 5	Partly indurated 5
8		Like 6	Partly indurated 6
9		Basin-floor-alluvial flat, playa, lake, and fluvial-lacustrine; distal-piedmont alluvial	Silty clay interbedded with sand, silty sand and clay
10		Like 9, with evaporite processes (paleophreatic)	Partly indurated 9, with gypsiferous and alkali-impregnated zones
a		River-valley, fluvial	Sand, gravel, silt and clay
	a1	Basal channel	Pebble to cobble gravel and sand (like 1)
	a2	Braided plain, channel	Sand and pebbly sand (like 2)
	a3	Overbank, meander- belt oxbow	Silty clay, clay, and sand (like 3)
b		Arroyo channel, and valley-border alluvial-fan	Sand, gravel, silt, and clay (like 5)
c		Basin floor, alluvial flat, cienega, playa, and fluvial-fan to lacustrine plain	Silty clay, clay and sand (like 3,5, and 9)

Table 2-2. Summary of properties that influence groundwater production potential of Santa Fe Group lithofacies assemblages (modified from Haase and Lozinsky 1992) [>, greater than; <, less than]

Lithofacies	Ratio of sand plus gravel to silt plus clay[1]	Bedding thickness (feet)	Bedding configuration[2]	Bedding continuity (feet)[3]	Bedding connectivity[4]	Hydraulic conductivity (K)[5]	Groundwater production potential
1	High	>5	Elongate to planar	>1000	High	High	High
2	High to moderate	>5	Elongate to planar	>1000	High to moderate	High to moderate	High to moderate
3	Moderate	>5	Planar to lobate	500 to 1000	Moderate to high	Moderate	Moderate to high
4	Moderate to low*	>5	Planar to elongate	100 to 500	Moderate to high	Moderate	Moderate
5	Moderate to high	1 to 5	Elongate to lobate	100 to 500	Moderate	Moderate to low	Moderate to low
5a	High to moderate	1 to 5	Elongate to lobate	100 to 500	Moderate	Moderate	Moderate
5b	Moderate	1 to 5	Lobate	100 to 500	Moderate to low	Moderate to low	Moderate to low
6	Moderate to low	1 to 5	Lobate to elongate	100 to 500	Moderate to low	Moderate to low	Low to moderate
6a	Moderate	1 to 5	Lobate to elongate	100 to 500	Moderate	Moderate to low	Moderate to low
6b	Moderate to low	1 to 5	Lobate	<100	Low to moderate	Low to moderate	Low
7	Moderate*	1 to 5	Elongate to lobate	100 to 500	Moderate	Low	Low
8	Moderate to low*	>5	Lobate	<100	Low to moderate	Low	Low
9	Low	>5	Planar to lobate	>500	Low	Very low	Very low
10	Low*	>5	Planar to lobate	>500	Low	Very low	Very low

[1]High >2; moderate 0.5-2; low <0.5

[2]Elongate (length to width ratios >5); planar (length to width ratios 1-5); lobate (lenticular or discontinuous planar beds).

[3]Measure of the lateral extent of an individual bed of given thickness and configuration.

[4]Estimate of the ease with which groundwater can flow between individual beds within a particular lithofacies. Generally, high sand + gravel/silt + clay ratios, thick beds, and high bedding continuity favor high bedding connectivity. All other parameters being held equal, the greater the bedding connectivity, the greater the groundwater production potential of a sedimentary unit (Hawley and Haase 1992, VI).

[5]High, 30 to 100 ft/day; moderate, 3 to 30 ft/day; low, <3 ft/day; very low, <0.1 ft/day.

Table 2-3. Summary of properties that influence groundwater production potential of post Santa Fe Group lithofacies assemblages [>, greater than; <, less than]

Lithofacies	Ratio of sand plus gravel to silt plus clay[1]	Bedding thickness (feet)[3]	Bedding configuration[2]	Bedding continuity (feet)[3]	Bedding connectivity[4]	Horizontal hydraulic conductivity (K)[5]	Groundwater production potential
a	High to moderate	>5	Elongate to planar	>1000	High to moderate	High to moderate	High to moderate
a1	High	>5	Elongate to planar	>1000	High	High	High
a2	High to moderate	>5	Planar to elongate	500 to 1000	Moderate to high	Moderate	Moderate
a3	Moderate to low	>5	Planar to elongate	100 to 500	Moderate to high	Moderate to low	Moderate to low
b	Moderate to low	1 to 5	Elongate to lobate	>300	Moderate	Moderate to low	Moderate to low
c	Low to moderate	1 to 5	Elongate to lobate	100 to 500	Low	Low	Low

[1]High>2;moderate 0.5-2; low <0.5

[2]Elongate (length to width ratios>5); planar (length to width ratios 1-5); Lobate (lenticular or discontinuous planar beds).

[3]Measure of the lateral extent of an individual bed of given thickness and configuration.

[4]Estimate of the ease with which groundwater can flow between individual beds within a particular ligholacies. Generally, high sand + gravel/silt + clay ratios, thick beds, and high bedding continuity favor high bedding connectivity. All other parameters

[5]General ranges: high 30 to 100ft/day; moderate, 3 to 30ft/day; low, <3ft/day; very low, <0.1ft/day.

2.5.2 Hydrostratigraphic Units

Most intermontane-basin fills in the southern New Mexico region can be placed in one or the other of two broad lithostratigraphic categories, the Santa Fe Group in the Rio Grande rift (Hawley et al. 1969; Hawley 1978; Chapin and Cather 1994) and the Gila Group (“Conglomerate”) in the Mexican Highland and Datil-Mogollon sections to the west (Hawley et al. 2000). The bulk of these deposits are of Late Neogene age (Miocene and Pliocene; ~23 to 1.8 Ma). In many previous hydrogeologic studies, clear distinctions have not been made between "bolson or basin fill” and contiguous (formal or informal) subdivisions of the Santa Fe and Gila Groups. As a first step in organizing available information on basin-fill stratigraphy and sedimentology with emphasis on aquifer characteristics, a provisional hydrostratigraphic classification system has been developed that is applicable to most basins of the southeastern Basin and Range province. This is an ongoing process, with progressive system refinement occurring with each new study phase. To date this informal classification scheme has been used

successfully in the Albuquerque and Mesilla Basins and in adjacent "Southwest Alluvial Basins" (Hawley 1984, 1996; Hawley and Haase 1992; Hawley and Lozinsky 1992; Hawley and Kernodle 2000; Hawley et al. 1995, 2000, 2001).

In Rio Grande rift basins south of Elephant Butte Dam (Palomas-Rincon, Jornada del Muerto, Mesilla and Hueco basins); the Santa Fe Group has been further subdivided into five major formation-rank units that record stages of basin filling and tectonic evolution prior to incision of the present river-valley system (Fig. 2-6). From youngest to oldest, these mappable units are formally named the Camp Rice, Palomas, Fort Hancock, Rincon Valley, and Hayner Ranch Formations (Section 2.6.5; Strain 1966; Seager et al. 1971; Gile et al. 1981; Lozinsky and Hawley 1986; Seager et al. 1982, 1984,1987; Seager 1995; Mack et al. 1998; Collins and Raney 2000).

Hydrostratigraphic units (HSUs) defined in the region are mappable bodies of basin and valley fill that are grouped on the basis or origin and position in both lithostratigraphic and chronostratigraphic sequences. The informal upper, middle, and lower Santa Fe hydrostratigraphic units (HSUs: USF, MSF, LSF) form the major basin-fill aquifer zones, and they correspond roughly to the upper (Camp Rice-Palomas), middle (Fort Hancock/Rincon valley, and lower (Hayner Ranch) lithostratigraphic subdivisions of the Santa Fe Group used in local and regional geologic mapping (Fig. 2-5). Dominant lithofacies assemblages in the upper Santa Fe HSU are LFAs *1-3, 5 and 6*. The middle Santa Fe HSU is characterized by LFAs *3, 4, 7-9*, and the lower Santa Fe commonly comprises LFAs *4,7-10*. Basin-floor facies assemblages *3* and *9* are normally present throughout the Santa Fe Group section in closed-basin (bolson) areas.

The other major hydrostratigraphic units comprise channel and floodplain deposits of the Rio Grande (HSU–RA) and its major arroyo tributaries (VA). These valley fills of Late Quaternary age (<130 ka) form the upper part of the region's most productive shallow-aquifer system. Surficial lake and playa deposits, fills of larger arroyo valleys, and piedmont-slope alluvium are primarily in the *vadose* zone. However, they locally form important groundwater discharge and recharge sites. Historical *phreatic* conditions exist, or have recently existed,

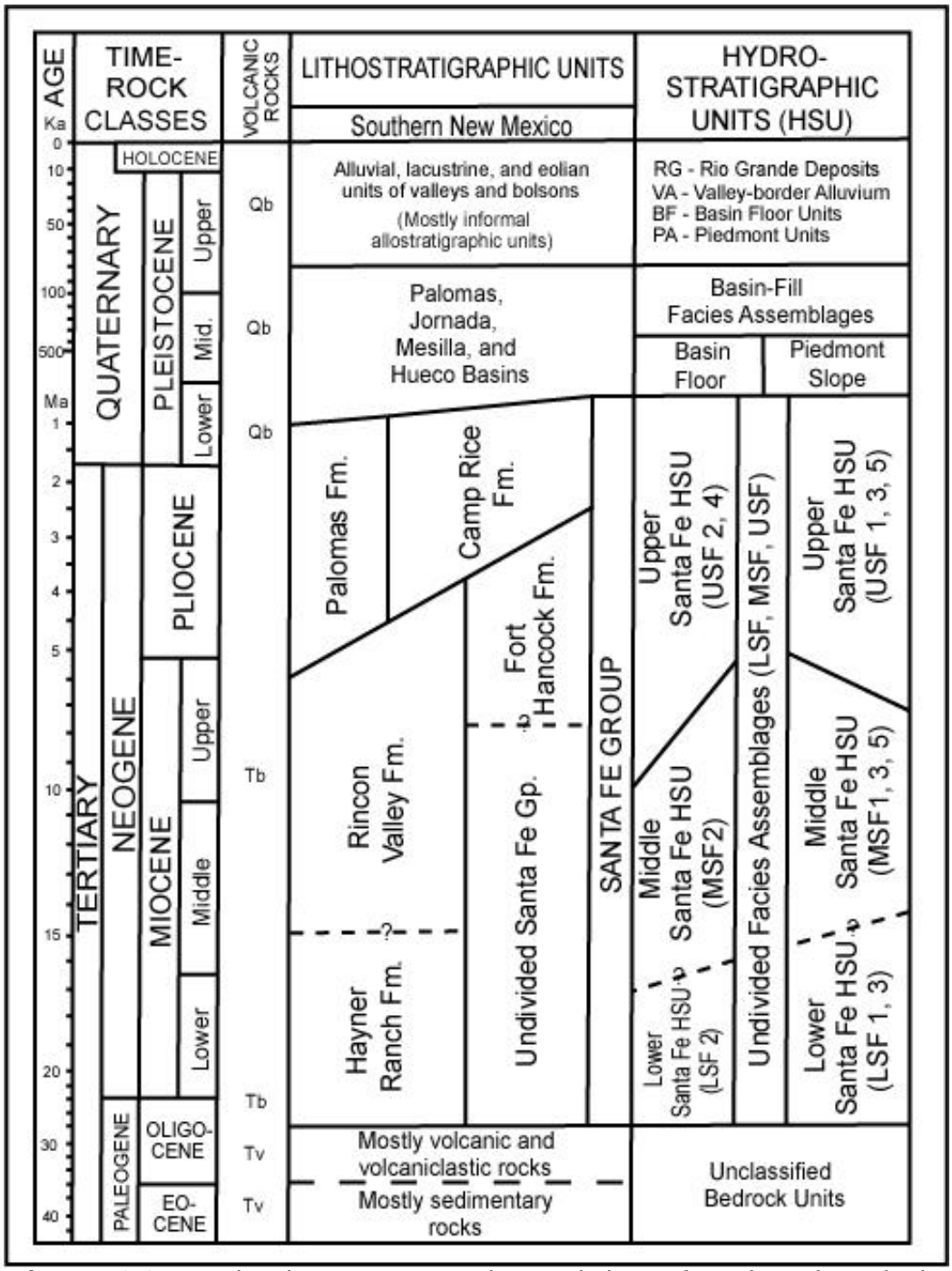

Figure 2-6. Regional summary and correlation of major chronologic, lithostratigraphic, and basin-fill hydrostratigraphic units in the Mesilla Basin region of southern New Mexico and Trans-Pecos Texas. Igneous rock symbols: Qb–Quaternary basalt, Tb–Tertiary mafic volcanics, and Tv–older Tertiary intermediate and silicic volcanics, and associated plutonic and sedimentary rocks. Modified from Hawley and Kernodle (2000).

in a few playa remnants of large pluvial lakes of Late Quaternary age (Hawley 1993). Notable examples are gypsum or alkali flats in the Tularosa, Jornada del Muerto and Los Muertos basins, which are contiguous to, but outside the area of discussion (Figs. 1-1 and 1 - 2; Hawley 1993; Lucas and Hawley 2002).

2.5.3 Bedrock and Structural-Boundary Components

Bedrock and structural-boundary that controls the behavior of basin-fill aquifer systems include bordering mountain uplifts, bedrock topography beneath the basin-fill, fault zones and flexures within and at the edges of basins, and igneous (intrusive and extrusive) rocks that penetrate or are interbedded with basin fill. Tectonic evolution of the fault-block basins and ranges of the Mesilla Basin region during the past 25 Ma has had a profound effect on the distribution of lithofacies assemblages and the timing and style of emplacement of all major hydrostratigraphic units (Figs. 2-4 and 2-5). Most of the significant bedrock- and structural-boundary features in the area now are well documented on geologic maps and sections by Collins and Raney (2000), Seager (1995), Seager and others (1982,1987), and Woodward and Myers (1997). These topics are addressed in more detail in the following section (2.6, 2.6.1) and in Sections 2.7.1 and 2.7.4.

2.6 GENERAL HYDROGEOLOGIC SETTING

2.6.1 Regional Overview

Detailed discussion of the area's geologic history is beyond the scope of this paper, and the reader is referred to excellent reviews in Sawyer and Pallister (1989), Chapin and Cather (1994), Keller and Cather (1994), Mack and others (1998), and Faulds and Varga (1998). Emphasis here is on those key elements of the geologic setting that directly apply to the Mesilla Basin's hydrogeologic framework and related aspects of groundwater flow and chemistry.

The Mesilla Basin is near the southern end of the north-trending series of structural basins and flanking mountain uplifts that constitute the Rio Grande rift tectonic province (Figs. 1-1, 1-2, 2-1; Plate 1; Chapin and Seager 1975; Hawley

1978; Seager and Morgan 1979). The ongoing rifting process began in Oligocene time, about 34 million years ago (Ma). During this long interval, extensional forces have stretched the earth's crust, causing large basin blocks to rotate and sink relative to adjacent mountain uplifts. North-trending half-graben structures, many with accommodation-zone terminations, are the dominant tectonic forms of the regional geologic terrane (Figs. 1-1, 1-2); and they are commonly superimposed on mid-Tertiary volcano-tectonic features (e.g., Organ and Doña Ana uplifts), and still older Laramide structural highs and depressions (e.g., parts of the Franklin Mountains and Mesilla Basin).

All rift basin fill that was deposited prior to entrenchment of the present valley system is included in the Santa Fe Group (Spiegel and Baldwin 1963; Hawley et al. 1969; Hawley 1978, Charts 1 and 2; Chapin and Cather 1994). Geologic mapping and geochronologic studies throughout the region (Fig. 2-6) demonstrate the Santa Fe Group continuity that was originally recognized by Kirk Bryan (1938). The river itself flows southward through New Mexico in a series of canyons and valleys that follow the N-S trends of most of the rift basins from the San Luis basin to the southern end of the Mesilla Valley. Beyond El Paso Narrows (El Paso del Norte) between the Franklin and Juárez-Cristo Rey uplifts, the El Paso Valley reach of the Rio Grande follows the SE trend of the Hueco Bolson.

2.6.2 Basin-Scale Setting

The geologic setting of the Mesilla Basin is illustrated by an index map (Fig. 2-7) that shows basin-scale structural features and locations of two schematic cross sections, which extend across the northern (Las Cruces) and south-central (Anthony, NM-TX) parts of the basin (Figs. 2-8 a, b). Section base elevation is 10,000 ft below sea level, and there is no vertical exaggeration. A much more detailed view of the basin's hydrogeologic framework is provided by the hydrogeologic base map and cross-sections (Plates 1 to 9, Section 2.7, Appendix A). These illustrations are based primarily on a compilation of surface and subsurface geologic information by Hawley (1984) and Seager and others (1987), and interpretations of subsurface geophysical, and hydrogeologic data by

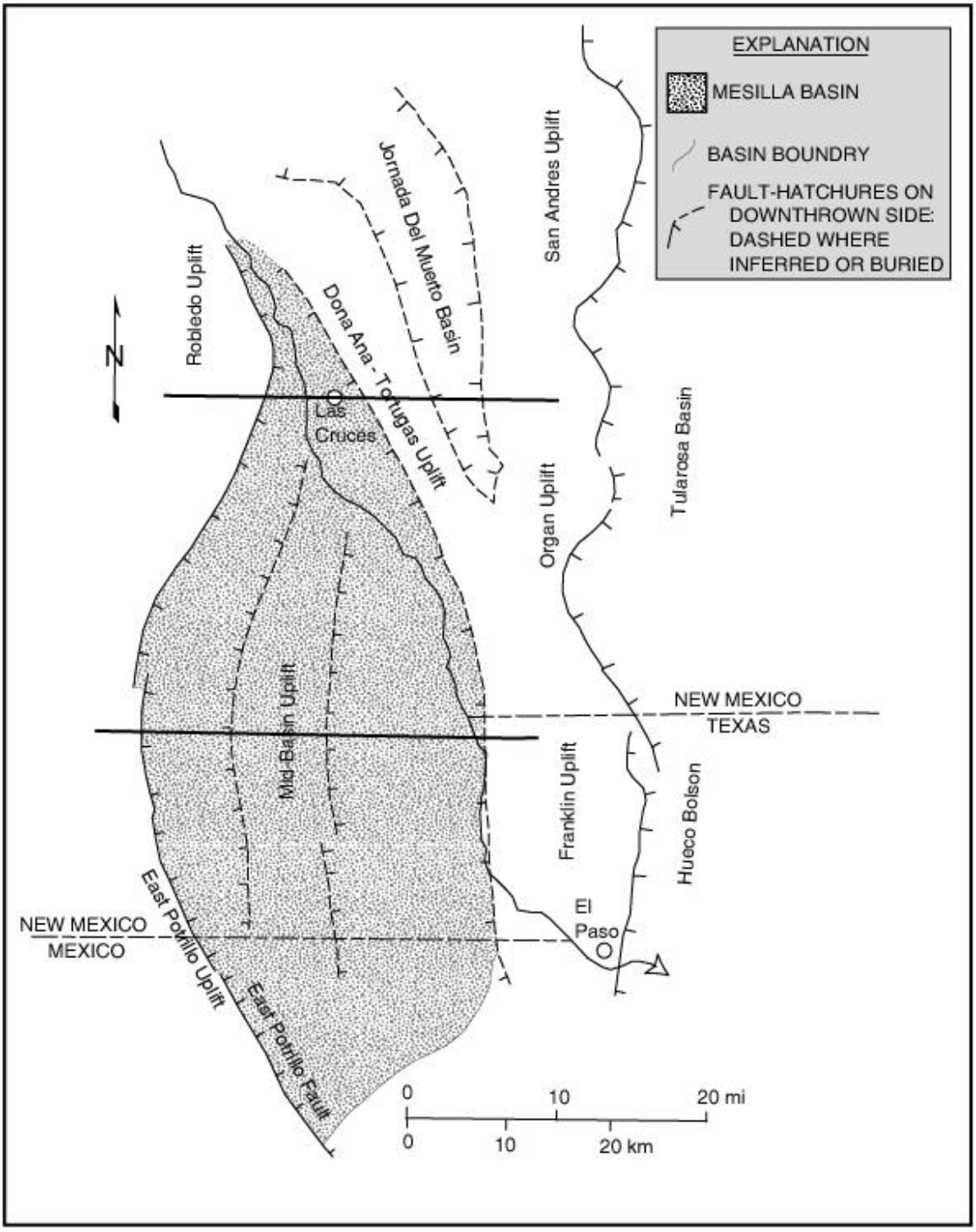

Figure 2-7. Index map of Mesilla Basin area showing major basin-boundary and intrabasin fault zones and uplifts. Locations of structural-geologic sections (Fig. 2.7a,b) are also shown. Modified from Hawley and Lozinsky (1992).

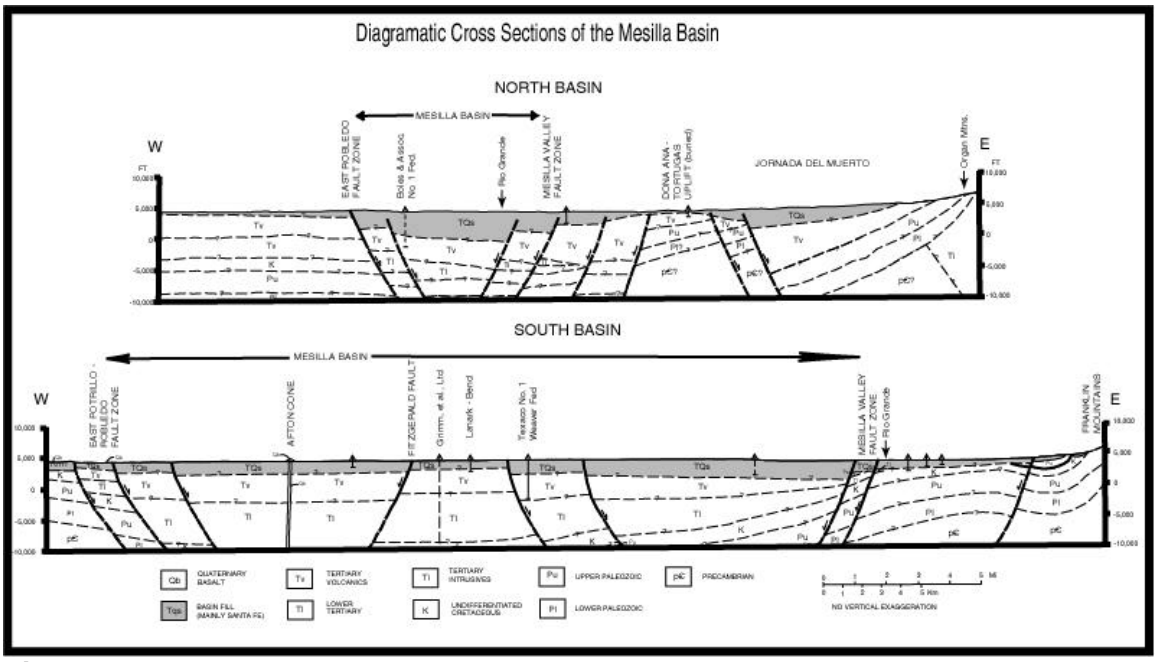

Figure 2-8. Schematic structural-geologic sections of the northern and central Mesilla Basin: **a**. West to east section from Robledo to Doña Ana-Tortugas uplifts across Las Cruces Metro-area. **b**. Section along 32nd Parallel from Aden-Afton volcanic field to Franklin uplift, NM-TX. Section locations shown on Figure 2.6. No vertical exaggeration. Modified from Hawley and Lozinsky (1992).

Hawley and Lozinsky (1992). Other major contributors to the geologic interpretations on Figures 2-8 a, b include Leggat and others (1962), Cliett (1969), Hawley and others (1969), King and others (1971), Gile and others (1981), Wilson and others (1981), Wilson and White (1984), Myers and Orr (1986), Seager and Mack (1986, 1994), Seager (1995), and Ken Stevens (USGS-WRD unpublished).

The Mesilla Basin is bounded on the east by the Organ-Franklin-Juarez mountain chain and on the west by fault-block and volcanic uplands, which extend northward from the East Potrillo Mountains (near the International Boundary) to the Aden and Sleeping Lady Hills. The Robledo and Doña Ana Mountains bound the northern end of the valley; but, in terms of topography and some surface inflow, the northeastern border is transitional with the Jornada del Muerto Basin (Figs. 1-2, 2-1, 2-7; Plate 1; Seager et al. 1987; Frenzel and Kaehler 1992). The basin extends southward at least 60 mi (100 km) from the upper end of the Mesilla Valley, between the Robledo and Doña Ana Mountains,

to a poorly defined structural-boundary zone located about 15mi (25km) south of the International Boundary and southwest of Sierra Juárez (Figs. 2-1, 2-7). This part of the basin merges southward with the Bolson de Los Muertos in north-central Chihuahua (Córdoba et al. 1969; Hawley et al. 2000).

Basin width varies from about 5 mi (8 km) at its northern end to about 25 mi (40 km) in its central part. Flanking mountain uplifts (Plate 1) are narrow and relatively low-lying (most less than 8,000 ft (2,400 m) elevation) in comparison with ranges of the northern and central Rio Grande rift (Hawley 1978). Broad plains with low relief (less than 500 ft, 150 m) characterize much of the 1,600-mi² drainage area of the Mesilla topographic basin (Hawley 1975). The only major erosional feature is the entrenched Mesilla Valley of the Rio Grande near the basin's eastern edge. The area of the floodplain is about 215 mi². The deep structural basin that contains the bulk of the Santa Fe Group and valley-fill aquifer systems has been designated the "Mesilla ground-water basin" in recent USGS-WRD reports (e.g., Frenzel and Kaehler 1992; Nickerson and Myers 1993). Its area is about 1,100 mi². An extensive basin-floor remnant of late Pliocene and early Pleistocene age is preserved between the Valley and the western basin-boundary uplifts (Plate 1, Fig. 2-1). This geomorphic surface is called "La Mesa" in many earlier reports on the area (Conover 1953; King et al. 1971; Gile et al. 1981); but it is here designated the "West Mesa" following the place-name terminology used in USGS-WRD publications starting with Wilson and others (1981).

A distinctive feature of Santa Fe Group deposits in the Mesilla Basin fill is that they are relatively thin (maximum saturated thickness of about 3,000 ft) in comparison to fills in adjacent parts of the Hueco-Tularosa and Mimbres basin systems (Seager et al. 1987; Seager 1995). Deep test drilling in the basin since 1985 indicates that previous estimates of much greater rift-basin-fill thickness are incorrect. For example compare interpretations of Wilson and others (1981) and Hawley (1984) with those of Hawley and Lozinsky (1992) and Nickerson and Myers (1993). Basin-fill deposits (discussed in detail in following sections) are predominantly alluvial in origin, with eolian and lacustrine facies occurring

primarily in older parts of the depositional sequence. Interbedded basaltic volcanic rocks of Miocene age are also locally present, as are feeder conduits for the Quaternary basalts and ejecta from Maar (phreato-magmatic) eruptions, which cap the Santa Fe Group in some parts of the southwestern Mesilla Basin (Section 2.6.4).

2.6.3 Basin Structure and Bedrock-Boundary Units

In contrast with northern and central Rio Grande rift basins, the Mesilla Basin is not bound by high and continuous ranges of high mountains (Seager 1995; Seager et al. 1987; Collins and Raney 2000). Onlap of basin fill has buried much of the Doña Ana-Tortugas and southern Organ-Bishop Cap uplifts on the northeastern basin margin, and the East Potrillo and Robledo uplifts to the west. Only the Franklin and Juarez uplifts at the basin's southeastern edge form well-exposed structural highlands (Figs. 2-1, 2-7, 2-8; Plate 1).

Basin subsidence was initiated in late Oligocene time, but maximum differential displacement between the major basin and range structural blocks probably occurred between 4 and 10 million years ago (late Miocene to early Pliocene). By late Miocene time, rock debris eroded from adjacent highlands, and possibly from adjacent parts of the Rio Grande rift, had filled existing subbasins (mostly half grabens) to the point where intrabasin uplifts (horsts) were buried by lower and middle Santa Fe Group deposits. The broad topographic basin formed by this infilling process continued to aggrade as a single (*upper* Santa Fe) unit through the early middle Pleistocene when widespread basin filling ceased due to entrenchment of the Rio Grande Valley system. The thickest Santa Fe Group fills in the Mesilla Basin (about 3000 ft, 900 m) are located in areas adjacent to the most active segments of major boundary fault zones – the Mesilla Valley, East Potrillo, and East Robledo (Figs. 2-7, 2-8; Plates 8 and 9).

Tertiary igneous intrusives (granites to monzonites) and volcanics (rhyolites to andesites) are the dominant rocks exposed in the Doña Ana and southern Organ Mountains, with some Paleozoic and lower Tertiary sedimentary rocks being locally exposed (Seager et al. 1976; Seager 1981). Marine-

carbonate and siliciclastic rocks of Paleozoic and early Cretaceous age are the dominant lithologic units exposed in the Tortugas, Bishop Cap, Franklin, Juarez, East Potrillo, and Robledo uplifts (Harbour 1972; Kelley and Matheny 1983; Seager et al. 1987; Seager and Mack 1994; Collins and Raney 2000). Also of note is the common occurrence of gypsite beds in upper Pennsylvanian rocks of the Franklin Mountains—Bishop Cap area.

A variety of sedimentary and intermediate-intrusive rocks of Cretaceous and early Tertiary age crop out in the Paso del Norte area between the Franklin Mountains and Sierra de Juárez, which includes Cerro de Cristo Rey on the Chihuahua-New Mexico border (Fig. 2-1, Plate 1; Córdoba et al. 1969; Lovejoy 1976). Of special importance to the current study is the probability that the Paleozoic and Cretaceous rocks, which are widely exposed and/or shallowly buried along the basin's eastern and southwestern borders, can at least locally form conduits for significant volumes of deeply circulating groundwater. This inference is supported by the presence of extensive fracture systems associated with basin-boundary fault zones (Figs. 2-7, 2-8; Plate 1), and the fact that some dissolution features have been observed in carbonate and gypsiferous sedimentary rocks of this area, both in outcrop and subsurface. Refer to Sections 2.7.1, 2.9 and 3 for further discussion of this topic.

Middle Tertiary volcanic and intrusive rocks of intermediate to silicic composition are exposed in isolated upland areas such as the Sleeping Lady and Aden Hills at the southwestern end of the Robledo uplift, and Mount Riley northwest of the East Potrillo Mountains (Plate 1; Seager et al. 1987; Seager 1995; Seager and Mack 1994). Analyses of drill cuttings and geophysical logs from a few deep test wells (oil and gas, water, and geothermal), and surface geophysical surveys are the only sources of information on the lithologic character and structure of bedrock units beneath the rift-basin fill. Oil and gas test holes, including wells 25.1.32.141 and 26.1.35.333 in the central part of the basin (Plates 3 and 5), encountered a thick sequence of lower to middle Tertiary volcanic and sedimentary rocks (Uphoff 1978; Seager et al. 1987). The lower Tertiary sedimentary units were deposited in deep, northwest-trending basins of

Laramide age (Seager et al. 1986), and are exposed only in a few places along the northern and eastern basin margins (Seager et al. 1987). Cretaceous and upper Paleozoic underlie the middle to lower Cenozoic sequence at great depth in most parts of the basin; but Cenozoic units may rest directly on lower Paleozoic and Precambrian rocks in a few areas (Seager 1989; Seager et al. 1986).

All deep test drilling to date indicates that lower to middle Tertiary volcanic and volcaniclastic rocks of intermediate to silicic composition are the dominant units that immediately underlie Santa Fe Group basin fill. Besides the previously mentioned oil tests, water test wells that have definitely penetrated these units include wells 24.1.8.123, 25.16.333, and 27.1.4.121 in the central part of the basin; and wells 24.2.4.334, 29.3.2.243, and 49-04-109 east of the Mesilla Valley fault zone near the east edge of the basin (Plates 1, 8 and 9).

Almost all boundaries between the major subbasins and flanking uplifts appear to be formed by zones of high-angle normal faults. Many of the exposed mountain blocks are strongly tilted, and at least some of the basin blocks have a tilted half-graben morphology and listric boundary faults that are typical of most continental rift basins (Seager 1995; Seager et al. 1987; Mack and Seager 1990; Seager and Mack 1994; Leeder et al. 1996). Dips are usually very low in the central basin area, however; and the major subbasins and intrabasin uplifts are here interpreted as only slightly tilted graben and horst blocks that are bounded by high-angle normal faults that may or may not flatten significantly with depth (Fig. 2-8, Plates 8 and 9).

The northeastern basin boundary is formed by a partly buried bedrock ridge, designated the Doña Ana-Tortugas uplift on Plate 1, which marks the structural boundary between the Mesilla and Jornada basins. Recent surface geophysical surveys and test drilling by the U.S. Geological Survey (Woodward and Myers 1997) along the Doña Ana-Tortugas trend have confirmed previous inferences on its extent (King et al. 1971; Hawley 1984, Plate H-H'). This uplift is flanked on the west by a major intrabasin structure, the Mesilla Valley fault zone (MVFz). The two major western basin-boundary faults are the Robledo fault

(RoF) to the northwest and the East Potrillo fault (PoF) to the southwest. As already noted, the topographic basin merges northward with the Jornada Basin, northeast of Las Cruces, and southward with the Bolson de Los Muertos Plains, southwest of El Paso-Ciudad Juarez (Figs. 1-1, 1-2, 2-1, 2-7 and 2-8). Westward and eastward topographic transition zones with the Mimbres and Hueco-Tularosa basin systems, respectively, are along the I-10 corridor and at Fillmore Pass.

The internal structure of the Mesilla Basin is complex (Fig. 2-8, Plates 1, 8 and 9). Structural interpretations in this report are based on oil and geothermal test-well, water-well, and both surface and borehole geophysical data (Plates 2-9, Appendix A, Tables 1 and 2). The major structural elements include three large subbasins: Eastern, Southwestern, and Northwestern, with general north-south trends, a buried mid-basin uplift, and an inferred south-central basin that extends into Chihuahua west of Sierra Juárez. Geohydrologic implications of bedrock and structural controls are discussed in more detail in Sections 2.7 and 2.8.

2.6.4 Upper Cenozoic Volcanics

Late Oligocene to Quaternary sedimentary deposits of the Rio Grande rift are locally interbedded with, and capped by basalt and andesite flows, and pyroclastic deposits (Crumpler 2001; Crumpler and Aubele 2001). Associated with these extrusive rocks are intrusive bodies that include feeder dikes, plugs, sills and breccia pipes (Plate 1, Figs. 2-6, 2-8). Dated basalts in the southwestern New Mexico region include scattered occurrences of middle Miocene to Pliocene age and extensive lava fields of Quaternary age. Pleistocene basalt flows and associated vent units (e.g., cinder cones, lava shields, and maars) form a widespread cover on the *upper* Santa Fe Group in the west-central Mesilla Basin area, and they also cap parts of the southern Robledo and northeastern Potrillo uplifts (Hoffer 2001; Gile 1987; Seager et al. 1987; Seager 1987, 1989, 1995; Anthony and Poths 1992; Anthony et al. 1992; Williams et al. 1993; Williams 1999).

Basaltic andesites of late Oligocene age may also be present in the basal part of the basin fill (Fig 2-8). These rocks are locally interbedded with and intrude lower Santa Fe beds, and they are extensively exposed in the Sierra de Las Uvas area of northwestern Doña Ana County. Volcanic layers of basaltic to andesitic composition have been reported in drilling records of two water wells in the northern basin area, including the Mesilla Valley near Las Cruces (24.1.13.411); and they may be either flows of sills that are, respectively, interbedded with or intruded into the basin fill. A well drilled at the Las Cruces wastewater treatment plant (about 1.5 mi, 2.4 km WSW of 23.1.13.411) reportedly encountered a basalt layer at a depth of about 880 ft (270 m) in the middle to lower part of the basin-fill section (R.G. Myers, oral communication 7-14-92). A 563-ft ranch well at the eastern edge of the Aden-Afton volcanic field in the west-central part of the basin (26.1W.25.414) encountered 33º C water at 375 ft bls (Wilson et al. 1981, p. 294-295). The reported very high specific capacity of the well (789 gpm/ft of drawdown), if accurate, suggests that it is producing from a highly permeable basaltic intrusive or flow unit (see Section 2.7.5).

2.6.5 Santa Fe Group Lithostratigraphy

The Santa Fe Group (Spiegel and Baldwin 1963; Hawley et al. 1969; Chapin and Cather 1994) is the major component of Rio Grande rift basin fill. In southern New Mexico and western Trans-Pecos Texas, the Group ranges in age from about 25 to 0.7 Ma and includes alluvium derived from adjacent structural uplifts and nearby rift-basin areas, and locally thick eolian and playa-lake sediments (Fig. 2-6). Fill thickness in most of the central basin area (between the Mesilla Valley and East Potrillo-Robledo fault zones) ranges from 1,500 to 2,500 ft (460-760 m). In this report, the Santa Fe Group is subdivided into informal *lower, middle and upper* lithostratigraphic units defined on the basis of general lithologic character, depositional environments, and diagenetic features related to age and post-depositional history. Generally equivalent hydrostratigraphic units are discussed in the following section.

The *lower* Santa Fe Group is dominated by fine-grained, basin-floor sediments that intertongue with alluvial fan deposits beneath the distal parts of bordering piedmont slopes. Records from deep test borings (Plates 3 to 7) indicate that both *middle* and *lower* Santa Fe basin-floor facies include extensive and thick playa-lacustrine deposits in many parts of the central and southern Mesilla Basin. In addition, subsurface records from adjacent basins document the presence of calcium sulfate (gypsum-selenite) and sodium sulfate (mirabilite-thenardite) in the form of both primary evaporites, and secondary cements and segregations (e.g., Hawley et al. 1969; Reeves 1969; King et al. 1971; Seager et al. 1987; Lucas and Hawley 2002). Fill in the Tularosa and Los Muertos basins includes post-Santa Fe as well as Santa Fe units.

Lower Santa Fe eolian sediments also form thick sheets and lenticular bodies that are interbedded with both basin-floor and piedmont-slope deposits in the southern part of the Mesilla Basin. Buried dune complexes as much as 600 ft (200m) thick have been identified beneath the Mesilla Valley in the Anthony-Canutillo area (Cliett 1969; Hawley 1984) and are probably preserved in other parts of the eastern (La Union-Mesquite) subbasin (Plate 1). Thick eolian deposits possibly also occur in the deeper parts of the southwestern subbasin east of the East Potrillo fault zone.

Lower Santa Fe beds range in age from about 25 to 10 Ma. They were deposited in a *closed*-basin setting prior to the final interval of deep basin subsidence and uplift of the higher flanking range blocks (e.g., Organ, Franklin, East Potrillo, and Robledo Mountains). Formal lithostratigraphic subdivisions of the *lower* Santa Fe Group have not yet been proposed for the Mesilla Basin. However, the unit generally is correlative with the Hayner Ranch Formation and the lower part of the Rincon Valley Formation mapped in the Jornada del Muerto-Rincon Valley area of northern Doña Ana County (Seager and Hawley 1973; Seager et al. 1971, 1982, 1987).

The *middle* Santa Fe Group was deposited between about 10 and 4 Ma when rift tectonism was most active, and filling of subbasins adjacent to the major boundary fault zones (Mesilla Valley, East Potrillo, East Robledo) was

accelerated. In many areas, rates of erosion of uplifted basin borders and deposition on adjacent piedmont slopes increased relative to those of the preceding interval. Alluvial flats that terminated in extensive playa-lake plains dominated broad, rapidly aggrading basin floors; and most mid-basin uplifts were deeply buried by *middle* Santa Fe deposits. Alternating beds of clean sand, silty sand, and silt-clay mixtures are the dominant lithofacies (discussed in more detail in following section) in much of the central basin area. Eolian sediments also continued to accumulate in leeward (eastern) basin area; but the thickest buried dune sequences appear to be confined to *lower* Santa Fe Group. Formal lithostratigraphic subdivisions have not yet been proposed; but the middle Santa Fe unit probably correlates with at least the upper part of the Rincon Valley Formation (Seager et al. 1982, 1987) and the lower Fort Hancock Formation, which has a type area in the southeastern Hueco Bolson (Strain 1966; Hawley et al. 1969; Gustavson 1991).

The major *upper* Santa Fe subdivision in the region is the Camp Rice Formation of Strain (1966). This Plio-Pleistocene unit has been mapped in detail from the southern Palomas and Jornada del Muerto Basins, across the Mesilla and southern Tularosa Basins, and throughout the Hueco Bolson to its type area near Fort Hancock in Hudspeth County, Texas (Fig. 1-2; Seager et al. 1971, 1976, 1982, 1987; Gile et al. 1981; Gustavson 1991; Collins and Raney 2000). Camp Rice deposits are very well preserved throughout most of the Mesilla Basin, with significant dissection only occurring in the Mesilla Valley and valleys of a few major arroyos. The formation's thickness ranges from about 300 to 700 ft (90-215 m) in central basin areas.

The Camp Rice Formation contrasts markedly with older Santa Fe units in terms of lithologic character because its primary depositional environment was dominated by broad fluvial plains of a through-going river, the ancestral "upper" Rio Grande. The geomorphic transformation from a *closed* to an *open* system in the Mesilla basin area probably occurred between 3 and 4 million years ago. It is also important to note that the ancestral-river basin at that time already extended

as far north as the San Juan and Sangre de Cristo Mountains of southern Colorado and northern New Mexico (Southern Rocky Mountain province).

Braided distributary channels of “Camp Rice” fluvial system spread southward and eastward (via Fillmore Pass) and ultimately terminated in the extensive playa-lake plains of the Bolson de Los Muertos (northern Chihuahua) and the Tularosa-Hueco basin floor (Figs. 1.1, 1.2; Hawley 1969; Strain 1971; Hawley 1975; Gile et al. 1981; Seager 1981; Seager et al. 1987; Gustavson 1991; Mack et al. 1997). Sandy deposits of this complex fluvial-deltaic system continued to accumulate on the Mesilla Basin floor through early Pleistocene time. Recent research on basin-fill magnetostratigraphy and biostratigraphy, and dating of tephra lenses in the upper part of the Camp Rice Formation demonstrate that widespread basin-floor aggradation (and Santa Fe Group deposition) ended about 700 thousand years ago (Vanderhill 1986; Mack et al. 1993; Gile, Hawley et al. 1995; Mack et al. 1996; Mack et al. 1998; Lucas et al. 1999). Presence of Yellowstone-derived Lava Creek Ash in oldest inset-river deposits in Selden Canyon and El Paso Narrows (300 to 250 ft above the present Rio Grande floodplain), demonstrates that initial Mesilla Valley cutting occurred no later than about 0.65 Ma (Seager et al. 1975; Gile et al. 1981; Izett and Wilcox 1982; Gile, Hawley et al. 1995; Dethier 2001).

The dominant Camp Rice lithofacies is a thick sequence of fluvial sand and pebbly sand deposited by the ancestral Rio Grande during an interval of 2 to 3 million years. However, because of complex river-channel shifts (influenced by both tectonism and climatic factors) during basin-floor aggradation, fine-grained (slack-water) facies are also locally present. The other important Camp Rice lithofacies is a piedmont-slope assemblage that is primarily composed of fan alluvium and associated debris-flow deposits. To the south and southeast, the basal Camp Rice of the Mesilla Basin area appears to intertongue with and overlap fine-grained alluvial and playa-lake deposits of the upper Fort Hancock Formation. In their type areas near Fort Hancock in Hudspeth County, Texas, the Camp Rice/Fort Hancock Formation contact has been dated at about 2.5 Ma (Strain 1966; Vanderhill 1986; Gustavson 1991).

2.6.6 Santa Fe Group Sedimentary Petrography

Petrographic analyses of medium- to coarse-grained sediments of the Santa Fe Group and underlying Oligocene rocks (primarily drill cuttings) in the Mesilla Basin and Rincon Valley areas are described by R.P. Lozinsky in Section III and Appendix A of Hawley and Lozinsky (1992). His interpretations of the petrography of rock fragments and mineral grains that are major framework components of the major Santa Fe Group lithofacies assemblages are summarized here. Anderholm (1985) has also made preliminary x-ray analyses of clay-size materials from several Rio Grande rift basins (including the Mesilla Basin); and Mack (1985) has described the petrography of drill cuttings from two test wells in the Las Cruces West Mesa (including well 23.1.30.422**,** Plates 2, 5).

Tools needed to properly describe the sand-size fraction of basin-fill deposits include the binocular microscope for preliminary drill-cutting descriptions, the petrographic (light) microscope for rock and grain thin-section analyses, and x-ray equipment and the scanning electron microscope for characterization of ultra-fine-scale features (e.g., grain-surface features, cementing agents, and porosity). Only binocular and petrographic microscopes were used in this study to analyze sand-size material from selected sets of drill cuttings and outcrop samples (Appendix A: Methods). Cuttings from the Afton (MT1), Lanark (MT2), La Union (MT3), and Noria (MT4) test wells were analyzed initially with a binocular microscope in order to construct a stratigraphic column for each of these key wells (Plates 12-15 in Hawley and Lozinsky 1992), and to determine intervals (~100 ft) where sub-samples of representative sands would be collected for thin-section analyses. Samples were also collected from representative sandy intervals in the two wells in the Canutillo, Texas area (CWF1D and CWF4D; Nickerson and Myers 1993) and from six outcrops of the *upper* and *middle* Santa Fe units.

Sand samples analyzed from the six water wells and from outcrop areas in the Mesilla Basin were derived from more than one source terrane. The abundance of plagioclase (zoned and twinned) and andesitic lithic fragments

strongly suggest an intermediate volcanic source area for most of the detrital grains. Chert, chalcedony, and abundant quartz (many well rounded with overgrowth rims) indicate reworked sedimentary units as another major source. A granitic source area is also suggested by the presence of microcline, strained quartz, and granitic rock fragments. The paucity of metamorphic-rock fragments and tectonic polycrystalline quartz rules out a metamorphic terrane as a major source area. In the *middle* Santa Fe Group samples from the Rincon Valley area (Rodey site of Hawley and Lozinsky 1992), the abundance of plagioclase and intermediate volcanic lithic fragments and the paucity of quartz, chert and sedimentary lithic fragments strongly suggest an intermediate-volcanic terrane as the only major source area.

Due to lack of paleoflow indicators, it is difficult to determine the exact source area for these deposits. However, it appears that even in early to middle Santa Fe time (Miocene), the central Mesilla Basin was receiving sediment from a very large watershed area. A much larger source region was also available for sand and finer grain-size material when the mechanism of eolian transport is taken into account. By middle Pliocene time the ancestral Rio Grande was delivering even pebble-size material to the basin from source terranes as far away as northern New Mexico (e.g., pumice and obsidian from the Jemez and Mount Taylor areas). In most cases, visual and binocular microscopic examination of the gravel-size (>2mm) fraction is still the best way to establish local versus regional provenance of coarse-grained fluvial and alluvial deposits.

Most information on the mineralogy of clay-size material (<4 microns) in the Mesilla Basin area relates to soils and soil-parent sediments of the upper Camp Rice Fm that were sampled at NRCS-NMSU Desert Project sites (e.g., Gile et al. 1981; Gile, Hawley et al. 1995; Monger and Lynn 1996). A few analyses of clay-size material from older parts of the Santa Fe Group are reported by Anderholm (1985). There are, however, places in other Rio Grande rift basins (including Albuquerque, Socorro, and Jornada del Muerto-Rincon) where clay-mineral analyses from representative Santa Fe sections are available (e.g., Anderholm 1985; Bowie and McLemore 1987; McGrath and Hawley 1987;

Hawley and Haase 1992; and Machette et al. 1997). As with the sand fraction, the dominant clay-size component in these basins is detrital material that reflects the lithologic character of the various source terranes; however, some mineral varieties of authigenic and/or polygenetic origin have been identified.

Clay-mineral assemblages that are almost always present (but in varying proportions) in Santa Fe Group deposits include: illite (clay-size mica), smectite, mixed-layer illite/smectite (I/S clay), kaolinite, and montmorillonite (a dioctahedral sodium smectite). Authigenic clay minerals are commonly associated with alkaline-playa environments or partly indurated calcic-soil horizons, and include montmorillonite, I/S clay, and chain-lattice clays of the magnesium-rich sepiolite—palygorskite group. Zeolites are another secondary mineral group associated with feldspar alteration under alkaline-diagenetic conditions; and their occurrence as cementing agent has been reported primarily in piedmont facies derived from silicic-volcanic source terranes (e.g., Seager et al. 1975; Anderholm 1985; Hawley and Haase 1992). As noted in the preceding description of the *lower* to *middle* Santa Fe Group sequence, gypsum and selenite (of both primary and secondary origin) are common constituents of fine-grained playa-lacustrine facies; and if alkali-lake environments ever existed, sodium-sulfate-enriched zones may also be present.

Almost all of the above-mentioned rock and mineral types, from sand to clay size, play a significant role in the chemical evolution of groundwater moving through, or stored for long intervals in basin-fill aquifers (Section 2.9). Water-sediment interactions, including solution-precipitation and cation exchange, are a major topic covered in Section 3.

2.6.7 Post Santa Fe Deposits

Post-Santa Fe Group sediments were deposited in two contracting geomorphic settings: 1) valleys of the Rio Grande and tributary arroyo systems, and 2) extensive intermontane-basin areas still topographically *closed* (Fig. 2-1; Hawley and Kottlowski 1969; Reeves 1969; Hawley 1969, 1975; Gile et al. 1981).

Valley-fill units of middle and late Quaternary age were deposited during repeated episodes of the river incision separated by intervals of partial backfilling that produced the present landforms of the Mesilla Valley. The stepped-sequence of geomorphic surfaces (mainly alluvial terraces and fans) bordering the Rio Grande floodplain was produced by multiple episodes of valley entrenchment during glacial (pluvial) stages, and subsequent intervals of valley aggradation during interglacial (interpluvial) stages (Section 2.8.2). The 60 to 100 ft (18-30 m) of medium-to coarse-grained alluvium beneath the modern river floodplain ("flood-plain alluvium" of Frenzel and Kaehler 1990) is a product of 1) valley cutting by a high-energy fluvial system during the last glacial stage of the Pleistocene, which ended 10 to 15 thousand years ago (Ka), and 2) subsequent inner-valley filling that has continued during the Holocene interglacial stage (Fig. 2-6). Tributary alluvial systems have delivered more sediment to the valley floor than the river could transport out of the drainage basin during this 10-15 ka interval of net fluvial aggradation.

Older valley fills, of the tributary arroyo systems as well as the ancestral river, that are preserved in terrace remnants on the valley borders ("valley-border surfaces" Hawley and Kottlowski 1969) are generally above the water table; and they are not described in this report. Thin (<30 ft, 10 m) alluvial, eolian, and playa-lake sediments deposited in areas of the Mesilla Basin still not integrated with the Rio Grande are also not discussed. They are included with the *upper* Santa Fe unit in the hydrogeologic cross sections (Plates 2 to 9) that are described in the following section. Younger valley and basin fills, and soil-geomorphic relations are the subject of numerous reports by L.H. Gile and associates (e.g., Gile and Grossman 1979; Gile et al. 1966, 1981; Gile, Hawley et al. 1995).

2.7 HYDROGEOLOGIC-FRAMEWORK OF AQUIFER SYSTEMS

2.7.1 Overview

From a geohydrologic perspective, the Mesilla Basin occupies a broad topographic depression, which, in turn, overlies a hydrologically linked group of

deep structural subbasins and intervening buried-bedrock highs (Plate 1, Figs. 2-7, 2-8 a, b). Both intrabasin and basin-boundary structures play a major role in terms of groundwater flow and geochemistry. Figure 2-9 is a schematic hydrogeologic cross-section of the south-central Mesilla Basin, and it is aligned approximately along the 32nd Parallel and close to the position of Figure 2-7b and Plate 3. Basic concepts of hydrogeologic framework and groundwater flow in incompletely *closed* and *partly drained* intermontane-basin systems like the Mesilla Basin have been introduced in Sections 2.4 and 2.5 (Figs. 2-3 to 2-5; Tables 2-1 to 2-3). The following general description of the basin's hydrogeologic framework is supplemented by more detailed characterization of individual hydrostratigraphic, lithofacies, and structural components of the Santa Fe Group and valley-fill aquifer systems in Appendix A, Tables 1 and 2).

The most-productive aquifer zones are in the eastern half of the Mesilla Basin and vary in thickness from about 300 to 2,000 feet (Wilson et al. 1981; Wilson and White 1984; Nickerson 1986 and 1989; Frenzel and Kaehler 1992; Nickerson and Myers 1993). The thickest section underlies the east-central West Mesa and adjacent parts of the Mesilla Valley floor in an area extending from Las Cruces to near Cañutillo (TX) and La Union (Plates 1–3, 6, 7, 8a-d, 9a). Basic aquifer properties of Santa Fe HSUs in the Mesilla Basin are very similar to those in adjacent parts of the Hueco-Tularosa and Jornada del Muerto basins (Cliett 1969; Wilson et al. 1981; Hawley 1984; Orr and White 1985; Orr and Myers 1986; Bedinger et al. 1989; Ashworth 1990; Orr and Risser 1992; Shomaker and Finch 1996; Hibbs 1999). The extent of these partly connected aquifer systems, and the amount of interbasin groundwater flow is controlled in great part by the hydraulic properties of basin-boundary faults and lithofacies distribution patterns (depending, of course on existing flow gradients). While fault zones and fine-grained facies commonly form effective barriers to interbasin flow, a small amount of underflow may enter or leave the basin at low barrier points associated with zones of relatively high permeability (Appendix A; Sections. 2.7.5, 2.8.1).

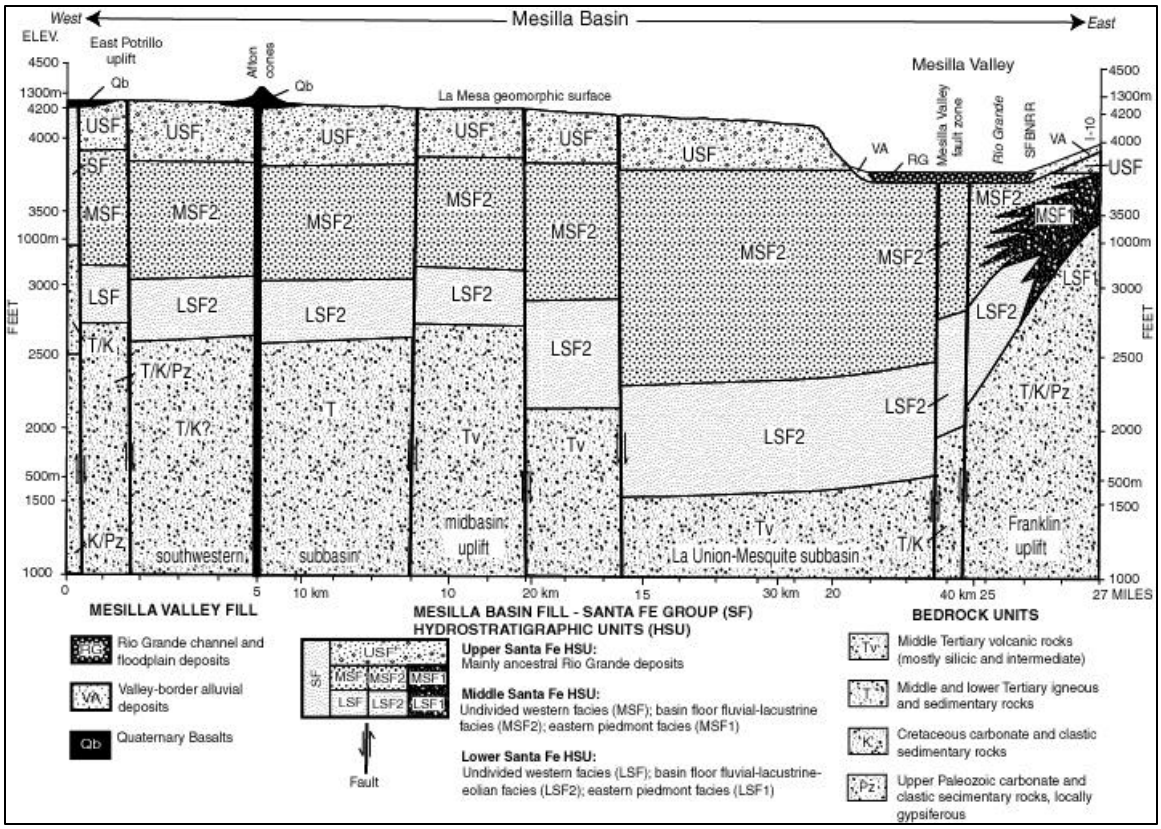

Figure 2-9. Schematic hydrogeologic cross section of the south-central Mesilla Basin near the 32nd Parallel in Doña Ana County, N M and El Paso County, TX, Vertical exaggeration about 10x. Modified from Hawley and Lozinsky (1992).

The major sources of fresh to slightly saline groundwater in the Mesilla Basin are from basin-floor facies assemblages (LFAs 1 to 4) in the middle to upper parts of the Santa Fe Group (HSUs USF2 and MSF2). The dominant central-basin facies group comprises 1) thick sequences of fine-grained alluvial and lacustrine sediments that 2) interfinger with (LFA 3) and are overlapped by coarser-grained, ancestral-river deposits (LFAs 1 and 2). Along basin margins, both of these upper and middle Santa Fe facies units are transitional with piedmont-slope alluvium (USF1, 3 and MSF1, 3; LFAs *5* to *8*).

Inferred subsurface distribution patterns of lithofacies assemblages with aquifer potential in the basin are shown on Plates 8 and 9. They are components of five HSUs (LSF, MSF, USF, RA and VA) and include LFAs 1 to 5. Documentation of these patterns varies from good (where petrographic analysis

of drill cutting, borehole geophysical logs, and detailed drilling records are available) to strictly inferential (where few or no field data exist). This variation in data quality is clearly illustrated in the lithofacies interpretations presented on Plates 2 to 9. In the large areas and/or depth zones without adequate subsurface control only the most general attributes of the hydro-stratigraphic units can be shown. However, all information collected to date does indicate that the entire basin-fill sequence is increasingly thinner and finer grained to the south. Fine- to medium-grained basin-floor facies are dominant units near the International Boundary west of Cerro de Cristo Rey, an area that includes the Santa Teresa and Noria well sites (Plates 8e, 9b, LFAs *3*, *9* and *10*). How far this basin-fill fining and thinning trend continues towards the Bolson del Muertos area of northern Chihuahua has not yet been determined; limited test drilling, geophysical data, and photogeologic interpretations suggest that the Mesilla "structural" basin extends no more than 15 mi (25 km) into Mexico (Figs. 1-1,1-2; Section 2.6.2).

As in basin areas to the north and the Hueco Bolson to the southeast, the most productive and thickest aquifers are ancestral Rio Grande fluvial deposits (LFAs *1* and *2*) of the *upper Santa Fe* HSU (*USF2*). However, coarse-grained fluvial facies are only saturated in the northeastern part of the basin near Las Cruces (Hawley and Lozinsky 1992). In the southern and western part of the basin the *upper Santa Fe* HSU is entirely in the vadose zone; and the most productive aquifers comprise the *middle* and *lower Santa Fe* HSUs (MSF2/LSF2*:* LFAs 3 and 4). A particularly productive aquifer is the "deep aquifer" of Leggat and others (1962), which underlies the southern Mesilla Valley in the Anthony-Cañutillo area (HSU-LSF 2, Fig. 2-9). This unit includes a distinctive eolian sand facies (LFA 4) that intertongues mountainward with piedmont fanglomerates (LFAs 7-8), and basinward with basin-floor facies assemblages (LFAs *3, 9* and *10*?). The latter facies are here interpreted as playa-lake and fluvial-deltaic- deposits (Fig. 2-6).

2.7.2 Structural and Bedrock Elements

In terms of overall basin and range architecture, the major hydrogeologic-framework component includes the bedrock units and tectonic features that form important boundary zones with respect to the basin-fill aquifer system and related aspects of groundwater flow and chemistry. Distribution patterns of large-scale framework components, including major fault zones and volcanic-feeder conduits, are shown on Plate 1 (map view) and Plates 2 to 9 (cross-section view). Relatively impermeable igneous and sedimentary bedrock units of Oligocene and older age, crop out along the basin margins, and underlie the basin fill at depths ranging up to about 3,500 ft. One of the significant contributions of the present study is that there is now much better definition of the contacts between bedrock boundary units and the basin fill. Compare Plates 8 and 9 with earlier cross-section interpretations (e.g., Wilson et al. 1981; Hawley 1984).

We need to emphasize here, however, that there is still much to be learned about the basin's internal structure. Based on recent experience in other parts of the Rio Grande rift, notably the Albuquerque Basin, additional drilling and geophysical studies (including aeromagnetic, gravity and seismic-reflection surveys) should lead to greater precision in the identification of structural-boundary conditions throughout the Mesilla Basin (Keller and Cather 1994; Hawley 1996; Allen et al. 1998; Connell et al. 1998; Grauch 1999; Grauch et al. 2000; Plummer et al. 2000; Sanford et al. 2000; Kucks et al. 2001).

Locations of the major basin-boundary faults are shown on Plate 1, and Figures 2-7 and 2-8. The Robledo and East Potrillo faults (RoF and PoF), respectively, form the northwestern and southwestern boundaries of the "deeper" basin used in recent groundwater-flow models (Peterson et al. 1984; and Frenzel and Kaehler 1992). The broad Mesilla Valley fault zone (MVFz) is entirely buried by Late Quaternary valley fill, but it still forms the major eastern-boundary feature of the Mesilla "structural basin." In the Las Cruces metro-area, the MVFz marks the western edge of the bedrock high that 1) includes the partly buried Tortugas-Doña Ana Mountain uplift, and 2) the area of topographic and structural transition

between the Mesilla and Jornada del Muerto Basins (Woodward and Myers 1997). This fault zone, however, has not been used as a numerical-model boundary (Frenzel and Kaehler 1992).

The structural segmentation of the Mesilla Basin into three major subbasins (Northwestern, Southwestern, and Eastern) and a N-S trending, "Mid-Basin uplift" is well illustrated on Figures 2-7 to 2-9, and Plates 1, 8 and 9. A maximum basin-fill thickness of about 3,000 ft (905 m) is inferred from borehole data in Eastern (La Union-Mesquite) subbasin, but probably rarely exceeds 2,000 ft (610 m) in the Northwestern and Southwestern subbasins (Plates 1 to 4, 8 b-e, 9). The Eastern subbasin is bordered on the east by the MVFz; and its western boundary with the Mid-Basin uplift is the "Mid-basin fault zone" (MBFz, Figs. 2-8, 2-9; Plates 1, 3, 9), informally named by Hawley and Lozinsky (1992). The poorly defined MBFz is locally expressed by alignment of volcanic centers and some low scarps on the West Mesa surface (Plate 1); but it is most prominently displayed in the subsurface as offsets of distinct stratigraphic-marker units on borehole electric logs (e.g., Plate 4, Appendix A, 1.3, 1.4). The Santa Fe Group is only about 1,500 ft (457 m) thick above the central part of the Mid-Basin uplift near the Lanark test-well site (Plates 1 to 5, 8 b-c, 9 b-c). The best-documented surface expression of the uplift's western boundary is the (down-to-west) Fitzgerald fault zone (Plates 1, 3, 8c).

2.7.3 Basin-Fill Hydrostratigraphic Units and Lithofacies Assemblages

Three hydrostratigraphic subdivisions of the Santa Fe Group form the basin-fill aquifer system (Appendix A). These HSUs are ordered in upper to lower (younger to older) stratigraphic sequence (Figs. 2-6, 2-9). The *upper* Santa Fe HSU (USF1, 2) is generally correlative with the Camp Rice Formation, and the most productive aquifer zone (LFAs 1&2, Table 2-3) consists of ancestral Rio Grande channel sand and gravel (HSU-USF2). However, only the lower part of this unit is saturated. The *middle* Santa Fe HSU (MSF1, 2) correlates with much of the Fort Hancock Formation in the Hueco Bolson, which is dominated by fine-grained, alluvial-flat and playa-lake sediments. In the Mesilla Basin, however, the

dominant basin-floor facies assemblage (HSU-MSF2; LFA 3) includes extensive layers of clean fluvial and eolian (?) sand that are interbedded with silty clay; and it probably forms the major aquifer zone in the basin, because its saturated thickness is locally as much as 2,000 ft (610 m). HSU-MSF2 was originally identified by Leggat and others (1962) in deep wells of the EPWU-Cañutillo well field in the southeastern Mesilla Valley (Figs. 2-8b, 2-9).

The *lower* Santa Fe HSU (LSF) is primarily fine grained and partly consolidated throughout much of the basin (LFAs 3, 9, 10); and it only forms a significant part of the aquifer system in the lower Mesilla Valley area that extends from near Mesquite (NM) to Cañutillo and La Union (NM). Leggat and others (1962) first identified this part of the LSF unit in deepest wells of the Cañutillo well field; and they informally named it the "deep aquifer" zone (HSU-LSF 2, Fig. 2-9). The major LSF component in the lower Mesilla Valley area is a distinctive eolian-sand facies (LFA 4) that intertongues mountainward with piedmont fanglomerates (LFAs 7, 8), and basinward with basin-floor facies assemblages (LFAs 3, 9, 10). The latter facies are here interpreted as fluvial-deltaic and playa-lake deposits (Fig. 2-6, Table 2-1).

2.7.4 Valley-Fill Hydrostratigraphic Units and Lithofacies Assemblages

The Rio Grande Valley-fill aquifer system (primarily HSU RA, LFAs a and b) underlies the Mesilla Valley floor between Leasburg dam and the El Paso Narrows. HSU RA comprises river-channel and overbank facies ranging in texture from sand and gravel to silt and clay (Tables 2-1, 2-3). The base of these fluvial deposits is about 60 to 80 ft (18-24 m) below the inner-valley floor, which ranges up to 5 miles (8 km) in width. The basal-channel gravel and sand layer is as much as 40 feet (12 m) thick; and it extends laterally for hundreds of feet beyond the present floodplain in some areas. Most of this unit was deposited during the last interval of maximum valley incision and widening in Late Pleistocene (Wisconsinan) time (Section 2.6.5). Valley-fill HSUs RA and VA extend continuously from Elephant Butte and Caballo reservoirs, through the Rincon, Mesilla and El Paso Valleys, to the Fort Quitman area of the lower

Hueco Bolson (Fig. 1-2). The shallow aquifer system of the Rio Grande Valley is formed by 1) the saturated parts of the inner-valley fill (HSUs RA and VA), and 2) fluvial sand and gravelly sand in underlying Santa Fe HSUs. The latter were deposited by the ancestral-river system during the Pliocene interval of basin filling (primarily HSUs USF2/MSF2 and LFAs 1 to 3).

2.7.5 Late Cenozoic Evolution of the Hydrogeologic System

Because the Mesilla Basin is part of an active tectonic zone in the Rio Grande rift that has been evolving for more than 25 million years, the distribution of hydrostratigraphic units and lithofacies assemblages (Plates 8 and 9) must be interpreted in terms of ongoing, but episodic crustal extension and basin subsidence. Regional and local extension and differential displacement, including rotation of basin and range blocks, clearly act as effective controls on basin sedimentation. On the other hand, obvious climate controls on geomorphic processes in the Quaternary stratigraphic record, which locally relate to Quaternary glacial-interglacial cycles, demonstrate that forces other than rift tectonism will also materially influence depositional processes (Gile et al. 1981; Smith 1994; Leeder et al. 1996). The major geologic processes that control the character and distribution patterns HSUs, LFAs, and bedrock-structural boundaries are reviewed in Appendix A.

With respect to the evolution of groundwater-flow and hydrogeochemical systems in most of the Mesilla Basin, the onset of river-valley entrenchment has had profound implications (Sections 2.8, 2.9). Prior to 700 thousand years ago, in the early Pleistocene, almost all of the Santa Fe Group beneath the floor of the Mesilla Basin was saturated. Subsequent (Middle and Late Pleistocene) RGV incision has caused a water-table drop of 300 to 350 ft (91-106 m) beneath much of the West Mesa area. An analog of the early Pleistocene groundwater-flow regime and hydrogeochemical environment, however, still exists in the southern Mimbres basin system and the Bolson de Los Muertos (Hawley et al. 2000, Chapters 3 and 4). Recent studies in that area provide excellent models of early stages of flow-system evolution throughout the Mesilla Basin (e.g., Hanson et al.

1994; Love and Seager 1996; Mack et al. 1997; Hawley et al. 2000). It must be emphasized, however, that because the lower Mimbres—Los Muertos basin complex has continued to aggrade during the Middle and Late Quaternary, it is the only basin-boundary zone with significant groundwater-inflow potential (Sections 2.8.3 and 2.8.4). The lacustrine deposits of "pluvial" Lake Palomas in the Bolson de los Muertos demonstrate that paleo-water-table elevations during Late Pleistocene and Early Holocene deep-lake intervals were as much as 200 ft (61 m) higher than the potentiometric surface at the lower end of the Mesilla Valley (3,960 vs. 3,760 ft or 1,207 vs. 1,146 m).

2.8 THE MESILLA BASIN GROUNDWATER-FLOW SYSTEM

2.8.1 Overview

The hydrogeologic interpretations presented in preceding discussions and in Appendix A. support the basic conceptual model of the Mesilla Basin groundwater-flow system developed by Frenzel, Kaehler and Anderholm (Frenzel and Kaehler 1992, Figs. 11, 15; p. C64-C74). The following discussion emphasizes aspects of geohydrology that have not had much attention in prior descriptions of the flow system, and its geochemical and geothermal properties.

With respect to surface flow, the Mesilla Basin is a geomorphic feature with both *open and closed* (topographic) components (Section 2.4); but it is externally *drained* in terms of groundwater flow (Fig. 2-3). The general potentiometric-surface map (Fig. 2-1) shows the major, near-surface elements of a flow system that discharges at the lower end of the Mesilla Valley above El Paso Narrows. Groundwater in the New Mexico and Texas parts of the basin generally moves from its flanking highlands and the upstream (Selden Canyon) Rio Grande Valley segment toward and sub-parallel to the Mesilla Valley. The hydraulic gradient in the shallow aquifer system in and near the valley (primarily in HSUs RA and USF2) is essentially the slope of the floodplain (~0.001; ~5 ft/mi). In the West Mesa area the hydraulic gradient in the upper basin-fill aquifer zone (primarily HSU MSF2) ranges from about 0.002 in the northwest to 0.0004 near the International Boundary. The amount of groundwater underflow that

enters the southern Mesilla Basin from the Bolson de los Muertos area of north-central Chihuahua may be quite large (Section 2.8.4).

As in other intermontane-basin flow systems (Fig. 2-3) basinwide flow gradients have a downward component in upslope recharge areas and an upward one in discharge zones. In the Mesilla Basin, the ultimate discharge zone is at and near the southern end of the Mesilla Valley, because there has been very little groundwater outflow through El Paso Narrows since the early Pleistocene (see Sections 2.6.5 and 2.8.3). Most pre-development discharge from the combined Mesilla Valley aquifer systems was by evapotranspiration from the extensive valley-floor wetlands that still existed when W.T. Lee (1907) initially mapped the Mesilla Valley water table.

In and adjacent to heavily developed areas, such as the Mesilla Valley, local-flow direction is influenced by a new set of hydrologic conditions, such as the river, canals, drains, well pumpage, and heavily irrigated fields (Richardson et al. 1972; Frenzel and Kaehler 1992). At the present time, the water table is approximately 10 to 25 ft (3 to 7.5 m) below the floodplain surface in most of the inner Mesilla Valley; and detailed hydraulic-gradient measurements at hydrologic sections near the Las Cruces, Mesquite, and Cañutillo well fields demonstrate that the river is a losing stream in those areas (Nickerson and Myers 1993; Nickerson 1998). Present discharge occurs primarily through evapotranspiration from irrigated croplands and riparian vegetation, flow to drains, and an increasing amount of pumping from all available aquifer zones (including both municipal-industrial and irrigation-agriculture consumption).

Much of the groundwater pumped for irrigation is derived from the unconfined to semi-confined parts of the shallow aquifer zone, which are no more than 250 to 600 ft (76 to 183 m) thick. The *middle* Santa Fe HSU is the most heavily developed aquifer zone, in terms of both drinking-water production and industrial consumption; and this unit is increasingly being pumped for irrigation (Wilson and White 1984). Most discharge from the *lower* Santa Fe unit occurs as municipal and industrial pumping in the Anthony (NM-TX) to Cañutillo (TX) area.

2.8.2 Hydraulic Properties of Hydrostratigraphic and Lithofacies Units

Irrigation-well specific-capacity data and a few aquifer-performance tests provide the basis for many of the published interpretations of hydraulic properties and sustained production potential of Mesilla Valley aquifer systems (Wilson et al. 1981; Frenzel and Kaehler 1992; Wilkins 1998). Almost all of the large irrigation wells and centers of municipal pumping (Las Cruces and El Paso areas) are located in the inner Mesilla Valley. Well yields range from a few to more than 3,000 gpm, and average discharge rates of deep irrigation wells in the central part of the valley are about 2,300 gpm (Wilson and White 1984).

Published information on well specific-capacities, transmissivity and hydraulic-conductivity estimates from aquifer tests, and other hydraulic properties are reviewed and summarized in Appendix A.5. Estimated aquifer transmissivities (T) of the upper 1,200 ft of saturated fill are as high as 50,000 ft^2/d at a few localities; but most values range from 10,000 to 40,000 ft^2/d in the central part of the basin (Santa Fe Group and Rio Grande Valley deposits); and the average T for the West Mesa area may be only about 10,000 ft^2/d (Wilson et al. 1981). Aquifer-test and well-performance data compiled by Frenzel and Kaehler (1992, Fig. 13) indicates that horizontal-hydraulic conductivities are moderate to high (median values of 22-70 ft/d) in the upper 600 ft of saturated basin fill, while conductivities in the lower 600 to 1,800-ft of tested-aquifer zones are low (median value of about 5 ft/d). The upper zone consists primarily of HSUs USF2/MSF2 (LFAs 1, 2, 3 & 5), while saturated basin fill below 600 ft is part of the middle to lower Santa Fe sequence (MSF2, 1 / LSF: LFAs 3, 4, 5 & 7). Almost all permeability estimates made to date clearly indicate that the hydraulic-conductivity ranges (and groundwater-production potential) listed in Tables 2.2 and 2.3 are reasonable values for basinwide modeling (see Section 2.7.2).

Vertical hydraulic conductivity values were found to range from about 0.2 ft/d to 3.0 ft/d for the entire thickness of the confining layers at West Mesa aquifer-test sites (Frenzel and Kaehler 1992); and Kernodle (1992a) suggests that appropriate anisotropy values (ratio of horizontal to vertical hydraulic conductivity) used in groundwater-flow models may range from 200:1 to 1,000:1

in aquifer systems of the Rio Grande rift region. Specific yield estimates vary from 0.1 to 0.2, assuming unconfined aquifer conditions; and specific storage values used in modeling groundwater flow in confined parts of the basin-fill aquifer system range from $1x10^{-5}$ to $1x10^{-6}$/ft (Kernodle 1992a; Frenzel and Kaehler 1992). The reported range in storage coefficients is $2x10^{-3}$ to $3x10^{-5}$ (Wilson et al. 1981).

2.8.3 Recharge: Present and Past

Most recharge to the basin-fill aquifer system occurs 1) through vertical and lateral underflow from the "shallow" alluvial-aquifer zone of the inner Mesilla Valley, and 2) by mountain-front mechanisms (Fig. 2.4; Richardson et al. 1972; Peterson et al. 1984; Hearne and Dewey 1988; Nickerson and Myers 1993; Anderholm 1984; Wasiolek 1995; Anderholm 2000). Recharge estimates for the arid to semiarid Chihuahuan Desert region are based on the conservative assumptions that 1) only 1 to 2% of mean-annual precipitation contributes to recharge, 2) this contribution is distributed very unevenly, and 3) it is most effective in mountain-front zones adjacent to larger and higher watersheds, and in the valleys of perennial streams and major arroyos (Hawley et al. 2000; Scanlon et al. 2001). Recharge to the shallow aquifer zone of the Mesilla Valley area, comprising integrated parts of the valley- and basin-fill aquifer systems, occurs primarily as vertical flow from the surface-water system (river, canals, laterals, irrigated cropland, and drains) except in times of extreme drought. This inner-valley-aquifer unit is, in turn, the major source of recharge to underlying and laterally adjacent basin fill of the Santa Fe Group (mainly HSUs USF2 and MSF2).

Except for a few perennial springs and seeps, and short reaches of intermittent mountain streams, there are no permanent surface-water bodies in the small highland watersheds on the flanks of the basin. Mountain-front recharge is, therefore, very low; and losing reaches of the Rio Grande channel and associated irrigation-canal systems are the major present sources of groundwater replenishment. The mountain-front recharge contribution to Mesilla

Basin aquifers, exclusive of the 215mi² Mesilla Valley area, is probably less than 12,000 ac-ft/yr. This estimate is based on the assumption that about 2% of the mean annual precipitation of 8 to 9 inches actually contributes to recharge outside the inner river valley. It must be emphasize that present and projected basinwide groundwater use greatly exceeds this amount. Frenzel and Kaehler (1992, Fig. 18) estimate that average-annual mountain-front recharge is about 9,700 ac-ft, with about two thirds being derived from higher and larger watersheds of the Organ and Franklin Mountains. They also estimate that another 2,200 ac-ft/yr is derived from the western group of uplands that includes the East Potrillo Mountains and the West Potrillo volcanic field. Small highland areas with relatively low relief, such as the Doña Ana and Robledo Mountains, and Aden-Sleeping Lady Hills are very small recharge sources.

Much of the basin area west and southwest of the Mesilla Valley (West Mesa-La Mesa) is a very gently sloping plain (<5ft/mi) with numerous shallow depressions and a discontinuous veneer of eolian sand (Plate 1). An indurated calcic-soil zone is normally present 3 to 10 ft below the surface. Due to common presence of fractures and pipe-like discontinuities, indurated soil-carbonate horizons is not necessarily the major factor limiting deep percolation of soil moisture in the uppermost vadose zone. This 300 to 400-ft thick zone, which is primarily composed of interbedded layers of clean sand to gravelly sand and silty to sandy clay, forms an effective barrier to downward movement of soil water, particularly in the context of an arid climatic regime during the past 5 to 10 thousand years. The other major limiting factor affecting basin-floor recharge simply relates to the very high efficiency of desert vegetation in soil-moisture extraction (e.g., Gile et al. 1995, 1998).

The significance of present and past climatic conditions on "predevelopment" groundwater-flow regimes is very well documented by both modern meteorological data, and the historic and pre-historic tree-ring record (U.S. Dept. of Commerce 1999; Thomas 1962, 1963; Schmidt 1986; D'Arrigo and Jacoby 1992). For example, the region experienced prolonged droughts from the late 1940s until the late 1970s; and the following two decades were abnormally

wet. Whether or not we are entering another drought period remains to be seen. Major climate cycles of the past two millennia are also well documented. The information compiled by Scurlock (1998) and review papers by Ackerly (1998, 2000) on the Rio Grande basin above Fort Quitman are particularly useful resource documents.

Much larger-scale, glacial-interglacial and pluvial-interpluvial cycles of the Quaternary Period have also had a major impact on both groundwater and surface-water flow regimes, and are of particular relevance to geohydrologic concerns in the Mesilla Basin as well as in other parts of the northern Chihuahua Desert region (Section 2.8.4; Hawley et al. 2000, Table 3-1). The pluvial-lake record in nearby *closed* and *undrained* basins, and other geomorphic and paleoecologic indicators of major environmental shifts associated with glacial-interglacial cycles of the Quaternary Period, is especially important (Hawley 1993, Hawley et al. 2000). Emphasis here is on the fact that groundwater-flow regimes observed during the past century have major recharge and storage components inherited from thousands to tens of thousands of years ago. This observation is confirmed by recent research on groundwater geochemistry and ^{14}C age in other basins of the Rio Grande rift (e.g., Plummer et. al. 2000; Sanford et al. 2000; Scanlon et al. 2001).

Relict shorelines and other lacustrine features, ancient river-channel deposits, and plant and animal fossil assemblages, most dating from Late Pleistocene through mid-Holocene time (~130 to 2 Ka), demonstrate that environmental conditions of the relatively recent past differed markedly from those of historic and late pre-historic time. Detailed discussion of this topic is beyond the scope of this report; but it is very well documented that long intervals of the last glacial (Wisconsinan) stage, and even parts of the Holocene, were significantly wetter and cooler than the present (Metcalf 1967,1969; Gile et al. 1981; Betancourt et al. 1990; Hawley 1993; Harris 1997; Wilkins and Currey 1997; Krider 1998; Connin et al. 1998; Castiglia and Fawcett 2001; Metcalfe et al. 2002). While glacial-pluvial paleoclimatic and associated hydrologic regimes obviously varied depending on basin and range physiographic setting, it is now

clear that cool-season precipitation/runoff increased, evapotranspiration was suppressed, and groundwater recharge was enhanced during much of the recent geologic past. The great importance of the Late Quaternary history of “pluvial“ Lake Palomas in the Bolson de los Muertos to the evolution of the Mesilla Basin groundwater-flow system is discussed in the following section (2.8.4).

2.8.4 Movement

All work to date on the hydrogeologic framework of the Mesilla Basin groundwater-flow system leads to one conclusion: Essentially all groundwater in the basinwide-flow system that is not intercepted by evapotranspiration and pumping must ultimately move to a discharge area in the southernmost part of the inner Mesilla Valley. In terms of large quantity and relatively short residence time, the dynamic part of the groundwater-flow system is in the shallow aquifer zone beneath and adjacent to the valley floor (Frenzel and Kaehler 1992). This is the zone where upper and middle Santa Fe HSUs (USF2/MSF2; LFAs 1,2,3) are well integrated with both valley-fill aquifer (HSU RA; LFA a) and surface-flow systems. Saturated thickness ranges from about 600 ft near Las Cruces to about 250 ft at Cañutillo (Plates 6, 7, 9a; Nickerson and Myers 1993). Compared with *middle* and *lower* Santa Fe HSUs (LFAs 3, 4, 7, 8), upper-zone hydraulic conductivities are high (Tables 2-2, 2-3). The hydrogeologic controls on underlying components of the basinwide flow system are also significant, however; and of special importance are those parts of the deeper flow regime (characterized by long flow paths and travel times) that ultimately discharge to the shallow aquifer zone and surface-flow system in the lower Mesilla Valley (Section 2.8.1).

Paleozoic and Cretaceous carbonate rocks, such as those exposed in most of the basin-boundary uplifts (Plate 1), probably provide conduits for inter-basin groundwater flow in some areas (Sections 2.4, 2.6.3). A temperature log in carbonate rocks at the south end of the East Potrillo uplift (Plate 4, borehole 29.1W.6.410; Snyder 1986) has a distinct isothermic profile segment that indicates significant groundwater circulation at that locality. Similar geothermal

and groundwater-flow conditions occur along much of eastern border zone of the Mesilla Valley (Sections 2.8, 2.9, and 3; Swanberg 1975; Gross and Icerman 1983; Gross 1988; Ross and Witcher 1998; Frenzel and Kaehler 1992, Fig. 47).

The buried bedrock high between the Doña Ana and Tortugas Mountains east of Las Cruces (Section 2.7.1; King et al. 1971; Wilson et al. 1981; Woodward and Myers 1997) restricts, but doesn't block underflow contributions from the Jornada del Muerto Basin (Fig. 2-8a). The same observation can be made concerning the small groundwater inflow through valley fill at the mouth of Selden Canyon near Leasburg Dam. Moreover, while there is 400 to 500 ft of saturated basin fill (mainly HSUs USF2/MSF) at Fillmore Pass between the Organ Cap and Franklin uplifts (Hawley 1984; Orr and White 1985), there is no evidence of any significant outflow from the Mesilla Basin to the Hueco-Tularosa aquifer system. Orr and Risser (1992) assign an underflow contribution of about 260 ac-ft/yr in northern Hueco Bolson groundwater-flow model. Flow at the southern end of the basin near the International Boundary is eastward toward the ultimate discharge zone of the Mesilla Basin groundwater-flow system at the upper end of El Paso Narrows (Wilson et al. 1981).

Slichter (1905) clearly demonstrated that the valley constriction at the International Dam site in El Paso Narrows (Plates 1, 4 and 8e) is an effective barrier to underflow discharge into the upper El Paso Valley. The bedrock-boundary units at the Narrows are Cretaceous and Lower Tertiary rock types that have very low hydraulic conductivities (primarily mudstone, sandstone, limestone and andesite). No zones of enhanced permeability due to limestone dissolution or open-fracture systems have ever been identified. The saturated valley fill (HSU RA) is no more than 75 ft thick, and it is restricted to an inner-valley area that has a maximum width of about 1,000 ft. Hydraulic conductivity also appears to be relatively low (probably in the low to moderate range, Table 2-3), and the hydraulic gradient of both surface and subsurface flow components is about 0.001. Therefore, Slichter's (1905) estimate of about 81 ac-ft/yr (50 gpm, 0.1cfs) of groundwater outflow through the Narrows is probably at the upper limit of potential subsurface discharge to aquifer systems of the western Hueco Bolson.

There is excellent documentation at several sites in the Texas section of the lower Mesilla Valley that an upward groundwater-flow gradient existed in that area prior to development of municipal and industrial wells in intermediate and deep aquifer zones (HSUs MSF2 and LSF). Leggat and others (1962, p. 16, well Q172) reported that the artesian head in the deep aquifer zone in Well JL 49-04-402 (Plate 7; Appendix A, Table 2) was 8 ft above the shallow water table and 1.25 ft above the land surface in 1957. This well site is near Vinton at the east edge of the floodplain (Plate 8d). Another flowing well, the 1,074-ft Lippincott oil test drilled in 1922, produced warm saline water from Cretaceous bedrock that was penetrated below 822 ft (Plates 7 and 9a, Table A2; Leggat et al. 1962-well Q138). Precision temperature logs of USGS-WRD monitoring wells near Cañutillo also record upward-flow gradients in the intermediate and deep aquifer zones at depths greater than about 600 ft below the shallow water table (Nickerson and Myers 1993; Wade and Reiter 1994; Reiter 2001).

Much work still needs to be done with respect to transboundary underflow conditions in the broad Mesilla Basin area between the southeastern uplifts formed by Sierra Juárez and Cerro de Muleros (del Cristo Rey), and the East Potrillo Mountains (Fig. 2-1). Unpublished water-level data from several I,000-ft test wells in the Mexican part of the basin indicate that, at least the shallow part of the groundwater-flow system in HSU MSF2 (mostly LFA 3) is northeastward toward the Santa Teresa area. Current research on the Late Quaternary history of pluvial Lake Palomas (Reeves 1969) by Castiglia and Fawcett (2001) demonstrates that the floor of Bolson de los Muertos, and adjacent parts of the Mimbres, Casas Grandes Santa Maria, and Freznal basins were periodically inundated by very large and deep lakes as late as early to middle Holocene time (8,400 to 6,500 ^{14}C yrs BP). The watershed contributing to these basin systems is about 12,650 mi^2. Elevations of the deep-lake stages are in the 3,900 to 3,965-ft range, or 120 to 185 ft above the potentiometric surface (~3,780 ft) in the Noria to Santa Teresa area about 30 mi (50 km) to the northeast (Plates 1 and 4; Wilson et al. 1981). Therefore, during these Lake Palomas high stands the northeastward gradient of (at least) the shallow part of the groundwater-flow

system would have been about 5 ft/mi. Since the present potentiometric surface in the north-central part of the Bolson de los Muertos is about 3,775 ft (Córdoba et al. 1969, p. 7), there may still be a slight northeast-trending pressure gradient toward the International Boundary area west of Cerro de Muleros (Fig. 2-1).

2.8.5 Storage and Production Potential

The maximum saturated thickness of the Santa Fe Group in the deepest structural subbasins of the Mesilla Basin is about 3,000 ft (Plates 8, 9; Hawley and Lozinsky 1992). As emphasized throughout this report, however, productive aquifer zones are usually restricted to the upper 1,000 ft of saturated basin fill (HSUs RA/USF2/MSF2; LFAs a, 1-3). Buried bedrock highs between the eastern and western structural subbasins may also restrict or "partition" deeper parts of the groundwater-flow system beneath the West Mesa; but head distribution and water quality/temperature changes with depth in that area can (at best) only be inferred until data from deep-piezometer nests are available.

The most productive aquifers in the 1,100-mi^2 Mesilla "groundwater" basin are formed by 1) unconsolidated to weakly indurated basin fill of the *upper* and *middle* Santa Fe HSUs, and 2) overlying Mesilla Valley fill deposited by the Rio Grande (HSU RA). The total saturated thickness of the latter unit rarely exceeds 60 ft; while the *upper* and *middle* Santa Fe units extend from about 600 to 1,600 ft below the water table in the structurally deepest parts of the basin (Plates 2 to 7)**.** Limiting assumptions used in this study for preliminary estimates of available water stored in the basin-fill aquifer system include: 1) the estimated average thickness of the unconfined to semi-confined part of the system is about 200 ft in an inner-basin area of about 1,000 mi^2, 2) specific yield is 0.1, and 3) quality is potable (or fresh, <1,000 mg/L TDS). If these assumptions prove to be valid, then our estimate of available water in storage is about 13 million ac-ft. Based on review of data in the Frenzel and Kaehler (1992) flow model, Balleau (1999, p. 46) estimated that about 14 million ac-ft of available fresh water is stored in the upper 100 ft of saturated fill in the West Mesa area (about 360,000 acres in NM).

The estimated average thickness of fill that is saturated with fresh to slightly saline water is about 1,000 ft in the deepest parts of the basin. Since the areal extent of the deeper Mesilla Basin subbasins is about 750 mi^2, there could be as much as $480x10^6$ ac-ft of saturated, poorly consolidated basin fill in the central and eastern parts of the basin. As noted above, essentially all of the aquifer zones more than 200 ft below the potentiometric surface are confined. So even if an assumed value of 10% for "available porosity" proves to be reasonable, there will always be large variations in our estimates of the amount of recoverable groundwater (e.g., as much as $50x10^6$ ac-ft), given the constraints imposed by technology, economics, socio-political forces, and time itself.

2.9 HYDROGEOLOGIC CONTROLS ON GROUNDWATER SALINITY

2.9.1 Introduction

Hydrogeologic factors that have a significant affect on the chemical and thermal properties of the Mesilla Basin groundwater-flow system are emphasized in this concluding part of Section 2. In the context of the present study, hydrogeologic conditions that influence the large salinity increases observed in the uppermost groundwater-flow system of the lower Mesilla Valley area are of special importance. With our increased understanding the basic hydrogeologic controls on groundwater flow in the Santa Fe Group and Mesilla Valley aquifer systems, we are now in a much better position to identify the major "sources of salinity." These remarks also serve as an introduction to the detailed presentations on Mesilla Basin groundwater geochemistry and Rio Grande Project salt balance in Sections 3 and 4**,** respectively. Moreover, it must be noted that the hydrogeologic interpretations developed during this study phase (including information summarized in Appendix A) support S. K. Anderholm's basic conceptual model of the Mesilla Basin groundwater-geochemical system (*in* Frenzel and Kaehler 1992: C64-C74). The general model developed by Hibbs and others for the geochemical evolution of groundwater in other basins of the southern Rio Grande rift region are also applicable to the Mesilla Basin flow system (e.g., Hibbs 1999; Hibbs et al. 1998, 1999, 2000).

Groundwater evolves geochemically as it moves through the Santa Fe Group and Rio Grande Valley aquifer systems from recharge areas toward its ultimate discharge zone in the southern Mesilla Valley. In the above-cited conceptual models, groundwater in upland areas of active recharge is characterized by fairly low concentrations of dissolved ions, dominantly calcium, magnesium, and bicarbonate. Total-dissolved solid (TDS) concentrations are usually <250 mg/L. TDS content increases as groundwater moves laterally and vertically through bedrock-boundary units and the basin fill toward the Mesilla Valley, particularly along travel paths with a significant geothermal component. In intermediate to distal parts of the flow system, TDS values range from 500 to as much as 5,000 mg/L. A typical basinwide (recharge- to discharge-area) transformation is from calcium-bicarbonate to sodium-bicarbonate, and ultimately to sodium sulfate and/or sodium-chloride-sulfate groundwater. Major hydrochemical and salinization processes active in the basin include: Gypsum dissolution and reprecipitation, cation-exchange involving partly authigenic clay minerals and zeolites (e.g., Na for Ca and Mg), diagenetic alteration of sand and silt grains (e.g., calcite, mica, feldspar, and heavy minerals), some halite dissolution, and evapotranspiration where the water table is at or near the surface. Refer to Section 2.6.6 for information on major Santa Fe Group mineral constituents in the sand- to clay-size range, and to Section 3.4 expanded coverage of the topic of sediment- and rock-water interactions.

2.9.2 Discussion

Groundwater-quality in the shallow-aquifer zone of the basin's Mesilla Valley section (HSUs RA/USF2/MSF2) generally reflects the geochemistry of the well-integrated surface and shallow-subsurface flow system described in Sections 2.8 and 4. Reported TDS values range from about 500 to over 1,000 mg/L. At the extreme southern end of the valley, however, values locally exceed 10,000 mg/L (Appendix A, Tables 1 and 2). With respect to current practices of groundwater-resource development in the eastern Mesilla Basin, groundwater "mining" is of great concern. For example, long-term pumping will ultimately

move inferior quality water toward major drawdown cones and zones of decreased hydrostatic pressure. In many places, natural hydraulic gradients have already been reversed, and effective stresses on confining beds substantially increased. One current result of this process is enhanced downward flow from shallow, high-salinity zones in irrigated areas of the Mesilla Valley. Another involves release of saline porewater and possible land subsidence due to consolidation (compaction) of fine-grained layers and lenses in the upper basin fill sequence (primarily LFA 3).

As documented in preceding discussions and in Section 3, however, there also are deeper components of the groundwater-flow system that can deliver significant quantities of poorer quality (slightly saline to saline) water to almost all aquifer zones in the Mesilla Basin, particularly to aquifers of the lower Mesilla Valley area. These units include not only the *shallow, intermediate (medial),* and *deep aquifers* of Leggat and others (1962), but also shallowly buried, bedrock-boundary units and associated fault zones along the eastern and southwestern basin borders. In intermediate and deep parts of the flow system, much of the spatial variability in quality is related to the distribution patterns of fine-grained confining zones, which are for the most part poorly consolidated. Silty to sandy clays are an important component of LFA 3, and they are the primary constituent of LFAs 9 and 10 (Tables 1-2, 1-3). Basin-fill deposits in the clay-silt range contain large quantities of saline porewater; and their clay-mineral components play a major role in sediment-water chemical reactions (Section 2.6.6)

Water in the *middle* Santa Fe HSU (MSF2) is generally of better quality than in overlying valley-fill and basin-fill units. In the Las Cruces to Mesquite segment of the northeastern Mesilla Basin, however, more uniform quality reflects a well-connected shallow and intermediate flow system with a downward flow gradient (Wilson and White 1984; Nickerson and Myers 1993). Sand strata (LFA2) are a major component of both *middle* and *upper* Santa Fe HSUs in that area, and these units are well connected with overlying parts of the shallow aquifer zone (HSU RA/USF2). As described in Sections 2.7.3 and 2.7.4, the latter

sequence is dominated by medium- to coarse-grained fluvial facies (LFAs a,1 & *2*; Plates 2, 6, 8b, 9a; Appendix A, Table 1).

In the southern part of the Mesilla Basin, where LFA3 is the major HSU MSF2 component, deterioration of groundwater quality is noted at many well sites. Water quality in the *lower* Santa Fe HSU LSF (LFAs 4, 7 & 9) is generally poorer than in the *middle* unit except beneath the Mesilla Valley area between Mesquite and Cañutillo (Plates 3, 4, 7, 8c-e, 9a-c; Appendix A, Tables 1 and 2; Leggat et al. 1962; Wilson et al. 1981). The "historic" upward-flow gradient in the latter area is well documented (Section 2.8.3). The most prominent negative shift in water quality in both intermediate and deep aquifer units occurs across a narrow WNW-trending zone extending from near Cañutillo to the east edge of the "Mid-basin uplift" near the Lanark Test-Well site (Figs. 7, 8b, 9; Plates 1, 3: 27.1.4.121).

In summary, there is an enormous reservoir (probably at least 100 million ac-ft) of slightly to highly saline water stored in and slowly moving through the intermediate to deeper parts of the Mesilla Basin aquifer system. The primary destination of the mobile groundwater component that saturates this system is the inner Mesilla Valley, with the ultimate discharge zone in the lower valley area between Canutillo-La Union and El Paso Narrows. Major salinity sources related to the basinwide groundwater-flow regime include: 1) geothermal waters moving from zones of higher permeability in bedrock-boundary units, 2) release of saline water stored in fine-grained, basin-fill facies, and 3) and general upward and lateral migration of deep-circulating groundwater moving into local discharge zones, primarily along the eastern edge and at the southern end of the Mesilla Valley. Analogous conditions occur at the lower end of the Albuquerque Basin and have been recently well documented by Plummer and others (2000).

3.0 GROUNDWATER CHEMISTRY AND SALINITY

3.1 INTRODUCTION

Groundwater salinity in the Mesilla Basin is investigated with geochemical and geothermic approaches. Groundwater flow domains and aquifers are characterized by several distinct physical and geochemical processes that may allow fingerprinting of the salinity sources and mechanisms (Stuyfrzand 1999). Salinity can involve the flow path length or age of water since recharge, climate and geographic area of recharge, and the type of rocks that host water flow and react chemically with the water. The processes of cation exchange, hydration reactions, mixing, dissolution, precipitation, and evaporation or evapotranspiration can all play roles.

Temperature gradients can be a measure of basin hydrodynamics and may be used to distinguish and even quantify upward or downward groundwater flow (Reiter 1999 and 2001; Wade and Reiter 1994a and 1994b). Mass and energy analysis of terrestrial heat flow anomalies over a geothermal system in the Mesilla Basin can define the vertical water flux or minimum volumetric discharge of saline waters into shallow basin aquifers (Yeamans 1983).

Geochemical fingerprints comprise two general categories. The first involves the mapping of the ratios of conservative ions such as chloride (Cl), boron (B), bromide (Br), and lithium (Li). These ions are highly soluble or conservative and are, therefore, unlikely to be involved in precipitation of minerals and can be applied to study mixing, evaporative concentration, and dissolution of salts (Hem 1985).

A second category involves the isotopic characteristics of the water and dissolved chemical constituents. Isotopic information is useful to characterize recharge source and paleoclimate, age since recharge, and the type of rock that hosts water flow (Mazor 1997). Isotopic signatures, in conjunction with conservative dissolved ions, can also be used to investigate mixing of waters with different flow domain heritage or to delineate other salinity processes such as evaporation.

Aqueous geochemical models to define chemical and isotopic equilibrium or saturation indices with solid mineral phases provide additional interpretative tools to characterize salinity evolution and sources (Bethke 1996). This approach is not detailed in this report.

Several isotopic classes are applied to map groundwater salinity evolution and sources. The use of multiple isotopic systems, combined with solute chemistry, allows cross checking of results and interpretations.

The first and most commonly used system uses fractionation ratios of natural stable isotopes such as oxygen ($^{18}O/^{16}O$), hydrogen ($^{2}H/H$), carbon ($^{13}C/^{12}C$), and sulfur ($^{34}S/^{32}S$) (Clark and Fritz 1997). Recharge source and timing, temperature, rock-water reactions, organic processes, and evaporation can have an important impact on these ratios. In addition, the sulfur and carbon isotopes may point to specific geologic formations as salinity sources.

The second isotopic approach uses radiogenic stable-daughter isotope ratios such as the strontium (Sr) system of $^{87}Sr/^{86}Sr$ (Banner et al. 1989; Johnson and DePaolo 1994). The Sr system is useful to fingerprint the flow path and type of rock that the groundwater has predominantly encountered. The Sr isotope systematics can provide a proxy for the ultimate source(s) of calcium (Ca) and potassium (K) in mixed saline waters.

The third isotopic class of systems involves isotopes that preferentially accumulate in groundwater compared to other isotopes of the same element such as ^{234}U compared to ^{238}U (Gross and Cochran 1984; Banner et al. 1990). The uranium (U) isotopic disequilibrium ratio is useful to describe flow paths and mixing, and to fingerprint aquifers.

Available and reported groundwater chemistry, including geothermal waters, were compiled into a digital database (see Appendix B). An initial evaluation of this database, in conjunction with available subsurface information, was used to provide a preliminary interpretation of geochemical processes in shallow aquifers less than 400 ft deep. Delineation of geochemical processes combines the concepts of regional and local flow domains, hydrostratigraphy, water levels, and water chemistry and temperature (Hawley and Lozinsky 1992;

Toth 1963; and Stuyfrzand 1999). Geochemical interpretations rely on recent and ongoing hydrostratigraphic studies in the basin and other published hydrogeologic data and models (Hawley and Lozinsky 1992; Wilson et al. 1981; Leggat et al. 1962; Frenzel and Kaehler 1992; Stickel 1991).

Primary sampling sites were selected from wells with apparent production from representative end member hydrogeochemical facies and with documented well construction and suitable screened intervals. Less documented wells were used as secondary sampling sites to provide additional information.

Thirty-six samples were taken from a range of hydrogeologic settings in the Mesilla Basin. In addition to field sample filtering and preservation, the pH, conductance, and temperature were measured in the field. Analysis of dissolved ions includes:

Na, Ca, Mg, Sr, K, HCO^3, SO^4, Cl, SiO^2, Br, Li, B, U, Fe, F, TDS, and Mn

Samples taken for chemistry were also isotopically analyized for:

$^{18}O/^{16}O$, $^{2}H/H$, $^{13}C/^{12}C$, $^{34}S/^{32}S$, $^{87}Sr/^{86}Sr$, and, $^{234}U/^{238}U$.

Charge and mass balance were used to evaluate the quality of the results from sampled fluids and on analyses obtained from available databases and literature (Reed and Mariner 1991). Collection methods and preservation of samples were carefully coordinated with analytical laboratories.

An integrated approach of traditional solute chemistry and isotopic systematics was employed. Water temperature and hydrogeologic information complement geochemical and isotopic interpretations. Data interpretation focuses on sources, mixing, and relative contributions of geochemical processes to groundwater and surface water salt balance.

Temperature gradients, well production temperature, and heat flow information are used to further evaluate basin hydrodynamics (Reiter 1999). Because of the availability of much high quality temperature gradient information in the area, heat loss mapping above the water table allows a rough calculation of the minimum volumetric influx of upwelling saline geothermal water in selected areas (Icerman and Lohse 1983; Snyder 1986; Witcher unpublished temperature log files).

Primary results of this study include the identification of the groundwater sources of salinity and the delineation of the processes involved in salinity contributions such as dissolution, evaporation and evapotranspiration, and mixing. A preliminary relative ranking of groundwater salt fluxes and sources is discussed.

3.2 PREVIOUS STUDIES

To date, reconnaissance geochemical studies in the Mesilla Basin aquifers have focused upon the shallow aquifers because most water usage is from this domain (Bexfield and Anderholm 1997; Frenzel and Kaehler 1992; Peterson et al. 1984; Wilkins 1998; Wilson et al. 1981; Wilson and White 1984). The studies identify the distribution of salinity both areally and vertically within the Mesilla Basin, but not the sources or processes of the salinity with detail.

3.3 METHODS

Sampling was accomplished after allowing the installed pump to operate for at least 15 minutes. A 5-gallon (19.2 liter) plastic pail (well rinsed with the sample water) was used to take a grab sample. Temperature was determined using a digital thermometer. Aliquots were taken for pH determination with an Oakton pH 10 series meter, and conductivity using an Oakton Con5 Acorn series meter. Alkalinity was determined using a Hach digital titrator. A 50 mL sample was pipetted into a beaker with a stirring bar and placed on a portable, "homemade" battery-operated magnetic stirrer. A pre-measured packet of Bromcresol Green-Methyl red reagent was added and the solution was titrated with 0.1600N H_2SO_4 until the color changed to pink. The acid titrated times 2 gave a direct reading of mg/L as $CaCO_3$ total alkalinity. Eight water samples were collected for laboratory analysis. The D/H and $^{18}O/^{16}O$ sample was collected in amber glass bottles with septum caps, rinsed with sample water. All other samples were collected in high-density polyethylene bottles, which were washed with soap, then rinsed with tap water to remove the soap, and finally rinsed three times with distilled/deionized water. The last rinse was left in the bottles and emptied just prior to sampling. After the preceding wash and rinse, the $^{87}Sr/^{86}Sr$

sample bottles were placed in a 10% nitric acid bath for a minimum of 24 hours, followed by three additional rinses with distilled/deionized water. Filtration was accomplished on site with a 0.45 micron filter and vacuum flask. A “homemade” vacuum pump, constructed from a small marine bladder pump with cigarette lighter power supply, was connected to the vacuum flask for rapid and efficient filtering. Table 3-1 shows the amounts and treatments of the samples collected.

TABLE 3-1. Field Sample Preparation

SAMPLE	AMOUNT	FILTERED	TREATMENT
Anions	250 mL	Yes	None
Cations	250 mL	Yes	Acidified to pH < 2 with HCl
D/H and $^{18}O/^{16}O$	60 mL	No	None
$^{13}C/^{12}C$	250 mL	No	Sodium azide
$^{34}S/^{32}S$ sulfate	1L	Yes	BaCl w/ $BaSO_4$ precipitate filtrate
$^{87}Sr/^{86}Sr$	250 mL	Yes	Acidified to pH< 2 with ultra-pure H_2NO_3
$^{234}U/^{238}U$	1 L	Yes	Acidified to pH < 2 with H_2NO_3

3.4 GEOCHEMISTRY OF BASIN FILL AQUIFERS

3.4.1 Background

Section 3.4 provides a preliminary study on possible mixing and sources of anions and cations commonly associated with most classes of salinity and with some of the major constituents commonly associated with outflow from upwelling geothermal waters that may be entering the shallow basin aquifers and mixing with non-thermal water.

Dissolution of evaporite minerals no doubt occurs in the Mesilla Basin groundwater system. Dissolution of gypsum ($CaSO_4:2H_2O$) will add SO_4 and Ca to groundwater. However, an increase in calcium (Ca) can saturate the waters and result in precipitation of calcite ($CaCO_3$). With precipitation, the ratio of Ca to SO_4 and HCO_3 ($mCa/mSO_4 + mHCO_3$) changes due to the precipitation of calcite. The reaction $2Ca^{++} + SO_4^{++} + HCO_3^{-} = CaCO^0_3 + Ca^{++} + SO_4^{++} + H^{+}$ describes the process. Intragranular calcite cements are common in the basin

sands and gravels. Dissolution of halite (NaCl) will add Na and Cl to solution in a one to one fashion.

After dissolution of evaporite minerals, ion exchange may be a very important process for buffering Ca and Na concentrations in Mesilla Basin aquifers. Because of ionic charge balance considerations, one mole decrease in Ca would be balanced by two moles increase in Na.

Cations (Na, K, Ca, Mg) and silica (SiO_2) may also be contributed by irreversible weathering reactions of silicate minerals such as feldspars and amphiboles. High SiO_2, Na and Cl, along with high minor ionic contributions of potassium (K), lithium (Li), boron (B), and fluoride (F), are typically associated with geothermal waters.

3.4.2 Shallow Aquifers

Published data detailed by this report are mostly located within the inner Mesilla Valley or flood plain. Discussion of published data concentrates on wells and screened intervals that are less than 400 ft depth. Aquifers geochemically characterized from this interval include the post entrenchment Rio Grande fluvial deposits and adjacent arroyo drainage, the basal Camp Rice Formation, and the uppermost fine- to coarse-grained sediments of the middle Santa Fe Group (HSUs RA, USF2, and upper MSF2; Sections 2.6.3, 2.7.2-3). Data are from the U. S. Geological Survey (USGS) digital database of water quality (http://waterdata.usgs.gov/nwis/qwdata).

Piper diagrams (Piper 1944) provide an initial graphic display of geochemical data for the Mesilla Basin. A Piper diagram shows major cation and anions in terms of millequivalent percentages on respective cation and anion trilinear plots (Figs. 3-1 to 3-4). The anion and cation percentages are projected from the respective triangle plots on to a central diamond plot. As a whole, the Piper diagram allows immediate recognition of chemical type and some basic processes that may be occurring such as mixing, dissolution of evaporate minerals, and cation exchange between water and clay or silicate minerals. Figure 3-1 shows the general chemical quality definitions followed in this report.

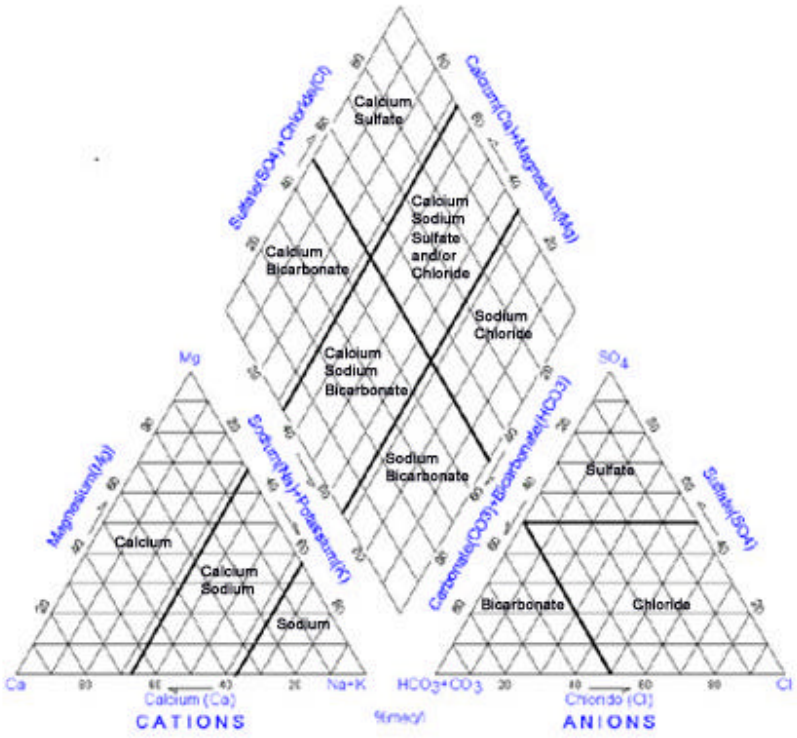

Figure 3-1. Piper diagram showing the water chemistry classification scheme used in Chapter 3

Because magnesium (Mg) and K are not major constituents in Mesilla Basin waters, the labeling scheme of water quality type shown in the diamond portion of the Piper diagram does not make use of Mg and K.

Figure 3-2 shows published water chemistry for wells with production or screened intervals less than 400 ft depth (USGS 2000, Water Quality Data, URL http://waterdata.usgs.gov/nwis/qwdata). The crosses represent water chemistry from wells 200 ft depth or less and the dots or solid circles represent water chemistry from wells between 200 and 400 ft depth. The dominant water types in order of importance include calcium-sodium-sulfate, sodium-sulfate, calcium-sulfate, and sodium-bicarbonate. Three of the four water types are dominated by sulfate (SO_4). Shallow wells less than 200 ft depth have the highest SO_4 percentages. Inspection of the anion and cation triangles of the Piper diagram

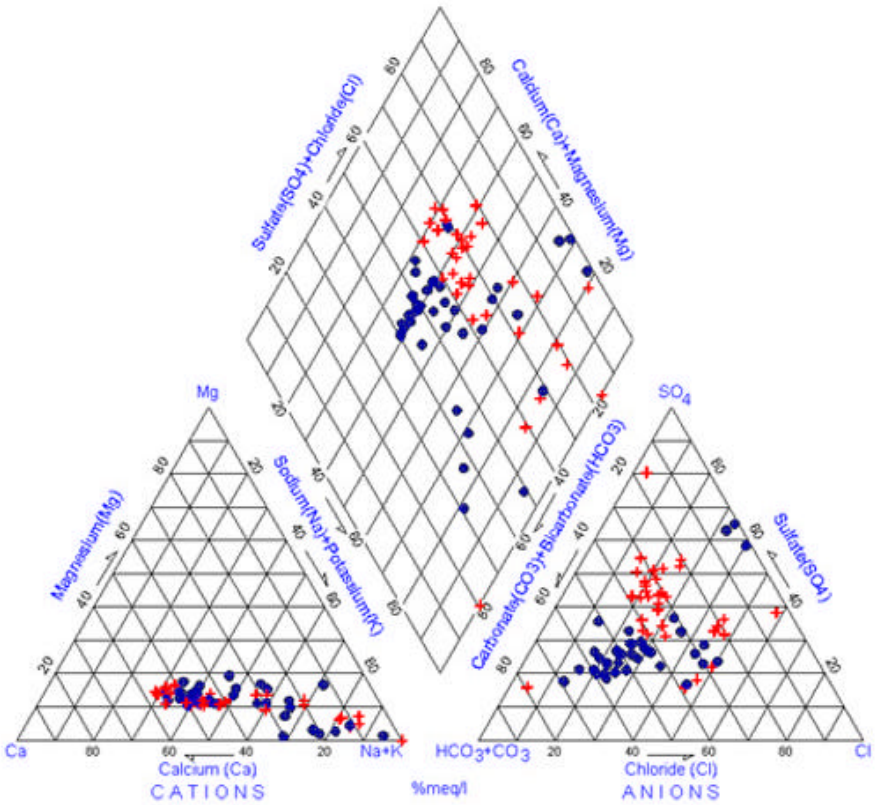

Figure 3-2. Piper diagram showing water chemistry for water produced from less than 400 ft depth in the Mesilla Basin. Cross symbols are for chemistry of water from less than 200 ft depth. Solid circles represent water chemistry between 200 and 400 ft depth.

shows two separate trends. The 200 to 400 ft water trends toward the bicarbonate ($HCO_3 + CO_3$) apex and the sodium (Na + K) apex and suggests that calcite and feldspar dissolution and possibly cation exchange is occurring. On the other hand, the 200 ft or less depth water shows a trend toward the sulfate (SO_4) apex and the sodium (Na + K) apex, indicating that gypsum ($CaSO_4{:}2H_2O$) dissolution and cation exchange is occurring. Scatter of the data percentages toward the chloride apex (Cl) may indicate concurrent dissolution of halite (NaCl) or mixing of more saline water with fresh water.

For comparison, Figure 3-3 is a Piper diagram showing published water chemistry for wells producing from screened intervals greater than 900 ft depth. The dominant water types in order of importance are sodium-sulfate, sodium-

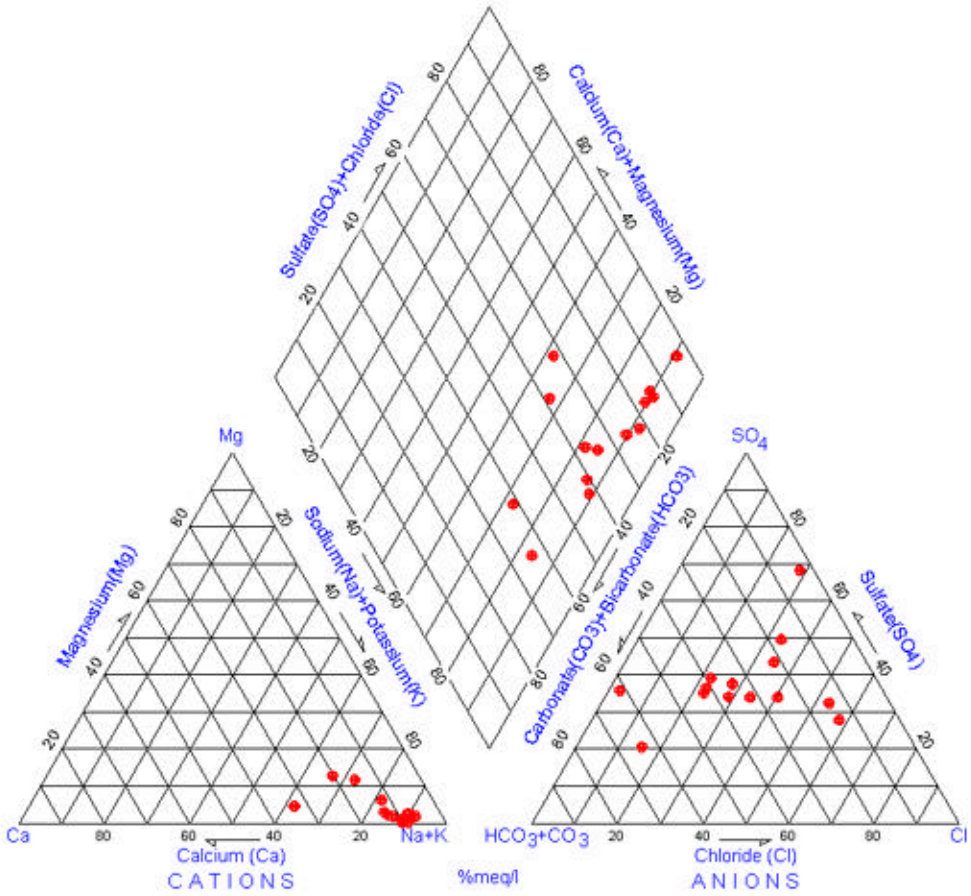

Figure 3-3. Piper diagram showing water chemistry for water produced from depths greater than 900 ft in the Mesilla Basin.

chloride-sulfate, sodium-bicarbonate, and calcium-sodium-sulfate. No dominant diagnostic trend is evident. However, mixing with deep, upwelling geothermal waters may be indicated, along with cation exchange.

Figure 3-4 is a Piper diagram of anion and cation chemistry for water samples collected for isotopic analysis. This data set contains several thermal or geothermal waters. The thermal waters (temperature greater than 26^{o} C) are almost all sodium-chloride-sulfate composition. Figure 3-5 is a map of the Mesilla Basin showing general water quality types for water sampled for isotope analysis.

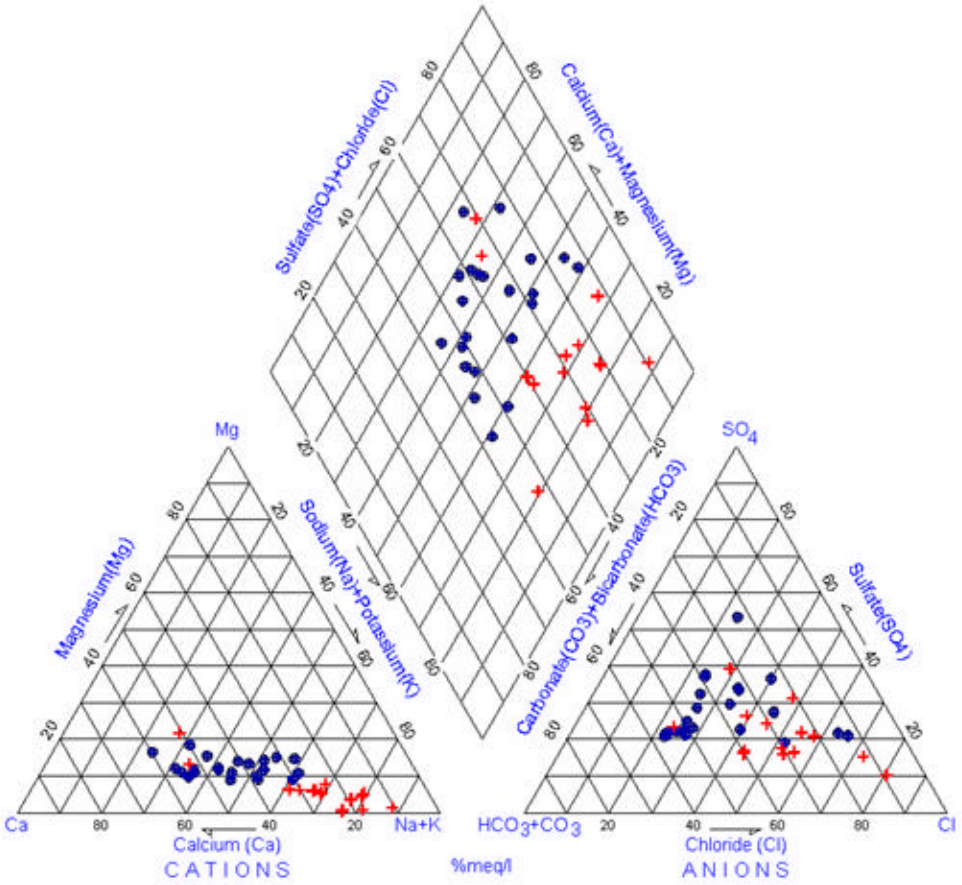

Figure 3-4. Piper diagram showing water chemistry of water samples collected for isotopic analysis in this study. Thermal waters (>26^{o} C) are shown with cross symbols. Non-thermal waters are shown with solid circles.

Swanberg (1975) noted that Mesilla Basin geothermal waters are characterized by high Cl, SiO_2, and K concentrations. The Mesilla Basin has waters with high K and two general trends are apparent when K data is plotted versus Cl data. Anderholm (in Frenzel and Kaehler 1992) suggested that two geothermal end member waters may be mixing with non-thermal water. Our data analysis for aquifers less than 400 ft deep shows the same pattern (Fig. 3-6). A

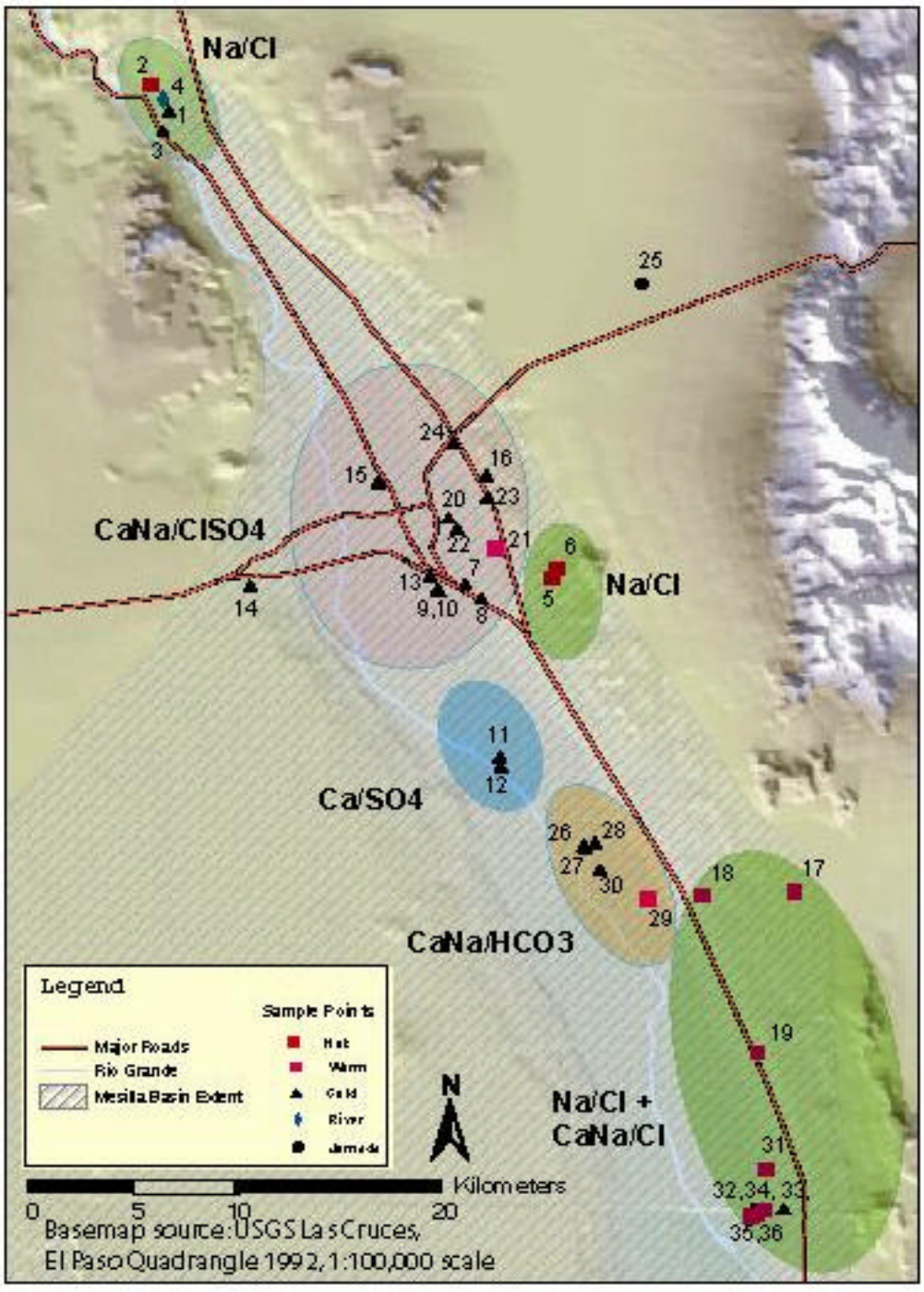

Figure 3-5. Map of the Mesilla Basin showing general types of water chemistry from wells sampled for isotopic analysis in this study

plot of moles per liter (molal) K versus molal Cl shows two general trends. An apparent trend with a shallow slope is associated with higher end member Cl and with abnormally warm temperatures at higher Cl concentrations. This shallow slope trend appears to indicate mixing of thermal and non-thermal water. The trend associated with the higher slope is associated with non-thermal waters. Because K, Cl, and Na can be rather conservative, except for ion exchange for the cations, a plot of molal Na and molal Cl was constructed (Fig. 3-7). As with K versus Cl, two general trends are noted with Na versus Cl; and the lower slope trend contains thermal water with high Cl. Because none of the trends has a slope of one, a simple model of salt or halite dissolution is not adequate to explain the Na (or K) versus Cl ratios.

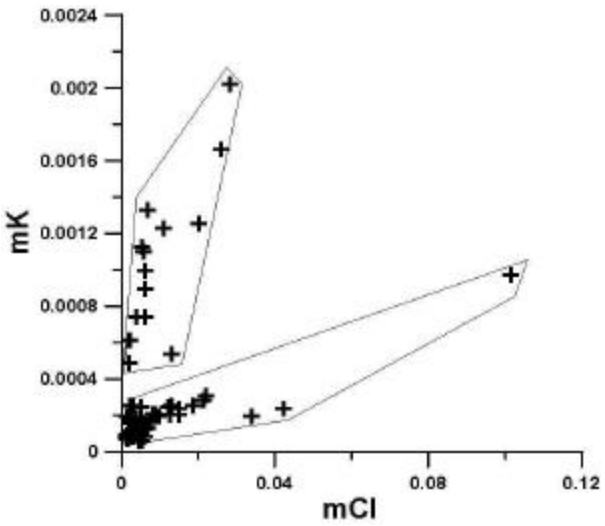

Figure 3-6. Molal concentrations of potassium (K) versus chloride (Cl) from wells less than 400 ft depth in the Mesilla Basin.

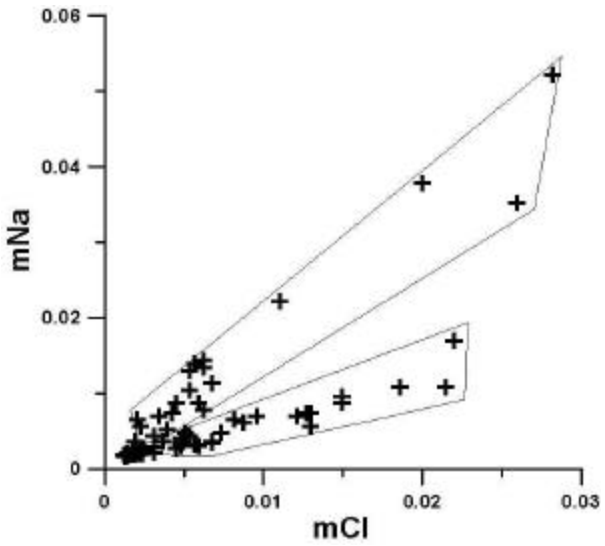

Figure 3-7. Molal concentrations of sodium (Na) versus chloride (Cl) from wells less than 400 ft depth

Figure 3-8 is a plot of molal K concentration versus location north to south (latitude) in the Mesilla Basin (Plates 6, 7, 9a). It is clear that most of the shallow (less than 400 ft depth) data are derived from around the Las Cruces area. However, two general patterns of K concentration are readily discerned. Most waters are clustered at low concentrations regardless of location. On the other hand, a wide range of high concentrations is noted in the Las Cruces area. The fact that this is only observed in the Las Cruces area may only represent a bias in the availability of data with complete major anion and cation analysis. However, the highest K concentrations are largely represented in the steep slope trend of Figure 3-6 and in Na/Cl ratios greater than one (see Fig. 3-7). The highest K data are from non-thermal water. Figure 3-9 shows a plot of depth to the top of the sampling (screened) interval versus K concentration. The low concentration cluster of K in Figure 3-8 is found at all depths in the upper 400 ft aquifers of the basin. While high concentrations of K occur at all depths, higher concentrations are more often observed at shallower depth. The lower K concentration field contains the bulk of the Na/Cl ratios less than one. High molal Na/Cl ratios are all associated with high K concentrations. Figure 3-10, a plot of K concentration as milligrams per liter (mg/L) versus temperature (^{o}C), confirms

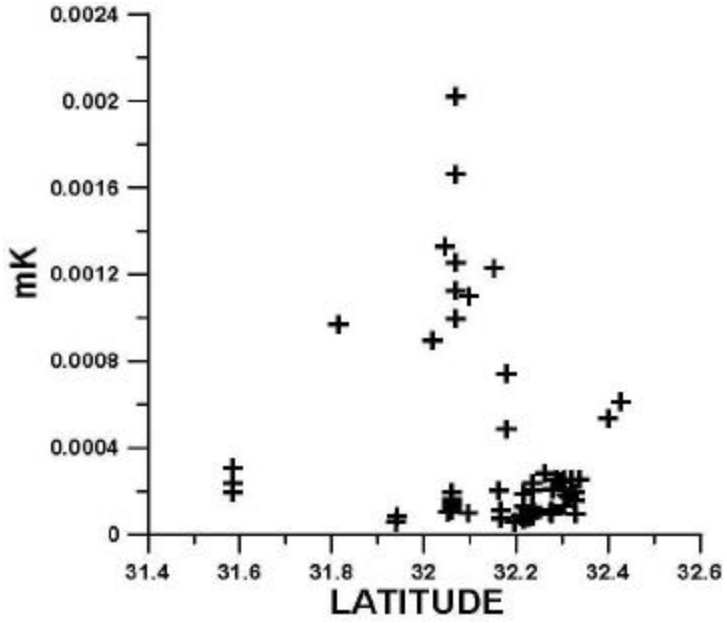

Figure 3-8. Molal concentration of potassium (K) versus latitude from wells less than 400 ft depth

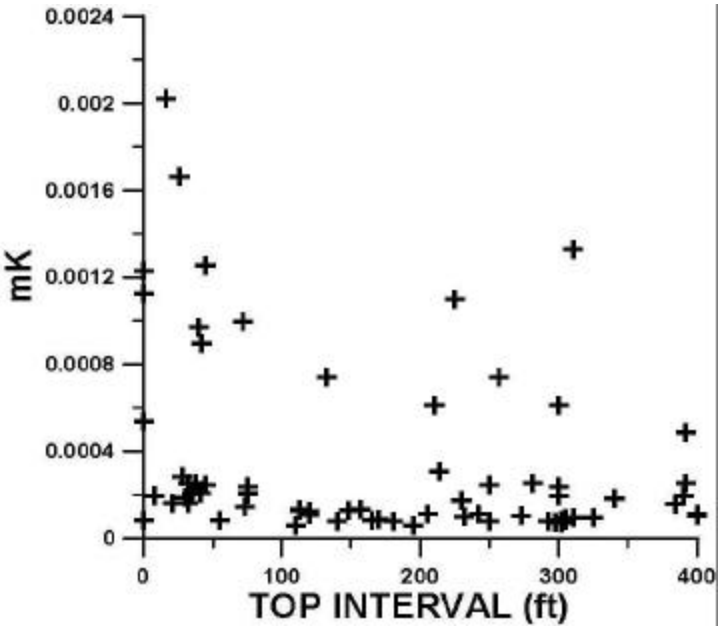

Figure 3-9. Molal concentration of potassium (K) versus feet to top of screened interval in wells less than 400 ft depth

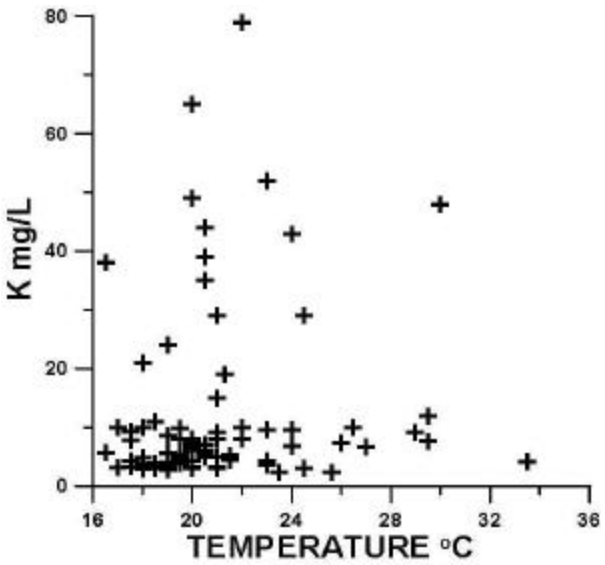

Figure 3-10. Molal concentration of potassium (K) versus temperature (^{o} C) from wells less than 400 ft depth.

that thermal (>26^{o} C) waters in aquifers less than 400 ft deep generally show no elevated K concentration. The highest K waters are not thermal. However, mixing and conductive heat loss could account for this apparent discrepancy. Apparently, important non-thermal processes are occurring to produce some of the "geothermal" constituents of Anderholm (in Frenzel and Kaehler 1992) and Swanberg (1975).

Silica (SiO_2) concentrations are temperature dependent and may indicate geothermal waters and mixtures of geothermal and non-thermal waters (Fournier 1960, 1977). With this preamble, a plot of SiO_2 versus K should show a trend. If SiO_2 is used as a proxy to temperature, this could point to geothermal water that has been conductively cooled. Figure 3-11 shows that a correlation between increasing SiO_2 and rising K concentrations does occur. On the other hand, SiO_2 shows no temperature dependency (Fig. 3-12). This may be reconciled by the slow kinetics of SiO_2 equilibrium at lower temperatures (Rimstidt and Barnes 1980). In other words, high SiO_2 concentrations are retained at low temperatures for long periods of time. Possibly more important, another process may best explain the correlation of higher SiO_2 and higher K.

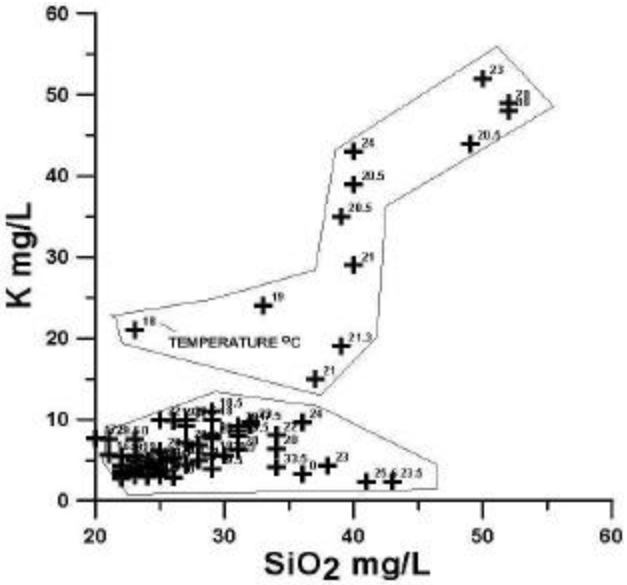

Figure 3-11. Dissolved potassium (K) versus dissolved silica (SiO_2) in wells less than 400 ft depth. Concentrations are in mg/L and point labels are measured temperature (^{o} C).

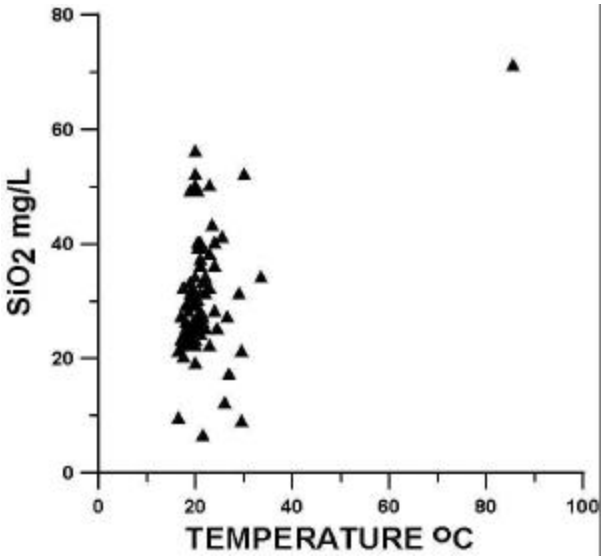

Figure 3-12. Dissolved silica (SiO_2) versus temperature (^{o} C) from wells less than 400 ft depth. Silica concentration is in mg/L.

Dissolution of aluminosilicate minerals such as potassium feldspar (orthoclase or sanadine) can release K and SiO_2 to solution and result in higher alkalinity or bicarbonate (HCO_3) concentrations. Feldspar-rich (arkosic) sands are common in the upper aquifer, especially in the Camp Rice Formation (HSU USF2, Section 2.6.4). Figure 3-13 is a comparison of HCO_3 concentration and dissolved SiO_2. A trend of higher SiO_2 with a correlative higher HCO_3 is observed. This suggests that higher SiO_2 is the result of low-temperature irreversible feldspar dissolution processes and not temperature dependent SiO_2 derived from geothermal processes. Figures 3-14 and 3-15 graphically represent bicarbonate versus K and Na, respectively, and also show apparent trends in concert with irreversible dissolution of aluminosilicate minerals. Figure 3-16 is a plot of SiO_2 versus Cl, and shows two patterns. A cluster of low Cl waters shows a wide range of SiO_2 from low to high concentration. However, waters with high Cl (>400 mg/L) tend to show a general trend of simultaneously increasing SiO_2 and Cl that is more typical of conductively-cooled or mixtures of geothermal fluids.

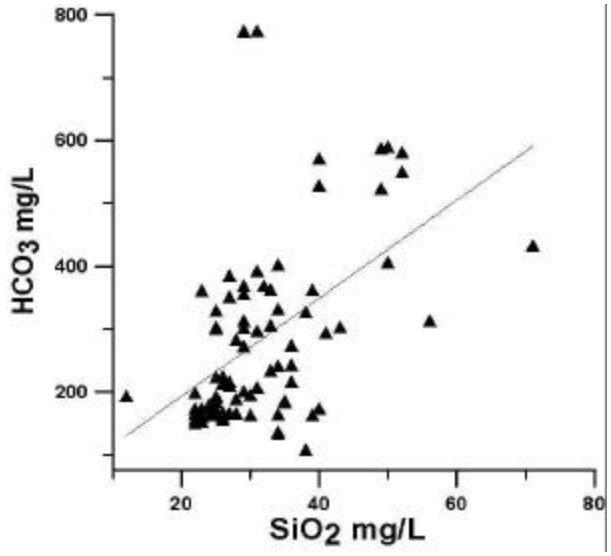

Figure 3-13. Dissolved bicarbonate (HCO_3) versus dissolved silica (SiO_2) in wells less than 400 ft depth. Concentrations are in mg/L.

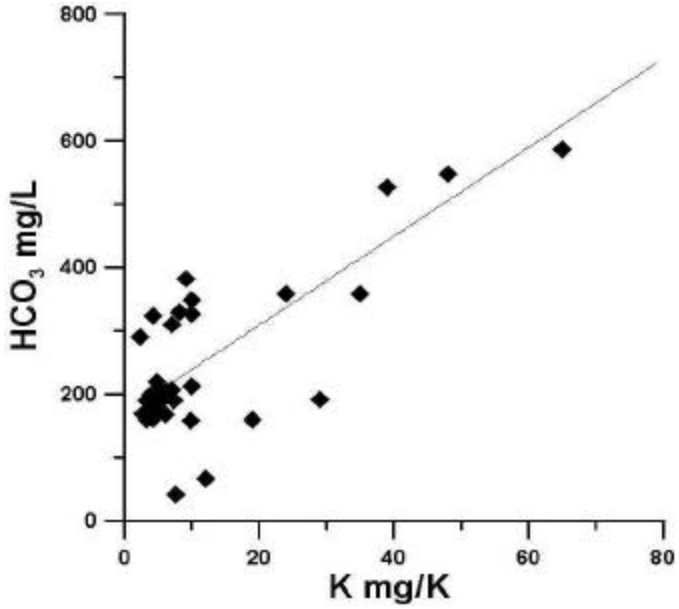

Figure 3-14. Dissolved bicarbonate (HCO_3) versus potassium (K) in wells less than 400 ft depth. Concentrations are in mg/L.

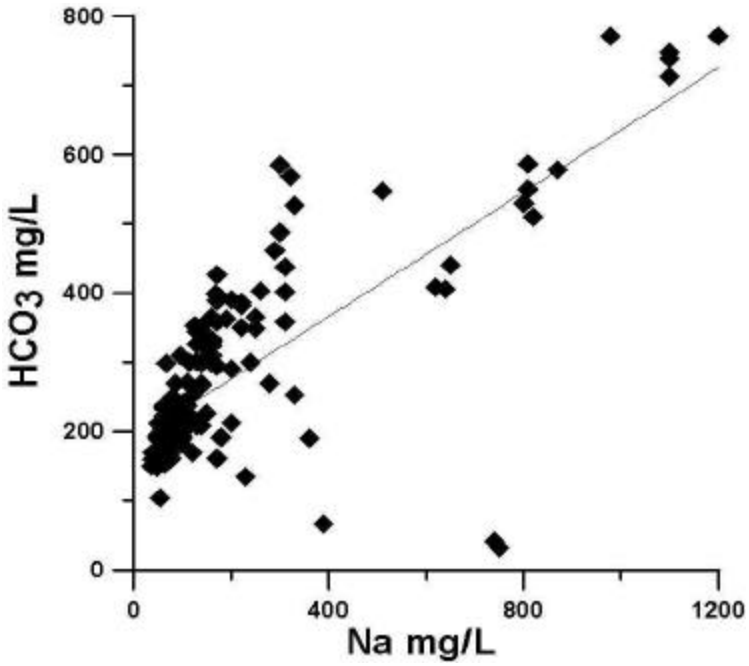

Figure 3-15. Dissolved bicarbonate (HCO_3) versus sodium (Na) in wells less than 400 ft depth. Concentrations are mg/L.

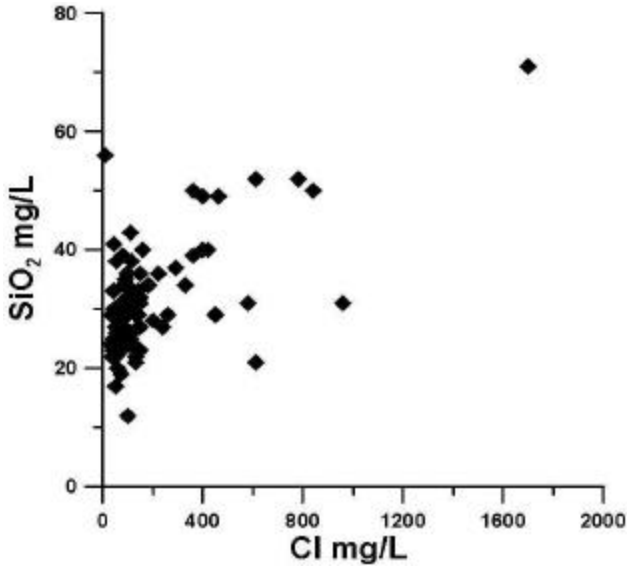

Figure 3-16. Dissolved silica (SiO_2) versus dissolved chloride (Cl) in wells less than 400 ft depth. Concentrations are mg/L.

Another view of salinity in the upper 400 ft of Mesilla Basin aquifers is gained by observing constituents commonly observed with dissolution and precipitation of mineral phases such as gypsum ($CaSO_4{:}2H_2O$), calcite ($CaCO_3$), and halite (NaCl). These are primary mineral sources of salinity in the subsurface rock units of the area (Sections 2.4, 2.6.1). Figure 3-17 is a plot of SO_4 versus Cl in mg/L concentration units. Three patterns of occurrence are noted. Most data cluster in a trend of rapidly increasing SO_4 at lower Cl concentration with only a slight increase in Cl at lower Cl concentrations. Waters with the highest SO_4 in this first trend show elevated temperature. A rapid increase in Cl with increasing SO_4 is observed in the second trend. This trend is also anchored by thermal water at the upper end. A third trend shows increasing SO_4 with no or very little increase in Cl at about 800 mg/L Cl. These waters are non-thermal and come mostly from wells or screened intervals at depths less than 100 ft. The group with high Cl (>1500 mg/L) and SO_4 less than 400 mg/L is from the Radium Springs geothermal area and represent geothermal waters.

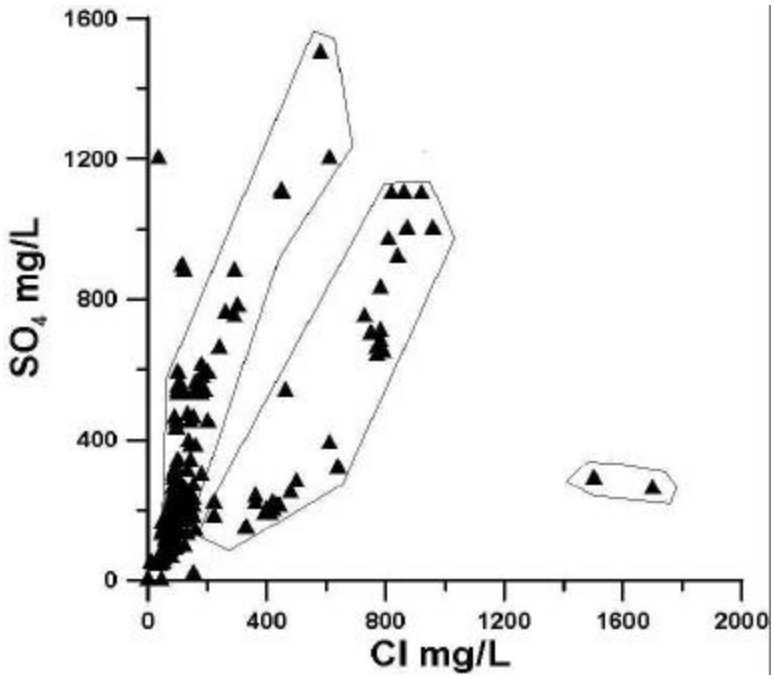

Figure 3-17. Dissolved sulfate (SO_4) versus dissolved chloride (Cl) in wells less than 400 ft depth. Concentrations are mg/L.

3.4.3 Bromide and Chloride/Bromide Ratio

Typically Cl acts as the most conservative major ion in groundwater and is not directly involved in most chemical reactions except for the dissolution of soluble minerals that are contained in evaporite rocks such as halite. Therefore, where evaporites are absent, Cl variation is largely the result of mixing of young low TDS waters and older thermal waters. Bromide (Br) acts much like Cl in solution, however, Br is considerably less abundant in natural groundwaters. In addition, Br is very conservative and even more soluble than Cl (Davis et al. 1998).

The Cl/Br ratio is sensitive to mineral and chemical sources or provenance. The Cl/Br ratio is very low in most natural systems like seawater (290), meteoric water (50-180), organic materials (20-200), and igneous and metamorphic rocks (100-500) (Davis et al. 1998). Higher Cl/Br ratios are generally associated with anthropogenic sources such as road salt, sewage, industrial chemicals or waste, agriculture processes, and with the natural dissolution of evaporite minerals or release of salts in mineral fluid inclusions during water-rock equilibration.

High Cl/Br ratios in evaporites are a result of the differential solubility between Br and Cl. Since Br is much more soluble than Cl, halite forms as nearly pure NaCl crystal with Br remaining in the brine. Dissolution and re-precipitation results in even higher Cl/Br ratios in the solid precipitate (Davis et al. 1998; Hounslow 1995; Hanor 1988, 1994).

Generally high Cl/Br ratios (349 – 661) in non-thermal groundwater in the Mesilla Basin may be the result of dissolution of evaporite minerals contained in the basin deposits or mixing with geothermal waters. Thermal groundwater generally has even higher Cl/Br ratios between 800 and 1361. The high Cl/Br ratios relate to geochemical processes along deep regional flow paths, in which water typically progresses from HCO_3 through SO_4 to Cl in anion character with increasing depth and flow path (Toth 1999; Mazor 1997). Processes may include dissolution of evaporate minerals from Paleozoic marine rocks. The large differences in Cl/Br between non-thermal and thermal water can be used to finger print local and intermediate flow paths from regional flow paths of geothermal waters and to identify mixing zones of groundwater flow domains.

When the Cl/Br ratios are plotted against Br, two separate linear trends are noted (Fig. 3-18). Bromide concentrations range from a low of 0.089 mg/L in non-thermal water to a high of 1.20 mg/L in thermal water. The shallow slope trend is anchored by thermal water and probably represents mixing of thermal and non-thermal water. The steep slope and nearly vertical trend may represent evaporation where Br increases in soil water and shallow aquifers at a greater rate than Cl. The nearly vertical trend is characterized by non-thermal water and shows increasing Cl concurrent with increasing Br even though the Cl/Br ratio remains roughly the same.

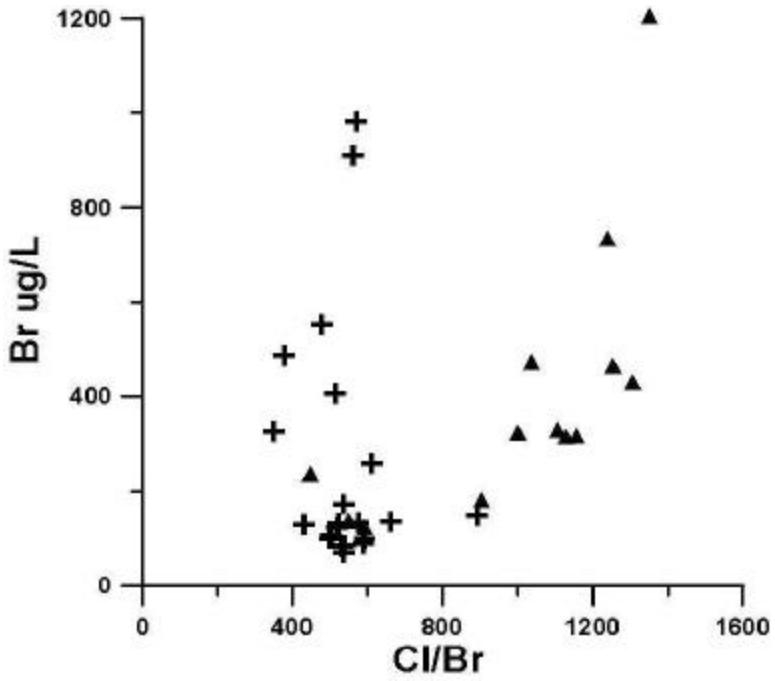

Figure 3-18. Bromide (Br) versus the Cl/Br. Solid triangles are thermal (>26^{o} C) waters and crosses are non-thermal-waters. Concentrations are ug/L.

3.5 ISOTOPE SYSTEMATICS

3.5.1 Introduction

Isotopic systems analysis helps to identify sources and processes associated with water chemistry and salinity. Isotopic data analyzed are almost entirely from the inner Mesilla Valley or flood plain; however, several geothermal wells on the east margin of the basin are included. Waters geochemically characterized from this interval include many water supply wells from the cities of Las Cruces and Anthony (NM) and Anthony (TX) and wells from the Mesquite Water Association. Locations for samples taken for isotopic analysis are shown in Figure 3-19. Appendix B provides tables with detailed location data, isotopic results, and completed cation and anion chemistry. For ease of discussion delta (δ) notation is used with isotopes. Delta (δ) is the per thousand (per mil) comparison of the ratio of heavy to light isotopes in a sample compared to a standard. Appendix B details the nomenclature used for reporting isotope analysis.

3.5.2 Hydrogen and Oxygen (δD and $\delta^{18}O$)

The stable isotopes of hydrogen (^{1}H) and deuterium (^{2}H), and oxygen (^{16}O and ^{18}O) are the most common isotopes in water (H_2O). In water, the light isotopes of hydrogen (^{1}H) and oxygen (^{16}O) comprise more than 99% of a water molecule, while the heavier isotopes comprise less than 1%. Because atomic mass is almost entirely protons and neutrons, addition of a neutron in a hydrogen (^{1}H) nucleus to form deuterium (^{2}H or D) practically doubles the mass. Addition of two neutrons to form ^{18}O increases the oxygen atomic mass by approximately 12.5%. Isotopic mass differences are significant enough to cause different chemical and physical reaction rates and allow measurable fractionation or separation of heavy and light water. For instance, the hydrologic cycle fractionates light and heavy water during evaporation and condensation. Lighter water evaporates more easily and heavy water condenses more readily (Faure 1986; Clark and Fritz 1997; Gat 1996; Mazor 1997). Enrichment of the heavy

isotope with respect to the standard is indicated by positive values of δD and $\delta^{18}O$, and depletion of the heavy isotope is noted by negative values.

Relative enrichment and depletion of isotope ratios in water can be characterized by plotting δD versus $\delta^{18}O$ (Fig. 3-20). Based on a large number of stable isotope analyses of precipitation from around the world, Craig (1961) found a systematic worldwide variation that described a sloping line or Global Meteoric Water Line. This line is quantified by the equation: $\delta D = 8\ \delta^{18}O + 10$. The intercept (10) is referred to as deuterium excess. Dansgaard (1964) found that temperature was a major determining factor in precipitation (meteoric water) isotope depletion. Other important factors include: 1) altitude, 2) storm duration, 3) a continental effect, 4) a seasonal effect, and 5) a paleoclimate effect (Fontes 1980). Higher altitudes and continental interiors receive isotopically lighter precipitation. In general, winter precipitation is isotopically lighter than in summer and longer storm events result in relatively lighter isotopic precipitation. Cooler paleoclimatic conditions also result in isotopically lighter meteoric water.

When local and regional meteoric water lines are constructed, the slopes are generally near 8 with variable δD intercepts or deuterium excess. Two processes can cause isotope values to plot to the right of the meteoric water line. With evaporation, residual waters attain heavier isotopic composition due to preferential evaporation of lighter molecules. Normally, residual waters plot as an “evaporation line” with a slope between two and five (Clark and Fritz 1997). Second, “old” groundwater and geothermal waters will gain heavy oxygen (^{18}O) from rocks by exchange processes associated with water-rock interaction and hydrothermal alteration. These waters typically plot horizontally to the right of the meteoric source water because rocks contain very little hydrogen for exchange and the δD value remains constant.

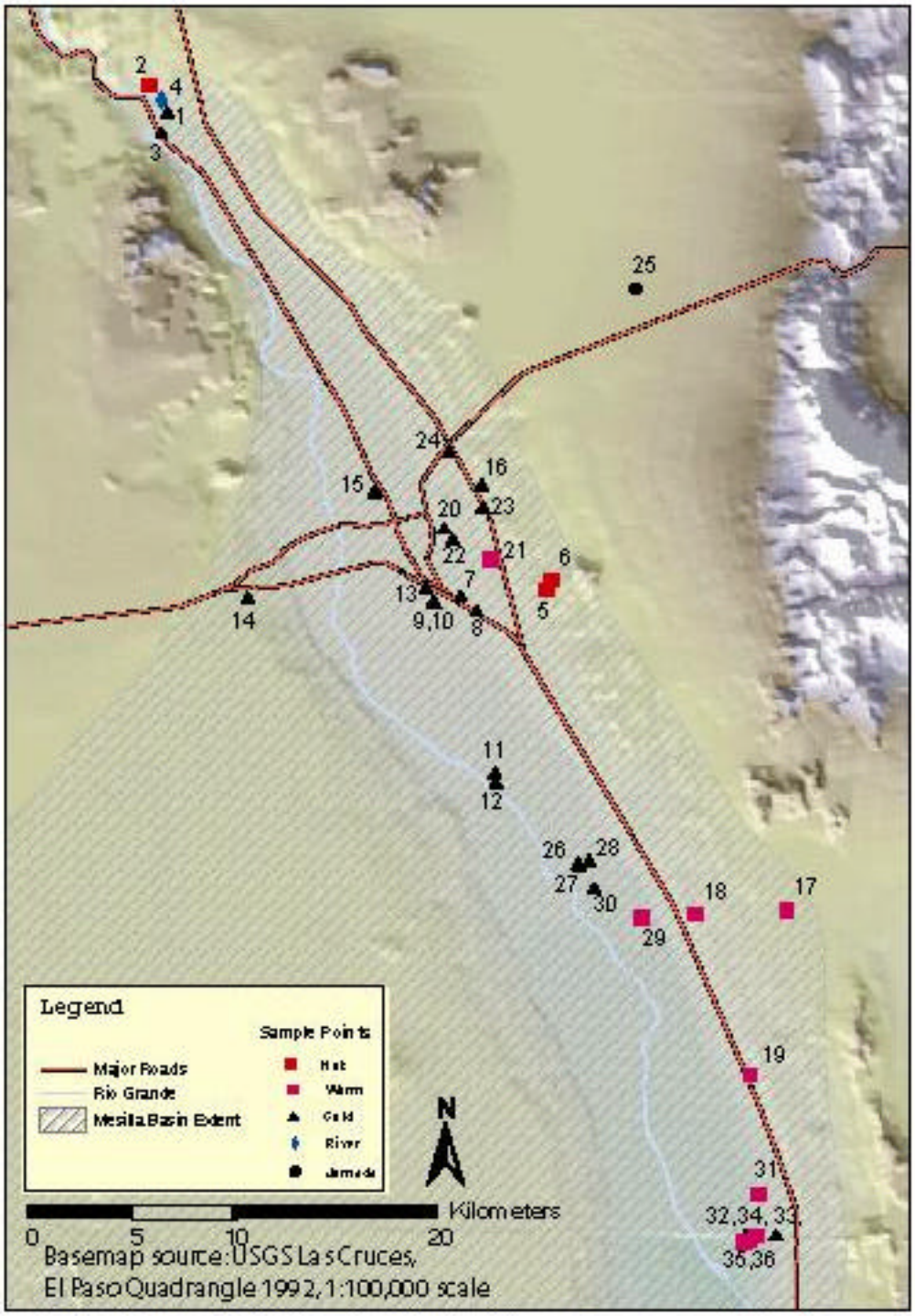

Figure 3-19. Location map of Mesilla Basin area of wells sampled for water chemistry and isotopic analysis in this study.

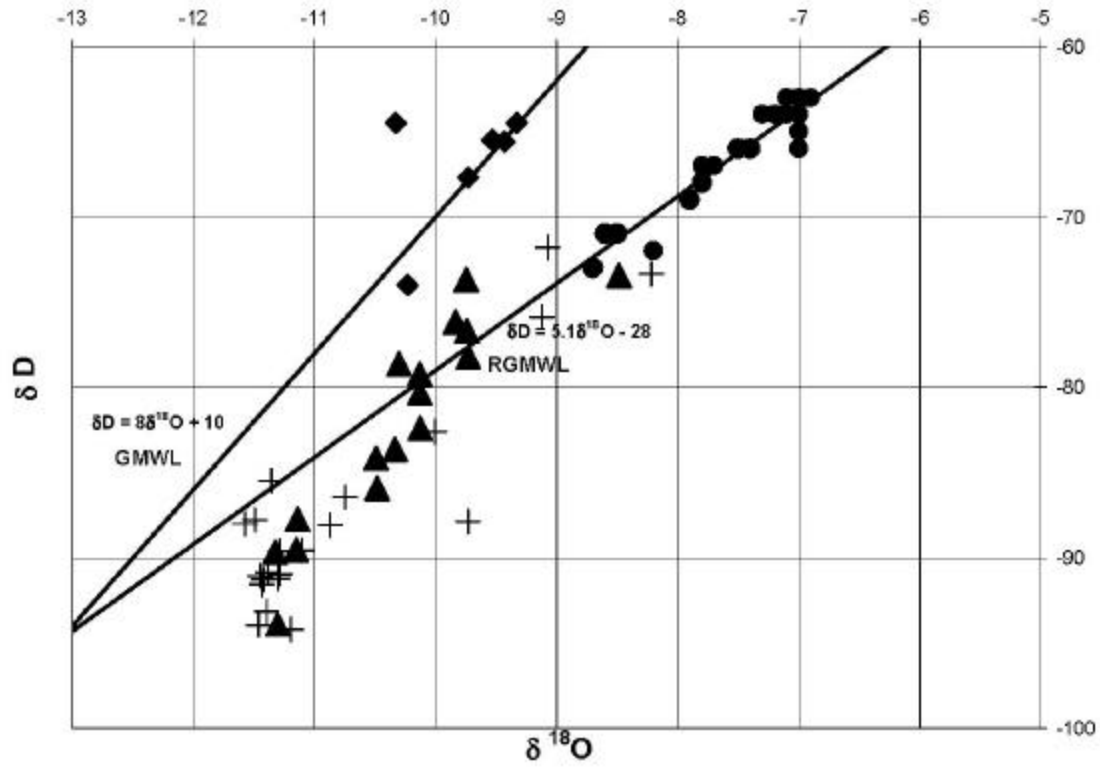

Figure 3-20. Oxygen ($\delta^{18}O$) stable isotopes versus hydrogen δD) stable isotopes for groundwater and surface water. Solid triangles are for thermal (>26^{o} C) groundwater and crosses are non-thermal groundwater (Appendix B, Table 4). Solid circles are for the Rio Grande and drainage canals (from Phillips et al. 2002) and solid diamonds are cold springs in the Organ Mountains (from Gross, 1988). GMWL is the Global Mean Water Line of Craig (1961) and RGMWL is the Rio Grande Mean Water Line of Phillips et al. (2002).

The amount of oxygen exchange or change in $\delta^{18}O$ is a function of rock composition, texture, temperature and length of contact (Fontes 1980; Nicholson 1993; Gat 1996; Mazor 1997).

Vuataz and Goff (1986) show local and regional meteoric water lines for the Jemez Mountains region of north central New Mexico to be parallel to the Global Meteoric Water Line with a deuterium excess of +12 or $\delta D = 8\ \delta^{18}O + 12$. Closer to the Mesilla Valley, Gross (1988) presents δD and $\delta^{18}O$ measurements for springs in the Organ Mountains just east of the Mesilla Basin that indicate the Organ Mountain spring water falls on the Craig (1961) Global Meteoric Water Line (Fig. 3-20). Figure 3-20 also shows the Rio Grande Mean Water Line of Phillips et al. (2002). The Rio Grande Mean Water Line ($\delta D = 5.1\ \delta^{18}O - 28$) represents an "evaporation" trend derived from river samples taken at regular intervals along 1,200 km of the Rio Grande from Colorado to Texas. Rio Grande waters of the Mesilla Valley are heavier in δD and $\delta^{18}O$ than Mesilla Basin groundwater samples. Thermally anomalous waters are generally heavier than non-thermal groundwater, but lighter than Rio Grande waters.

Because of arid climate in the region, surface water and shallow groundwater is subject to evaporation and evapotranspiration processes. With time and distance along the flow path, surface and shallow groundwater become progressively heavier in δD and $\delta^{18}O$ with a trend that is upward and to the right along the Rio Grande Mean Water Line of Phillips et al. (2002) because of evaporation. The isotopic lightness of Mesilla Basin thermal and non-thermal groundwater eliminates recent recharge from present day precipitation or Rio Grande water. Without evaporative fractionation, the Organ Mountain springs of Gross (1988) are heavier than groundwater and represent current day local meteoric water. In order to obtain the δD and $\delta^{18}O$ observed in Mesilla Basin groundwater and surface water, precipitation and recharge must have occurred during a much cooler climate (Plummer et al. 2000; Scanlon et al. 2001). High temperature geothermal waters can show a $\delta^{18}O$ shift to the right from hydrothermal alteration processes and show an upward to the right shift in δD

and $\delta^{18}O$ from subsurface boiling. However, δD and $\delta^{18}O$ chemical fractionation tends to act conservatively at temperatures below 100° C; therefore, the geothermal water, cold groundwater, and Rio Grande δD and $\delta^{18}O$ variation mostly represents fractionation processes associated with evaporation and original recharge variation. Evapotranspiration processes do not effectively fractionate water.

A plot of δD versus chloride suggests that three end member waters occur in the basin and that all other waters are mixtures of the three end members (Fig. 3-21) (Bothern 2003). The heaviest δD water with low Cl (<200 mg/L) is surface or Rio Grande water. The lightest δD with low Cl (<200 mg/L) is non-thermal groundwater. The intermediate δD composition water with high Cl (>800 mg/L) is geothermal water.

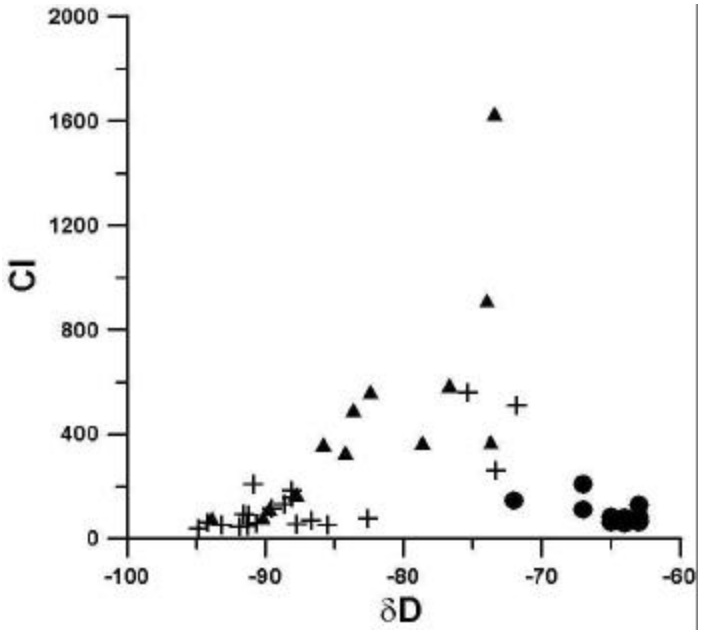

Figure 3-21. Hydrogen stable isotopes (δD) versus chloride (Cl) for groundwater and surface water. Solid triangles are for thermal (>26° C) groundwater and crosses are non-thermal groundwater (data, this study). Solid circles are for the Rio Grande and drainage canals (data from Phillips et al. 2002).

3.5.3 Strontium ($^{87}Sr/^{86}Sr$) Ratio

Strontium (Sr) frequently replaces Ca in mineral structures because of similar ionic radius. Strontium has four stable isotopes, ^{84}Sr, ^{86}Sr, ^{87}Sr, and ^{88}Sr. With time the natural reservoir of ^{87}Sr is slowly increasing due to beta decay of ^{87}Rb (rubidium), with a half-life of 48.8 X 10^9 years to form ^{87}Sr. Isotopes of Sr are reported as mass ratios such as $^{87}Sr/^{86}Sr$ (Faure 1986; Capo et al. 1998; Stewart et al. 1998).

Because of very small mass differences between the isotopes of Sr, the $^{87}Sr/^{86}Sr$ ratio is not changed by fractionation during chemical or physical processes as observed with lighter isotopic systems such as H and O. The Sr ratio is set at the time of mineral formation. Because Rb has an ionic radius similar to K, K-rich rocks may be enriched in ^{87}Rb. With sufficient time, a rock with high K content may have high ^{87}Sr contents as a result of ^{87}Rb beta decay.

The $^{87}Sr/^{86}Sr$ ratio of water in the Mesilla Basin reflects the flow paths and rock and mineral sources in the region. These sources include Precambrian granite and metamorphic rocks, Paleozoic carbonate rocks, Tertiary and Quaternary mafic and intermediate composition volcanic rocks and intrusions, Tertiary silicic volcanic and plutonic rocks, and Quaternary eolian dust. Flow paths through Tertiary and Quaternary sediments can reflect a mixture of all sources as these sedimentary units have varied mineral and rock provenance. Older (>1.5 b.y.) Precambrian granites have initial $^{87}Sr/^{86}Sr$ ratios between 0.700 and 0.708 while the younger (<1.5 b.y.) Precambrian K-rich granites in the region have initial $^{87}Sr/^{86}Sr$ ratios between 0.705 and 0.728 (Condie and Budding 1979). Today, measured Precambrian $^{87}Sr/^{86}Sr$ ratios may range up to 0.81 (Butcher 1990). Important variations in the initial $^{87}Sr/^{86}Sr$ ratio occur in marine carbonate rocks during the Phanerozoic (Burke et al. 1982; McArthur et al. 2001; Veizer et al. 1999). The ratio changes reflect large-scale plate tectonic related variance in weathering rates and terrestrial sources for initial $^{87}Sr/^{86}Sr$ ratios in Paleozoic seas. Most geothermal systems in the area are known to reside in Pennsylvanian carbonate rocks for at least a portion of the total flow history (Witcher

unpublished). During the Pennsylvanian, the average Sr ratio was generally between 0.7080 and 0.7085. Because of low K content and high Ca content, the $^{87}Sr/^{86}Sr$ ratios of today's Pennsylvanian rocks has probably not changed much. Tertiary and Quaternary basalts have initial $^{87}Sr/^{86}Sr$ ratios of 0.703 to 0.704 (Elston 1976). Mid-Tertiary basaltic andesites have initial $^{87}Sr/^{86}Sr$ between 7.07 and 7.08 (Elston 1976). Because of low K content and relatively high Ca content compared to K and likely low Rb content, the basalt and basaltic andesite initial $^{87}Sr/^{86}Sr$ ratios are roughly valid today. On the other hand, Tertiary silicic volcanics and plutons have initial $^{87}Sr/^{86}Sr$ ratios ranging from 0.71 to 0.73 (Elston 1976). Because these rocks may have high Rb contents as a consequence of high K, measured $^{87}Sr/^{86}Sr$ ratios of today are higher. Butcher (1990) reports measured present day $^{87}Sr/^{86}Sr$ values ranging from 0.7053 to 0.7488 for mid-Tertiary silicic rocks in the Organ Mountains east of the Mesilla Valley. Caliche provides a proxy for the Quaternary eolian dust $^{87}Sr/^{86}Sr$ ratio source reservoir. Caliche $^{87}Sr/^{86}Sr$ ratios range from 0.708 to 0.716 (Van der Hoven 1994; Capo et al. 1998). However, we believe that the contribution of Sr dissolved from eolian dust is minor when accounting for the $^{87}Sr/^{86}Sr$ ratio of groundwater in the Mesilla Basin.

Figure 3-22 shows the Cl/Br ratio versus the $^{87}Sr/^{86}Sr$ ratio for thermal and non-thermal groundwater in the Mesilla Basin. Thermal groundwater shows $^{87}Sr/^{86}Sr$ ratios ranging between 0.710 and 0.717 and end member thermal water have Cl/Br ratios greater than 1200. Non-thermal groundwater has less variation with $^{87}Sr/^{86}Sr$ ratios between 0.709 and 0.712 and Cl/Br ratios between 400 and 600. A rough upward to the right trend suggests that mixing is occurring between thermal and non-thermal groundwater in the Mesilla Basin**.**

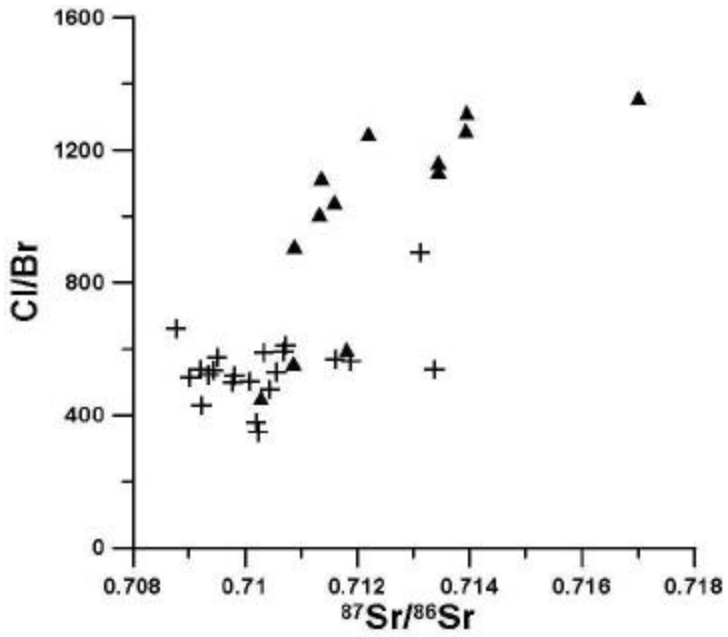

Figure 3-22. Strontium isotope ratio ($^{87}Sr/^{86}Sr$) versus Cl/Br. Solid triangles are thermal (>26° C) groundwater and crosses are non-thermal groundwater.

Geothermal groundwater has probably flowed through Precambrian granite and possibly mid-Tertiary silicic volcanics and granite plutons in order to acquire $^{87}Sr/^{86}Sr$ ratios greater than 0.712. Non-thermal groundwater has $^{87}Sr/^{86}Sr$ ratios (0.709 to 0.712 consistent with flow through clastic sediments with provenance that is dominated by Paleozoic carbonate and mid-Tertiary mafic to intermediate volcanic source terrain with local units dominated by mid-Tertiary silicic volcanics and/or Precambrian granite.

3.5.4 Carbon ($\delta^{13}C$)

Carbon (C) has three common isotopes; ^{12}C and ^{13}C are stable, while the ^{14}C isotope is radioactive. In this study, only the stable isotopes are discussed. The abundance of C stable isotopes is ^{12}C (98.89 %) and ^{13}C (1.11%). Carbon isotopes are fractionated by a variety of natural processes, including plant photosynthesis and isotope exchange reactions between carbonate minerals.

Plant photosynthesis can be important and result in ^{12}C enrichment of organic carbon inclusions in sediments, petroleum and coal (Faure 1986). Hoefs (1997) describes two separate pathways for sediment diagenesis, a shallow meteoric pathway and a burial pathway for deep-sea environments. The burial pathway creates carbonates enriched in ^{13}C from methane production even when ^{12}C enriched organic carbon is present in the original sediment. The resulting carbonates can have high $\delta^{13}C$ values (Faure 1986; Hoefs 1997).

In the Mesilla Basin**,** thermal waters have the highest $\delta^{13}C$ values (– 3.1 to +2.2). The heavier $\delta^{13}C$ values in thermal water may indicate water-rock equilibration along deep regional flow paths through marine carbonates of Cambrian to Pennsylvanian age. Marine carbonate rocks typically have $\delta^{13}C$ values from –4 to 6 (Clark and Fritz 1997; Veizer et al. 1999). Early Mississipian (Alamogordo Member of the Lake Valley Formation) in south central New Mexico has average $\delta^{13}C$ at 2.7 (Stanton et al. 2002). Algeo (1996) presents carbon isotopic data on the Middle Pennslyvanian Gobbler Formation in the Sacramento and San Andres Mountains of south central New Mexico. While $\delta^{13}C$ ranges from -5 to 5, most $\delta^{13}C$ values for the Gobbler Formation range from 2 to 4.

Waters with significant atmosphere-derived fractions of dissolved carbonate species will have $\delta^{13}C$ values lower than –4 but probably greater than –15. Average atmospheric $\delta^{13}C$ is about –7. Non-thermal waters in the Mesilla Basin are characteristically more negative or enriched in carbon-12 and have $\delta^{13}C$ values between –3.1 and –11.9. Calcite and carbonate in the upper basin fill deposits of south central New Mexico have $\delta^{13}C$ between –2.2 and –5.5 (Mack et al. 1994; Mack et al. 2000); while surface carbonate soils (caliche) $\delta^{13}C$ range between – 0.6 and –11 (Monger et al. 1998). Monger and others (1998) also report organic carbon $\delta^{13}C$ between –15.7 and –25 in near surface soils.

Figure 3-23 shows $\delta^{13}C$ values versus the Cl/Br ratio. Two trends are apparent. Thermal waters show an upward to the right trend that is consistent with mixing between thermal waters and non-thermal waters. The mixing trend shows a Cl/Br range of 400 to 1300. On the other hand, non-thermal water

shows no apparent mixing with a wide distribution of $\delta^{13}C$ (-2 to –12) in a relatively narrow zone of Cl/Br (350 to 650). The $\delta^{13}C$ depletion may in part indicate biogenic fractionation processes in the upper Mesilla Basin aquifers.

Figure 3-24 is a comparison of $\delta^{13}C$ and $^{87}Sr/^{86}Sr$. An apparent linear relationship among most sampling sites strongly suggests that most water in the basin is a varied mixture of thermal and non-thermal water.

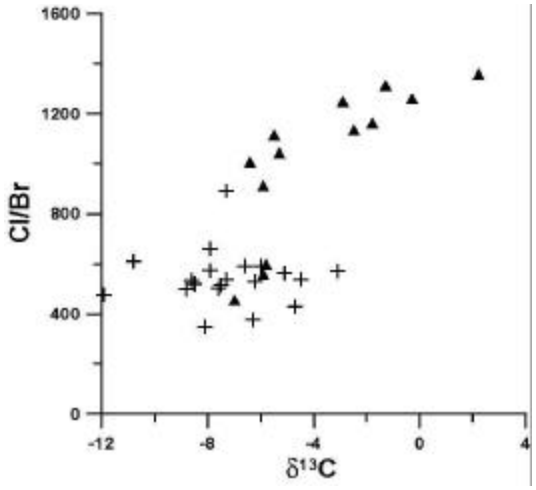

Figure 3-23. Carbon stable isotopes ($\delta^{13}C$) versus Cl/Br. Solid triangles are thermal (>26° C) groundwater and crosses are non-thermal groundwater.

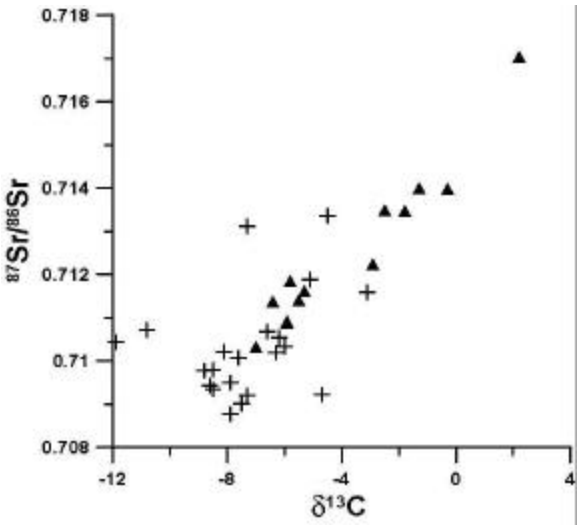

Figure 3-24. Strontium isotope ratio ($^{87}Sr/^{86}Sr$) versus carbon stable isotopes ($\delta^{13}C$). Solid triangles are thermal (>26° C) groundwater and crosses are non-thermal groundwater.

3.5.5 Sulfur $\delta^{34}S$

The main sources of sulfur for Mesilla Basin groundwater are probably dissolution of gypsum and weathering of sulfide minerals such as pyrite. Gypsum and anhydrite ($CaSO_4$) are associated with several Pennsylvanian and Permian rock units and with Tertiary-Quaternary playa deposits. While pyrite occurs as an accessory mineral in many rock units in the subsurface of the area, this reservoir probably contributes only minor sulfur to the basin groundwater systems. Dissolution and weathering releases sulfur into groundwater as a sulfate (SO_4) anion. Where acid geothermal conditions or subsurface boiling occurs and biogenic reducing processes are active, some sulfur may occur as dissolved hydrogen sulfide (H_2S).

Stable sulfur isotopic ratios of ^{34}S and ^{32}S can reflect source and geochemical processes such as biogenic reduction of sulfur. Marine evaporites of Permian age in west Texas typically have $\delta^{34}S$ of 9.6 to 12.5 (Thode and Monster 1965; Hill 1996). Late Permian brines in southeast New Mexico have $\delta^{34}S$ of 7.4 to 9.8 (Hill 1996). Where sulfur of biogenic heritage occurs, $\delta^{34}S$ can range downward to –30.

Sampled Mesilla Basin waters have $\delta^{34}S$ values between –2.7 and 9.4. Figure 3-25 shows $\delta^{34}S$ compared to the Cl/Br ratio with point labels representing temperature in degrees centigrade (^{o} C). Two general clusters or domains are apparent in the data. First, thermal waters with Cl/Br ratios above 800 show $\delta^{34}S$ values between 4 and 8. The thermal waters appear to have a component of late Paleozoic dissolved sulfate, although slightly lower than the $\delta^{34}S$ of Permian brines and gypsum in southeast New Mexico.

Non-thermal waters in Figure 3-25 show a band with narrow Cl/Br and wide $\delta^{34}S$ distributions. The narrow Cl/Br distribution indicates that the non-thermal waters have similar overall chemical evolution. However, the range of $\delta^{34}S$ indicates that most sulfate has a similar origin as the thermal water. On the other hand, the $\delta^{34}S$ values less than 4 may indicate that biogenic reduction of sulfur is important in local zones.

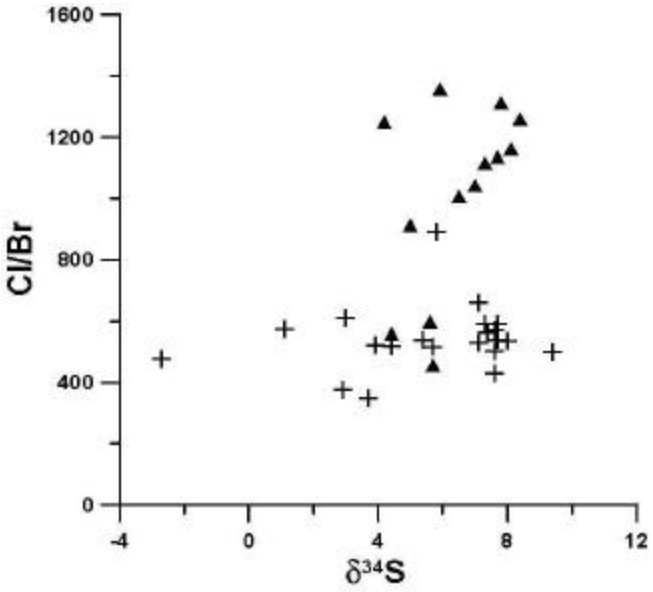

Figure 3-25. Sulfur stable isotopes ($\delta^{34}S$) versus Cl/Br. Solid triangles are thermal (>26° C) groundwater and crosses are non-thermal groundwater.

3.5.6 Uranium Isotopic Disequilibrium (Excess ^{234}U)

Uranium is the heaviest natural element and is comprised of three radioactive isotopes (^{238}U, ^{235}U, and ^{234}U). The most abundant ^{238}U comprises approximately 99.27% and ^{234}U and ^{235}U together have less than 1% abundance with ^{234}U at three orders of magnitude less abundant than ^{235}U. The decay of ^{238}U has a relatively short half-life and produces a radioactive and short-lived ^{234}U. In addition, $^{234}U/^{238}U$ shows considerable variability in geologic systems. In this report, ^{234}U is reported as a ratio for the actual measured activity of ^{234}U compared to the ^{238}U equilibrium decay activity for ^{234}U. The activity ratio is called ^{234}U excess. Processes that are important in the variation of ^{234}U excess are detailed in Osmond and Cowart (1976). Recoil of ^{234}U across the solid-water boundary during alpha decay of ^{238}U is probably the most important process leading to excess activity. Most groundwater and surface waters show ^{234}U in excess of equilibrium activity (>1.0). Waters with ^{234}U excess less than 1.0 are

probably the result of uranium dissolution or leaching from mineral sources that are depleted in ^{234}U.

Uranium in an oxidation state of 6^+ forms a variety of stable aqueous ionic complexes and tends to stays in solution. Because uranium dissolution and precipitation is typically not highly active in most groundwater environments, an aquifer will tend to retain a characteristic uranium concentration and ^{234}U excess activity. In reducing environments, uranium will be precipitated or adsorbed in the presence of H_2S and organic material. In this case, ^{234}U excess may be very high because alpha recoil becomes more important for uranium in solution.

Figure 3-26 shows excess ^{234}U versus $^{234}U/^{238}U$. Two general populations are shown for both the thermal and non-thermal groundwater in the basin. The first population has ^{234}U excess generally between 0 and 4, while the remaining sites show a wide variation of ^{234}U excess above 4. These distributions likely represent oxidation-reduction processes in the aquifers and do not appear to relate to mixing or evaporation processes.

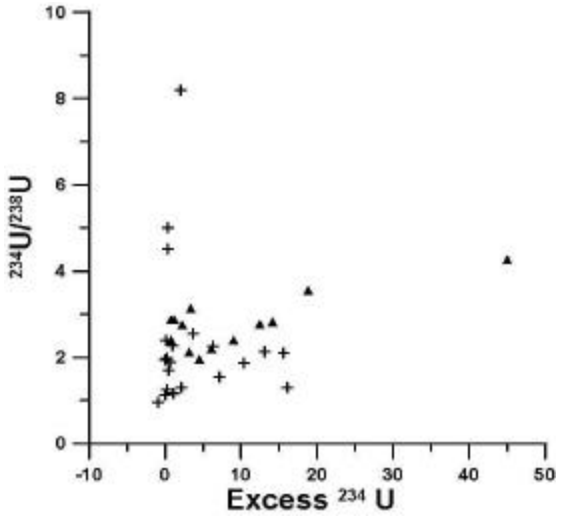

Figure 3-26. Uranium isotope ratio ($^{234}U/^{238}U$) versus excess ^{234} U. Solid triangles are thermal (>26^o C) ground-water and crosses are non-thermal groundwater.

3.6 MIXING AND EVAPORATION

Mingling of waters with different chemical evolution and provenance will create mixtures in proportion to each groundwater and/or surface water end member. Post mixing evaporation will concentrate highly soluble and conservative chemical species, but may not change conservative ratios.

In order to quantify or identify the relative importance of mixing and evaporation, several assumptions are required. First, are the appropriate ionic or isotopic constituents or parameters selected? The criteria used in this analysis selects highly soluble anions and isotopic species that show large variation among the Mesilla Basin water and are least likely to show modification by ion exchange, chemical hydration reactions or precipitation as solid salts or minerals. This study uses Cl, Br, δD and $^{87}Sr/^{86}Sr$. As with most other chemical and isotopic parameters, Cl, Br, and δD are subject to variation by evaporation and dissolution of evaporite minerals or rocks. On the other hand, evapotranspiration does not fractionate or change the δD of shallow groundwater. Also, evaporation will not change the $^{87}Sr/^{86}Sr$ ratio. Because brines are not involved in shallow Mesilla Basin waters, evaporation will not appreciably change the Cl/Br ratio either.

A second assumption involves selecting the appropriate end member sample sites for ground and surface water. Figure 3-27 is useful to show Mesilla Basin end members. End members are the apexes of a triangular field of analyses formed by a plot of Cl versus δD. The end members represent Rio Grande water, cold groundwater from the central and northern part of the basin, and geothermal water from the northern and eastern part of the basin. When Cl/Br versus δD is applied, the relationships remain unchanged (Fig. 3-28). Sample sites within the field of the triangle represent mixtures of end member waters that may have been modified by post mixing evaporation and dissolution processes.

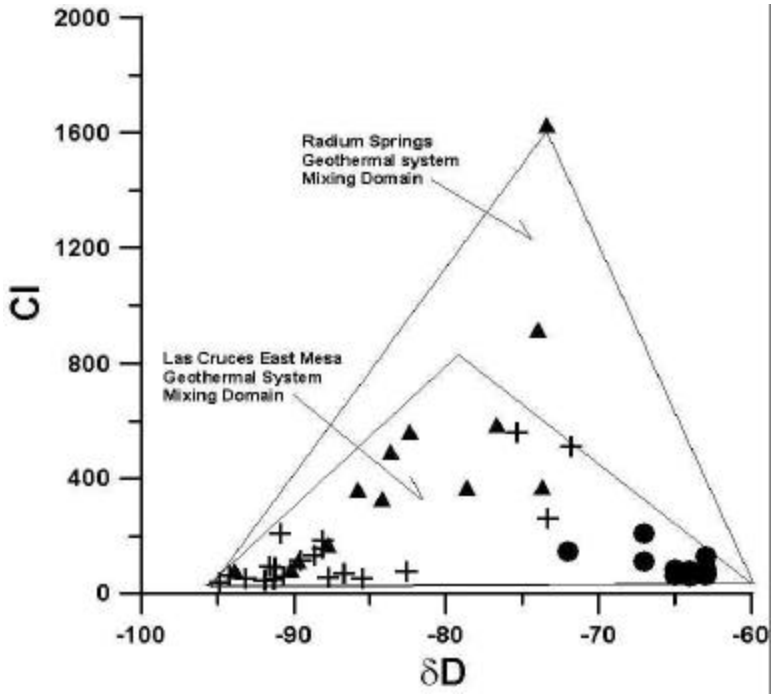

Figure 3-27. Hydrogen stable isotopes (δD) versus chloride (Cl) for groundwater and surface water. Solid triangles are for thermal (>26^{o} C) groundwater and crosses are non-thermal groundwater (data, this study). Solid circles are for the Rio Grande and drainage canals (data from Phillips et al. 2002). Solid circles are for the Rio Grande and drainage canals (data from Phillips et al. 2002).

A plot of δD/Cl versus Cl/Br is shown in Figure 3-29. Three features are readily apparent in the data. First, the majority of the geothermal or thermal waters plot on a tight linear trend that is up steeply to the left. This trend is interpreted as a mixing line for non-thermal ground and surface water in the basin. Second, the surface waters show a tight trend with a lower slope than thermal water that is up and to the left. Third, the non-thermal groundwater shows significant scatter along a rough horizontal trend.

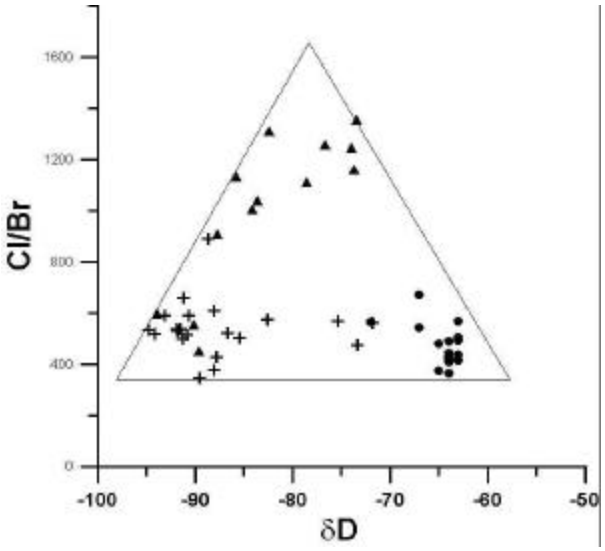

Figure 3-28. Hydrogen stable isotopes (δD) versus Cl/Br for groundwater and surface water. Solid triangles are for thermal (>26^{o} C) groundwater and crosses are non-thermal groundwater (data, this study). Solid circles are for the Rio Grande and drainage canals (data from Phillips et al. 2002). Triangle apexes are possible mixing end-member compositions for Mesilla Basin groundwater.

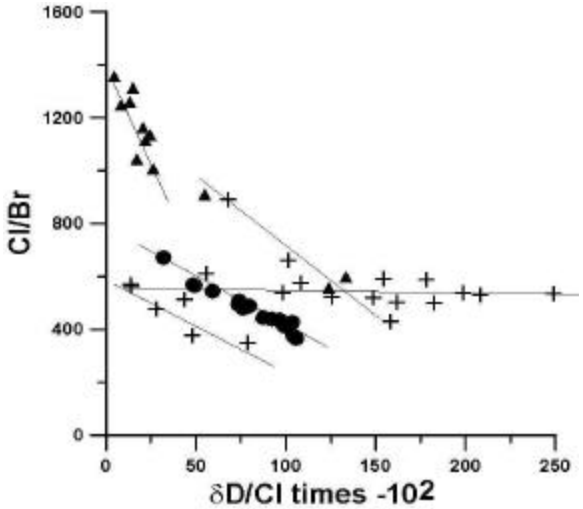

Figure 3-29. The ratio of hydrogen stable isotopes to chloride (δD /Cl) versus Cl/Br. Solid triangles are for thermal (>26^{o} C) groundwater and crosses are non-thermal groundwater (data, this study). Solid circles are for the Rio Grande and drainage canals (data from Phillips et al. 2002).

While trends in surface and thermal groundwater in Figure 3-29 are basically interpreted as the result of mixing processes, evaporation and dissolution may also play important roles. However, with evaporation the ratio of Cl/Br will not change. In others words, a plot Cl/Br compositions for various degrees of evaporation without mixing is horizontal. Chloride will increase and δD will become heavier by evaporation fractionation with the ratio of the two species showing trend to the right in the along the δD/Cl axis. A trend to the left would indicate mixing with lighter δD water. Phillips and others (2002) and Bothern (2003) show that Rio Grande and drain waters become lighter in the Mesilla Basin as a result of mixing inflows of groundwater with a variable fraction of geothermal water. This is especially is true for drains on the east and southern end of the valley.

Figure 3-30 is a plot of δD/Cl versus the $^{87}Sr/^{86}Sr$ ratio normalized with respect to Br ($^{87}Sr/^{86}Sr$/Br). Most thermal water shows a tight linear trend that is steep and upward to the right, while non-thermal groundwater and some geothermal waters show a lower sloped rising trend to the right. The scatter in the non-thermal groundwater trend is believed to be the combined result of evaporation, dissolution, and mixing processes with mixing and dissolution as the dominant processes. Because the $^{87}Sr/^{86}Sr$ ratio is not affected by evaporation, horizontal variation in the non-thermal groundwater trend may be the result of evaporative fractionation of δD.

Figure 3-31 is a Piper diagram for water in the southern Mesilla Basin portion of Texas, including the Canutillo area. Dominant water type is sodium-chloride-sulfate water typical of geothermal waters in the basin to the north in New Mexico. This indicates that groundwater in the southern end of the Mesilla Basin has significant components of geothermal water or deep-seated basinal water (regional flow systems).

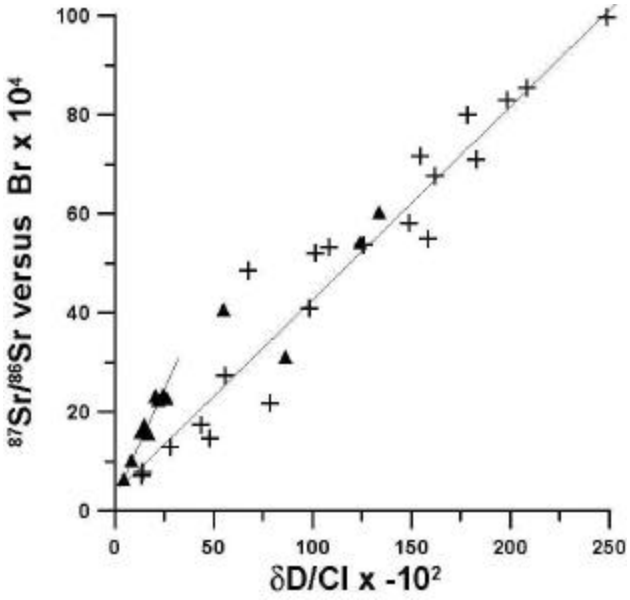

Figure 3-30. The ratio of strontium isotopes ($^{87}Sr/^{86}Sr$) to bromide Br) versus ratio of hydrogen stable isotopes to chloride (δD /Cl). Solid triangles are for thermal (>26^{o} C) groundwater and crosses are non-thermal groundwater.

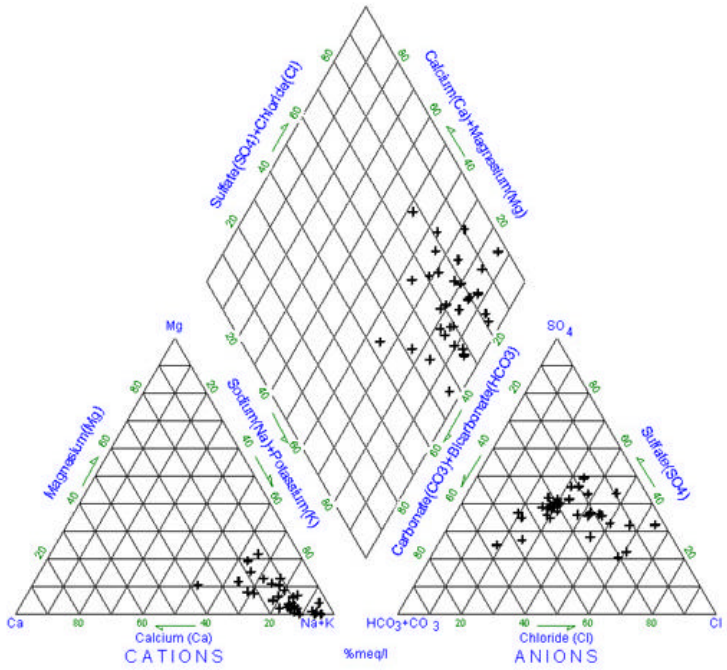

Figure 3-31. Piper diagram of groundwater in the Texas portion of the Mesilla Basin, including the Canutillo area

3.7 GEOTHERMAL INFLOW

Swanberg (1975), Frenzel and Kaehler (1992), and this study identify geothermal systems as possible major sources of salinity in shallow Mesilla Basin aquifers. The following discussion is an outline of one approach that can be used to quantify the salinity influxes. Our method makes use of a large temperature gradient and heat flow database measured and compiled from many sources over the past 20 years. With some knowledge of base reservoir temperatures, heat flow information can be used to quantitatively estimate geothermal mass inflow to the basin using a heat and mass balance calculation.

To make a heat and mass balance calculation, a dynamic three-dimensional system is defined. Geothermal systems can be characterized as having a deeply connected bedrock upflow zone and a shallow bedrock or alluvial aquifer outflow plume. One subsurface hydrogeologic boundary that is parallel to the earth's surface is located "deep" in the bedrock of the upflow area and allows the vertical mass and energy input to the system. "Deep" bedrock outside of the upflow zone is assigned a boundary with no vertical mass flow, but vertical conductive heat input is allowed from the regional background crustal heat flux.

The outflow plume represents the area of shallow lateral flow of geothermal water from the upflow zone. The outflow plume has distal and diffuse zones of lateral mixing with non-thermal water. Vertical boundaries, normal to the Earth's surface and above the "deep" basal boundary, are open to heat and mass inflow or outflow in all cardinal directions. Anomalous conductive heat loss occurs above the water table over the upflow zone and the entire extent of the outflow plume. Measurement of this heat loss gives the minimum total advective heat loss of the geothermal system.

Conductive heat flow is defined by $q_z = k(dT/dz)$, where q_z is the conductive heat flow (mW/m^2), k is the thermal conductivity (W/m^oK) of the material through which the conductive heat flow is determined, and dT/dz is the measured temperature gradient in $^oC/km$ across the interval. In order to perform

a heat and mass balance calculation, we determined the total heat conducted out of the geothermal system by integrating the vertical conductive heat flow over the upflow zone and outflow plume areas of the system: $Q = \int q_z dA - \int q_b dA$, where Q is the total advective heat output of the geothermal system in W, and dA is the area (km^2) of the integration, and q_b is the regional crustal heat flow of the area. We conservatively use 100 mW/m^2 as the regional crustal heat flux for the southern Rio Grande rift and Mesilla Basin region (Blackwell 1978; Reiter et al. 1986).

Vertical upflow zone geothermal fluid flow introduces heat to the system by advection. The amount of heat transported by advection (Q) depends on the difference in temperature between fluid discharging across the upflow zone area in bedrock (the base reservoir temperature or T_{gs}) and the surface mean annual temperature (MAT) and the fluid flow rate: $Q = pcV(T_{gs} - MAT)$ where *p* is fluid density, *c* is specific heat of the fluid, and V is the volumetric fluid flow rate. Because the geothermal system that is used in our example is low temperature (less than 100^o C), fluid density and specific heat are conservatively assigned unity values of pure water at standard temperature and pressure. The MAT for the Las Cruces area is about 16^o C.

An area that extends from the southern end of the Doña Ana Mountains to the Texas border area around Anthony known as the Las Cruces East Mesa Geothermal System has several probable upflow zones. It overlies a mostly buried bedrock horst block, forming the eastern margin of the Mesilla Basin (Sections 2.6.1, 2.7.1; Figs. 2-7, 2-8; Plate 1). The Tortugas Mountain area represents one of the better characterized areas along the Las Cruces East Mesa Geothermal System trend although it is not the hottest upflow zone. However, the area probably represents one of the larger heat and mass geothermal discharges. It is an area 8.5 by 7.5 km centered on the Tortugas Mountain area and includes the southeast part of Las Cruces, the NMSU campus, and the Las Alturas development. The upflow zones can show relative differences in geochemical character and base reservoir temperature, depending upon the deep flow path of the geothermal system.

Deep boreholes provide the base temperature and geochemical character of the Tortugas Mountain segment of the Las Cruces East Mesa Geothermal System. The hottest wells in the Tortugas Mountain area are NMSU PG-4 (MV-5 and Chaffee 55-57 (Gross 1988). The 980 ft deep NMSU PG-4 has a production temperature of 63.4^{o} C with a Cl content of 578 mg/L. Chaffe 55-57, 2645 ft total depth, has a measured reservoir temperature of 68^{o} C and a 482 mg/L Cl concentration (Gross 1988).

Chemical geothermometry is often applied to estimate base reservoir temperatures, using the basic assumptions discussed by Fournier et al. (1974). Cation and silica are the general types of geothermometers most commonly applied to evaluate reservoir temperatures. The most common cation geothermometers use the ratios of Na, K, Ca, and Mg (Fournier and Truesdell 1973; Fournier and Potter 1979). These empirical geothermometers are believed to represent temperature dependant reactions among feldspars, micas, and clay minerals (Giggenback 1988). Frenzel and Kaehler (1992) and Swanberg (1975) use the Na-K-Ca chemical geothermometer of Fournier and Truesdell (1973) to estimate base reservoir temperatures. The Na-K-Ca geothermometer calculates reservoir temperatures between 190 and 210^{o} C. These estimates may be too high; because the Las Cruces East Mesa Geothermal System is largely contained in fractured Paleozoic carbonate bedrock, the traditional Na-K-Ca geothermometer is probably not reliable because non-temperature dependent dissolution and precipitation processes are likely occurring such as gypsum dissolution and calcite precipitation. However, the Na-K-Ca with Mg corrections (Fournier and Potter 1979) gives temperatures in the 70 to 80^{o} C range.

Experience has shown that the silica geothermometers for chalcedony and quartz provide the most reliable estimates for lower temperature geothermal reservoirs such as those found in the southern Rio Grande. The quartz and chalcedony geothermometer formulas are found in Fournier (1977). With the silica concentrations observed in the Las Cruces East Mesa Geothermal System, the quartz geothermometer is around 100^{o} C and the chalcedony geothermometer ranges from 70 to 80^{o} C.

The 70^{o} C base reservoir temperature and an average chloride content of 500 mg/L was selected to perform a mass and energy balance, using the total conductive heat loss for the Tortugas Mountain area.

The total conductive heat loss is 10.8 MW_t (J/s) for the Tortugas Mountain area. This estimate does not determine the heat and mass balance of the entire Las Cruces East Mesa Geothermal System. For that purpose, the estimate may be low by several times as the outflow plume thermal signature continues southward (Fig. 3-32). Our purpose here is to show an example of how the heat flow data can quantify the salinity contribution to the shallow Mesilla Basin aquifers and ultimately the Rio Grande. A minimum natural mass flow rate of at least 760 gallons per minute of 500 mg/L chloride water is calculated for the area shown in Figure 3-24. This translates into a geothermal recharge to the Mesilla Basin of 1,229 acre/ft per year and a flux of 834 tons of chloride per year for the area selected for heat and mass balance. Because the area selected does not include the full thermal heat loss for the system, the actual mass input to the Mesilla Basin is greater. It is clear that the contribution of salinity by just one geothermal upflow zone to the shallow Mesilla Basin aquifer recharge provides significant salinity to the basin.

The error in these estimates is believed to be between 10 and 15% where the base subsurface or upflow zone temperature and chemistry is well characterized. The largest source of error is in the natural variability and measurement uncertainty in thermal conductivity. Of course, where temperature gradient data are sparse, additional error may be introduced in contouring the heat flow surface. However, concurrent interpretation with other geologic, geophysical, and hydrogeologic information helps reduce any error. In any case, the calculated mass and heat fluxes are considered as minimum values.

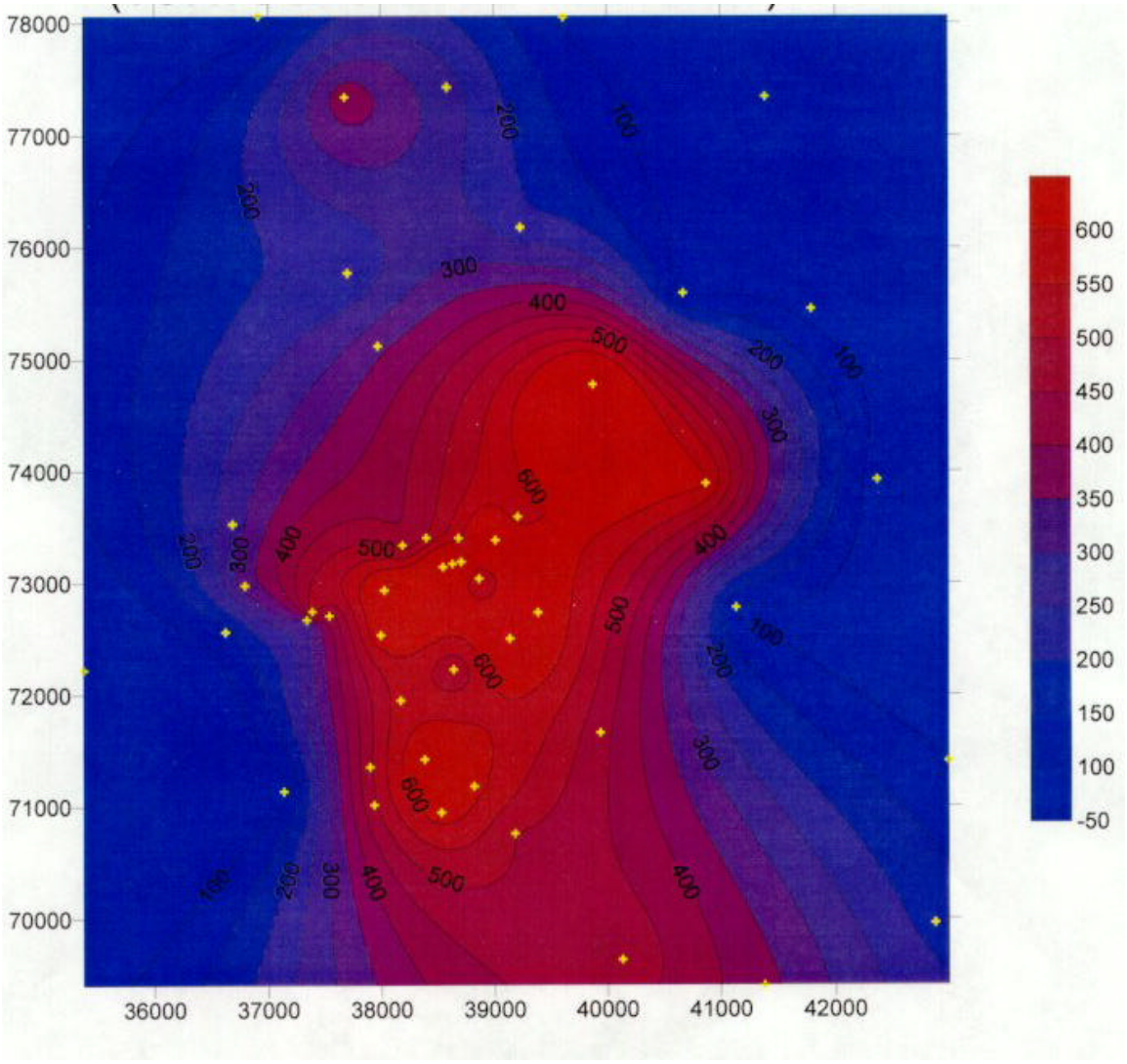

Figure 3-32. Heat flow map of a portion of the Las Cruces East Mesa geothermal field centered on the Tortugas Mountain area. Heat flow as milliwatts per meter squared (mW/m^2).

3.8 CONCLUSIONS

3.8.1 Summary of Results

Non-thermal groundwater in the New Mexico portion of the Mesilla Basin is dominated by calcium-sodium-sulfate, sodium-sulfate, calcium-sulfate, and sodium-bicarbonate waters. Thermal water (>26^{o} C) throughout the basin and non-thermal groundwater in the Texas portion of the basin is characterized by sodium-chloride-sulfate composition water. Mixing of thermal and non-thermal water is one possible explanation. However, several important water quality processes are identified in Section 3 through the use of major cation and anion chemistry and isotope systematics. These processes point to sources of salinity or water chemistry in the basin:

- High potassium and high silica concentrations are predominantly controlled by non-thermal aluminosilicate dissolution in low chloride and low sulfate waters (<400 mg/L for both chloride and sulfate).
- Potassium and silica have very limited use in fingerprinting waters in the basin with a geothermal component of salinity.
- Ion exchange of dissolved calcium with sodium is a common process in the basin. Cation exchange evolution progresses with greater maturity from north to south in the basin by adding sodium to the water.
- Ion exchange of dissolved calcium and sodium also appears to have greater evolution maturity with aquifer depth.
- Geothermal waters are characterized by high Cl/Br ratios over 800. Non-thermal waters have ratios between 400 and 600. The Cl/Br ratio is highly sensitive to mixing and water provenance.
- Oxygen and hydrogen isotope systematics (δD versus δ^{18}O) for geothermal, non-thermal groundwater and surface water show that geothermal waters, non-thermal groundwaters, and surface water fall on an “evaporation line” or Rio Grande Mean Water Line defined by Phillips and others (2002).

- The δD and $\delta^{18}O$ of geothermal water is generally heavier than non-thermal water, but lighter than surface water. This reflects the relative importance of evaporation, recharge source, timing, and paleoclimate. The differences are useful to identify mixing and relative importance of other processes.
- The $^{87}Sr/^{86}Sr$ ratios of water reflect the flow paths and residence time and degree of reaction with rock and mineral sources in the region. Geothermal waters have $^{87}Sr/^{86}Sr$ ratios between 0.710 and 0.717. Non-thermal groundwater has less variation with $^{87}Sr/^{86}Sr$ ratios between 0.709 and 0.712. The overlap in $^{87}Sr/^{86}Sr$ ratios between thermal and non-thermal groundwater probably reflects mixing. The high $^{87}Sr/^{86}Sr$ ratio for geothermal water reflect flow through Precambrian and possibly deeply buried mid Tertiary silicic volcanic and intrusive rocks.
- Positive stable carbon isotope ($\delta^{13}C$) indicates that thermal water has approached water-rock equilibrium along deep regional flow paths through marine carbonates of Cambrian to Pennsylvanian age. Mixing is strongly indicated in all thermal and non-thermal groundwater by an apparent linear mixing trend defined by a plot $\delta^{13}C$ versus the $^{87}Sr/^{86}Sr$ ratio.
- Stable sulfur isotope ($\delta^{34}S$) values for thermal water tend to indicate sulfate sources in Permian rocks.
- The stable sulfur and carbon isotopes ($\delta^{34}S$ and $\delta^{13}C$) show a wide variation in non-thermal groundwater within a narrow range of Cl/Br ratios. This is interpreted to indicate that biogenic fraction processes may be important in some of the non-thermal waters.
- Uranium isotopic ratios were not used in the analysis of basinwide processes such as mixing and evaporation. However, such data may have significant value for the understanding of water quality evolution on a local scale within the Mesilla Basin.

4.0 RIO GRANDE SALT BALANCE

4.1 INTRODUCTION

An analysis of surface water chemistry provides valuable information for interpretations of salinity processes in groundwater and surface water in the Mesilla Valley. This chapter on surface water chemistry covers the entire Rio Grande Project (Project), which extends beyond the Mesilla Valley and presents a summary of work by Williams (2001) (Fig. 4-1). While the chapter discusses surface water salinity upstream and downstream from the Mesilla Valley, the approach allows comparison of salt balances within all units of the Project and facilitates a better understanding of salinity sources.

The major purpose of the salt balance study is to determine the salinity variation, both temporally and spatially, within the Project, using available historic data. An understanding of salinity processes has important implications for sustaining surface water and shallow groundwater quality and build up of salts in soils during irrigation. Reductions in crop yield due to salinity occurs on over 25% of the 50 million acres of irrigated land in the western United States, with another 25% being threatened (Postel 1993, 1999). Locally, portions of the Project may also be threatened by salinity problems.

Scofield (1940) originated and defined the term “salt balance.” If the mass of the salt entering a hydrologic unit exceeds the mass of the salt leaving the unit then there is a net undesirable accumulation of salt. If the salt balance between the upper gage station and the lower gage station is negative, then the potential for salt accumulation within area soils and shallow groundwater is lower and salts are being removed and transported to the next hydrologic unit downstream.

4.1.1 Objectives

Study objectives include:

1. Compile all available monthly flow and water quality data (major ions) from river gage stations within the Project.

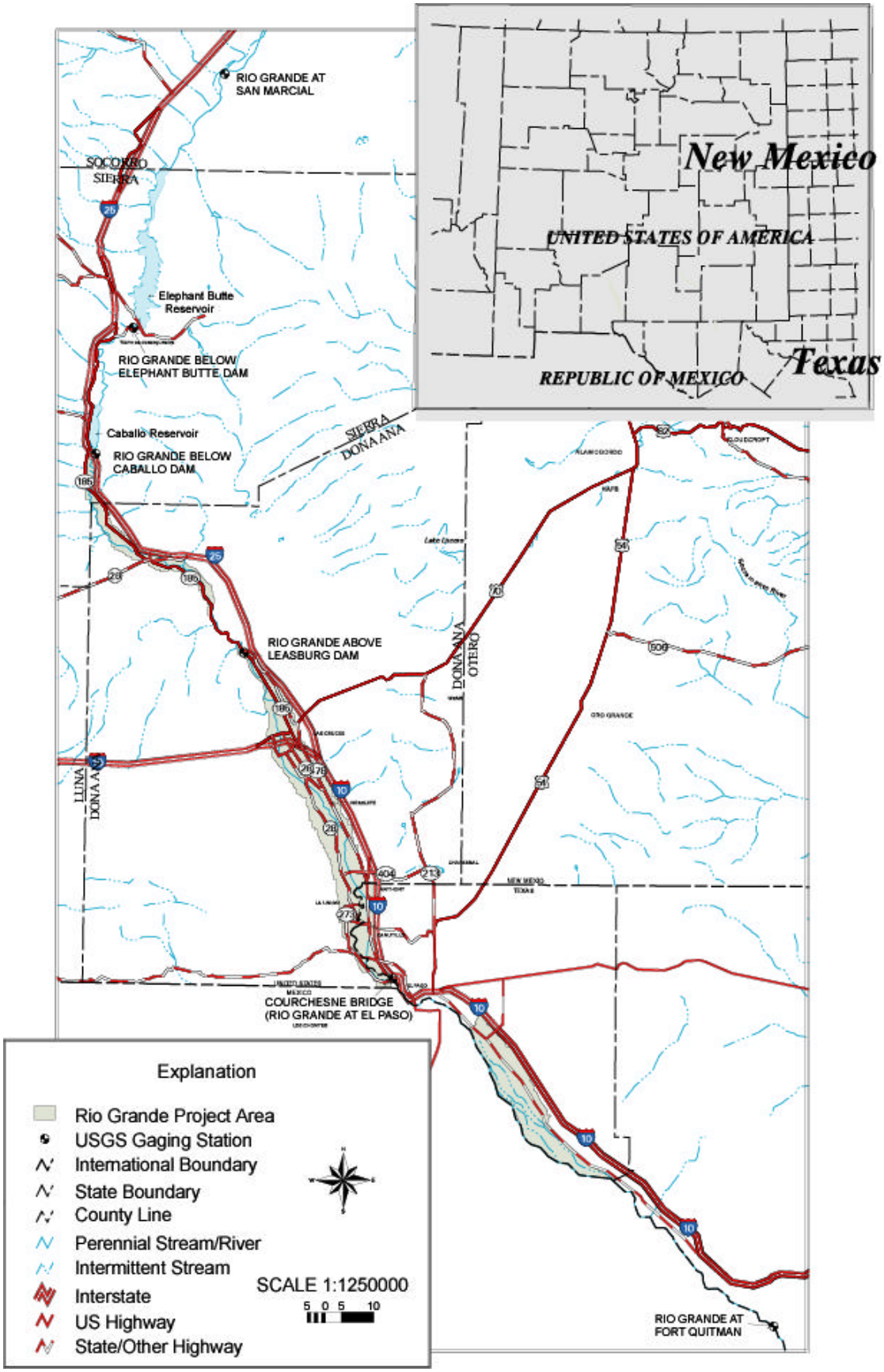

Figure 4-1. Index Map showing the main features of the surface water components of the Rio Grande Project.

Develop coefficients for relating total dissolved solids (TDS) to EC_{25} (electrical conductivity at 25° C) for the purpose of estimating TDS when only EC_{25} is measured.

2. Develop monthly ratios for each major ion to TDS (ion/TDS at each gage station) to facilitate estimates of major ion concentrations from the EC_{25} record.
3. Examine the monthly cumulative salt balance (mass inflow of salt minus mass outflow of salt) and balances of individual major ions for each of the three divisions or valleys in the Project.

4.1.2 Scope and Limitations

Existing historical flow and water quality data are used in this analysis and no new field measurements are reported. The focus in water quality is on major ions: calcium (Ca), magnesium (Mg), sodium (Na), sulfate (SO_4), bicarbonate (HCO_3), and chloride (Cl). However, if reported, boron (B) and nitrate (NO_3) are compiled into a digital database (see Appendix C).

The salt balance presented in this study is a gross simplification of a highly complex hydrologic and geohydrologic system. Each of the valleys is treated as a black box, with one source and one outlet. In reality, precipitation and dissolution processes, salinity and water inflows and outflows from local groundwater, imports of water and salts from aquifers not overlain or in direct communication with the river, addition of mineral fertilizers, and other anthropogenic factors are among the complex variables in the salt balance. However, on a long-term basis, the salt balance is a useful indicator of the overall health of the valleys hydrologic divisions in terms of salt accumulation in soils or shallow groundwater.

The monthly EC_{25} estimates of TDS and major ion concentrations at each gage station are not substitutes for chemical analyses for future studies. Changes in water use and in aquifer sources may cause the relationships presented here to change with time. However, EC_{25} measurements allow close approximation of missing data to produce continuous and consistent water

quality information for mass balance analysis. The TDS and ion conversions from EC_{25} can be used for future monitoring efforts; but regular checks are needed to ensure that EC_{25} derived from TDS and the monthly ion ratios for each site are not changing significantly.

4.2 RIO GRANDE PROJECT

Lee (1907) stated, “The Rio Grande is essentially a storm-water stream, subject to great and sudden floods.” Between 1897 and 1905, the annual Rio Grande discharge at El Paso varied from a minimum of 50,768 acre-feet (ac-ft) in 1902 to 2,011,794 ac-ft in 1905. Slichter (1905) reported that the river was dry for several months in 1904 at El Paso, Texas. To address fluctuations and depletions of the Rio Grande with long-term storage, Elephant Butte Dam construction began in 1915 with completion in 1916 (Elephant Butte Irrigation District 1998). Today, Elephant Butte Reservoir can store approximately 2 million ac-ft of water (EBID 1998).

Flows into the reservoir still vary dramatically. The minimum inflow (114,100 ac-ft in 1951) was only 4% of the maximum inflow (2,831,000 ac-ft in 1941). Hamilton and Maddock (1993) reported the average inflow from 1915 to 1990 as 872,588 ac-ft with a standard deviation of 537,969 ac-ft. Hamilton and Maddock (1993) state, “this high standard deviation reflects the incredibly variable nature of annual precipitation events and runoff within the region.” Outflows are managed or regulated releases. The average release from 1915 to 1990 was 723,147 ac-ft with a standard deviation of 265,537 ac-ft (Hamilton and Maddock 1993).

Completed in 1938, Caballo Dam is located about 25 miles downstream of Elephant Butte. Caballo Reservoir can store 343,990 ac-ft of water (EBID 1998). Its operations allocate the Rio Grande flow into the downstream Rincon, Mesilla and El Paso valleys. However, flow releases out of Caballo are dependent upon releases from Elephant Butte. Elephant Butte includes a hydroelectric power plant; consequently, water is normally released throughout the year. Winter

releases from power generation are then stored in Caballo for agricultural use during the irrigation season.

Between 1938 and 1989, the average release from Caballo was 667,792 ac-ft (Hamilton and Maddock 1993). Wilson and others (1981) report that 97% of Caballo releases occur during the irrigation season between March and September. Outflow from the Mesilla Valley is represented by discharge of the Rio Grande at El Paso, Texas.

The flow of the river at El Paso reflects a combination of reservoir releases from Caballo, canal wastes, irrigation water returned to the river from drain systems, discharge to the river from ephemeral tributaries, and sewage discharges from Las Cruces and Anthony. Rio Grande flow depletions between Caballo and El Paso reflect the amount of water that is consumptively used by crops and natural vegetation, evaporated from surface waters, recharged to groundwater, minus tributary water and groundwater inflow. The total depletion is calculated as outflow from Caballo minus flow past El Paso.

4.2.1 Physical Description

The Project provides irrigation water to the Rincon, Mesilla, and El Paso valleys and includes the river and a complex network of canals, laterals, and drains (Fig. 4.1). Canals and laterals deliver water to agriculture, while drains collect groundwater from agricultural areas to remove salt, to prevent soil water logging, and to return excess irrigation water for further use downstream. The system is gravity driven. Mostly unlined canals deliver water at higher elevation than the surrounding fields for efficient distribution of water. The drains receive water at lower elevation than the surrounding fields and canals, returning unused irrigation water. Drain water represents the diverted water in canals minus operational spills, consumptive water use by crops and natural vegetation, evaporation from surface water in both the canals and drains, and recharge to groundwater. In addition to the manmade features, there are several major ephemeral streams within the Project, including Percha Creek and Rincon

Arroyo, which can add significant flows to the Rio Grande after major precipitation events.

The Project extends along the Rio Grande from Caballo to the El Paso Hudspeth County line in Texas, a distance of 154 river miles (Fig. 4-1). The project is separated into three divisions by natural valley constrictions. The upper division or Rincon Valley starts at Caballo and extends downstream about 45 miles to Leasburg Dam. The middle division includes the Mesilla Valley and starts at Leasburg Dam and ends 63 miles south at the American Dam just above El Paso. The lower division extends across the upper El Paso Valley and starts at the American Dam and ends 46 miles downstream on the United States side of the Rio Grande to the El Paso-Hudspeth County line. The total irrigated area in the Project is approximately 159,650 acres, with 90,640 acres in the EBID and 69,010 acres in the El Paso County Water Improvement District (EPCWID).

The Caballo supplies two very small irrigation systems that pre-date the Project. The Bonito Lateral diverts water directly from Caballo; and the Percha Lateral diverts water from Percha Diversion Dam on the Rio Grande. The water delivered to the systems is not counted as part of the release from Caballo. Because water diversions are very small, it is believed that any influences on the Rio Grande salt balance are negligible.

EBID water for the Rincon Valley is diverted at Percha Diversion Dam approximately two miles downstream from Caballo. The Rincon Valley Main Canal carries water for the irrigation of 16,260 acres and has an initial capacity of 350 cubic feet per second (cfs).

Leasburg Dam diverts water into the Leasburg Canal near Radium Springs, which is 13.7 miles long with an initial capacity of 625 cfs, and irrigates 31,600 acres of the upper Mesilla Valley. The Mesilla Diversion Dam, approximately six miles south of Las Cruces and 40 miles north of El Paso, diverts water into the East Side and West Side Canals for delivery to the lower 53,650 acres in the Mesilla Valley. The distribution area of the Mesilla Dam system includes 42,770 acres in EBID and 10,880 acres in EPCWID. The East Side Canal is 13.5 miles long and has an initial capacity of 300 cfs. The West

Side Canal is 23.5 miles long and has an initial capacity of 650 cfs. Near its terminus, the West Side Canal system crosses beneath the Rio Grande channel through the Montoya Siphon.

Water for the El Paso Valley and Mexico is diverted at the American Diversion Dam two miles northwest of El Paso. The American Diversion Dam location is immediately above the point where the Rio Grande becomes the designated international boundary with Mexico. The American Canal is operated by the U.S. Section of the International Boundary and Water Commission (IBWC) in order to regulate delivery of water to Mexico in accordance with treaty provisions. The American Canal carries water 2.1 miles from the dam to the head of Franklin Canal. The initial capacity of the American Canal is 1,200 cfs. The Franklin Canal, serving 17,000 acres in the upper portion of the El Paso Valley, is 28.4 miles long and has an initial capacity of 325 cfs.

The Riverside Diversion Dam, the southernmost Project diversion is on the Rio Grande 15 miles southeast of El Paso and delivers water into the 17.2-mile long Riverside Canal with an initial capacity of 900 cfs. The Riverside Canal serves 39,000 acres in the lower portion of the El Paso Valley. Overflow from the EPCWID is delivered to the Hudspeth County Conservation and Reclamation District (HCCRD). The Tornillo Canal, a continuation of Riverside Canal, is 12 miles long and has an initial capacity of 325 cfs and accommodates excess flow from the Riverside Canal. The Riverside Diversion has not been used extensively since storm flows in the 1980s damaged the structure.

The HCCRD provides irrigation water to 18,000 acres. While the HCCRD is not a part of the Project, it does store and divert storm waters, drain flows, and canal tail water from EPCWID.

Final delivery of water to Mexico is provided to the Acequia Madre or Mexican Canal at the International Dam in El Paso that is located about 2 miles below the American Dam. Mexican farmers supplement the river diversion with sewage effluent from Ciudad Juarez and groundwater.

4.3 PREVIOUS STUDIES

From 1934 to 1963, L.V. Wilcox of the U.S.D.A. Salinity Laboratory in Riverside, California, systematically collected salinity data within the Project area. Wilcox worked primarily with U.S. Bureau of Reclamation (BuRec) personnel, who managed the Project at that time. BuRec personnel responsible for gate settings and flow measurement collected a small standard sample volume each day and poured it into a gallon jug at each collection site. At the end of the month, Wilcox collected all of the jugs and took them to a central laboratory in El Paso where the jugs were analyzed for EC_{25}, TDS by filtration and residue on evaporation, and major ions by standard methods. The Wilcox (1968) data represent a time-weighted monthly average rather than a flow-weighted monthly average. While a flow-weighted average would be preferable for determining the salt balance, errors introduced by the time-weighted average are small and unbiased, assuming no major changes in dissolved ions occur with changes in flow over a monthly cycle sampling. Hernandez (1976) compiled historical water quality data and periodically collected water quality samples from the major drains, canals, and effluent discharges in the Rio Grande for one year (1975). Water samples were taken in March, June, September, late October, and late December of 1975 at 45 stations from San Marcial to the head gate of the Riverside Canal. The sample timing characterized the varying seasonal water quality associated with the annual irrigation cycle.

Some of the pertinent findings of the Hernandez (1976) study are: (1) downstream increases in TDS and concentrations of both anions and cations in the river, (2) a distinct seasonal variation in TDS in the river and canal samples, (3) a general to inconsistent relationship between the ions and TDS, (4) greater downstream seasonal variations in quality, and (5) water quality degraded with low flow and improved during high flow that is associated with upstream reservoir water release and major storm precipitation events. One recommendation made by Hernandez (1976) was that an analysis be performed to determine the ratio of TDS to EC_{25} for sampling stations as a possible quick, efficient, and economic

method to monitor and supplement future water quality studies for greater detail and continuity.

The study by Miyamoto and others (1995), conducted for the years 1969-1989, focused on flow and water quality in the Rio Grande from El Paso to the Gulf of Mexico and was based on data obtained from the IBWC. Some of the significant findings include: (1) salt is the major constraint for full utilization of the Rio Grande, (2) salinity is increasing steadily at significant rates, (3) salinity is flow dependent at El Paso and Ft. Quitman, (4) salinity of the Rio Grande at El Paso averaged 1,000 mg/L and increases to around 3,000 mg/L at Ft. Quitman, (5) salinity decreases during the March 15 to September 15 irrigation season and increases during the rest of the year, and (6) salts are accumulating in the soils and shallow groundwater along the El Paso to Ft. Quitman stretch of the Rio Grande and will probably continue to accumulate.

4.4 METHODOLOGY

4.4.1 Data

Data used in this study are taken from reports compiled by Wilcox (1968), Hernandez (1976), and directly from the U.S. Geological Survey (USGS) for river gage stations at San Marcial, New Mexico below Elephant Butte Dam, below Caballo Dam, above Leasburg Dam, at the Courchesne Bridge in El Paso, Texas and at Ft. Quitman, Texas. Flow measurements and water quality are also compiled from the USGS, BuREC, and IBWC for the consistently recorded gage stations in the 1934 to 1963 time frame. Monthly flow measurements are associated with very little water quality data from 1963 to 1980. The stations at Courchesne Bridge and Ft. Quitman were the exceptions. At the Courchesne Bridge, the data are complete from January 1934 through September 1994 and at Ft. Quitman, from January 1934 through March 1988. From 1980 through 1994 only TDS measurements are available. After 1994, the water quality data are incomplete. Since the data are not continuous after 1963, the 30-year period from 1934 to 1963 serves as a bench mark or guide in this study for estimating missing ion and TDS data.

The data compiled and published by Wilcox (1968) and Hernandez (1976) were compared with original USGS and BuRec records. When differences were found, comparisons were made with adjacent measurements and the corresponding months of other years to determine which values were most likely the correct ones. In the few cases that remained questionable, the USGS data were used, except for the bicarbonate ion data at El Paso. The data published by the USGS are reported as equivalent carbonate concentration and values differed consistently by a factor of two from Wilcox (1968) and Hernandez (1976). This reflects the charge difference between carbonate (CO_3) and bicarbonate (HCO_3) as reported by the agencies analyzing the samples. Conversions were made to obtain consistent data in terms of bicarbonate concentration since bicarbonate is the dominant species at typical pH ranges for the Rio Grande.

With multiple data analysis for the same month, a time-weighted average was calculated and used for that month. In cases of occasional missing measurements or a short series of missing measurements, straight-line interpolation was used to complete the series. This method was used only to obtain TDS data.

Where conflicting data from different sources are available for a given month, the measurement that is most consistent with other temporally adjacent measurements is chosen.

Several gaps (TDS or individual ions) occurred in the available data. For short gaps, four months or less, missing data were estimated as described above. Where larger gaps occurred, no attempt was made to estimate the missing data. The data from hard-copy records in Wilcox (1968), Hernandez (1976), and the USGS are organized into Microsoft Excel® spreadsheets. As a means of checking for discrepancies, the individual ion concentrations are summed with the total ions reported as a percentage of TDS. When summed ions exceed 100%, the measurements for each individual ion are checked against the hard copy records from all sources. In most cases, the errors are relatively easy to detect and correct. However, in those remaining cases where it is not possible to determine the correct numbers with an acceptable degree of

certainty, the numbers are left as they are reported. When available, the USGS measurements are selected as the final choice**.** Data compiled are included in Appendix C.

4.4.2 Salinity-Ratio of TDS to EC_{25}

During the years from 1934 to 1963, EC_{25} measurements with units of microsiemens per centimeter (μS/cm at 25°C) are compiled concurrently with chemical analyses for each month at each of the Rio Grande gage stations and the major drains. The Wilcox (1968) data for both the gage stations and the drains represents approximately 3,800 chemical analyses taken monthly over the thirty-year span. After discarding the anomalies with total ion sums values exceeding 100% of TDS, statistical analyses were performed as a means of evaluating the results. There are some instances where only EC_{25} measurements are recorded. In these cases, the TDS is estimated from empirical EC_{25} conversion ratio (see Appendix C).

4.4.3 Individual Ions as a Percentage of TDS

Ratios of the major individual ions to TDS are calculated for all stations for each month, using complete data sets for 1934 to 1963. The ion/TDS ratios allow estimates for missing measurements for the years after 1980.

Estimated values and measured values are compared with the data for El Paso to check accuracy. This record is used to check accuracy because of the relative completeness for the 1934 to 1994 time frame. The estimated monthly ion/TDS ratios for each ionic species for El Paso are shown in Table 4-1. Except for bicarbonate in June and July, there is overlap of the 95% confidence intervals between the measured and estimated ion values for all twelve months in the El Paso record. Based upon the El Paso record it is assumed that estimated ion/TDS ratio values provide reliable data.

Table 4-1. Estimated average monthly ion/TDS ratios at Courchesne Bridge

Month/Ion	Ca	Mg	Na	HCO_3	SO_4	Cl
Jan	0.0826	0.0201	0.2239	0.0958	0.3174	0.2052
Feb	0.0841	0.0201	0.2183	0.0964	0.3226	0.1966
Mar	0.1132	0.0246	0.1936	0.1270	0.3434	0.1754
Apr	0.1152	0.0253	0.1872	0.1293	0.3462	0.1611
May	0.1091	0.0248	0.1839	0.1244	0.3376	0.1568
Jun	0.1125	0.0243	0.1754	0.1326	0.3312	0.1463
Jul	0.1115	0.0245	0.1749	0.1360	0.3264	0.1446
Aug	0.1121	0.0239	0.1717	0.1368	0.3196	0.1440
Sep	0.1081	0.0234	0.1816	0.1258	0.3228	0.1579
Oct	0.0887	0.0210	0.2096	0.1020	0.3198	0.1907
Nov	0.0869	0.0205	0.2163	0.1006	0.3184	0.1970
Dec	0.0870	0.0205	0.2144	0.1014	0.3138	0.1960

4.4.4 Salt Balances

Cumulative mass discharge in metric tons of total salts (TDS) or major ionic species is calculated for each month at each gage station by the following formula:

Mass discharge = (TDS or ion (mg/L)) X (Volume flow (L)) X (10^9)

The salinity balances or changes in salt storage (salt mass inflow – salt mass outflow) is presented for the following Project segments:

1) San Marcial to Elephant Butte,
2) Elephant Butte to Caballo,
3) Caballo to Leasburg,
4) Leasburg to El Paso,
5) El Paso to Ft. Quitman,
6) Elephant Butte to El Paso.

The cumulative mass discharge estimates are analyzed for seasonal trends, for long-term yearly trends within individual segments, and for comparison of temporal trends between Project segments.

4.5 RESULTS AND INTERPRETATIONS

The time gap from 1963 to 1980 in the water quality data requires starting over at "time zero" in 1980 for establishing cumulative salt and ion balance trends. However, there is value in comparing the relationships observed during each of the periods of active data collection. Because the analyses were performed over a relatively long period of time by different researchers and organizations, data used in this study have some inherent variation and errors due to different collection procedures and methods for chemical analysis.

4.5.1 EC_{25} to TDS Conversion Factor

For thirty years between 1934 and 1963, monthly EC_{25} measurements were obtained along with sample chemical analyses. A conversion ratio between TDS and EC_{25} of 0.66 was statistically derived from 3,573 measurements from all stations reporting in the Project. The relationship is as follows:

TDS (mg/L) = (EC_{25} as µS/cm) x (0.66)

The statistical analysis for determining this ratio is summarized in Table 4-2.

Table 4-2. Statistical analysis summary of the ratio of TDS to EC_{25}

Number Measure-ments	TDS/EC_{25} Ratio	Standard Deviation	Confidence 95% Interval Lower	Upper	Confidence 99% Interval Lower	Upper
3573	0.6581	0.0332	0.6570	0.6592	0.6567	0.6595

The 99% confidence interval for the mean ratio of TDS (mg/L) to EC_{25} (µS/cm at 25° C) measurements is between 0.657 and 0.660 or 0.66 when rounded to two significant figures. Miyamoto and others (1995) found the same ratio of 0.66 for the Rio Grande water for the reach from Ft. Quitman to Brownsville in the time interval from 1969 to 1989. However, the ratio during the same time frame for data

of El Paso was 0.69 (Miyamoto et al. 1995). On the other hand in this study, the 1934-1963 data for El Paso station shows no change in the ratio from 0.66.

4.5.2 Results of Ion/TDS Ratio Analysis

Simple averages of ion/TDS ratios for the Wilcox (1968) data from 1934 to 1963 for each major ion species at each gage station are analyzed. When the estimates are compared with the actual measurements at El Paso, significant seasonal variations are observed with ion/TDS ratios versus month (Figure 4-2).

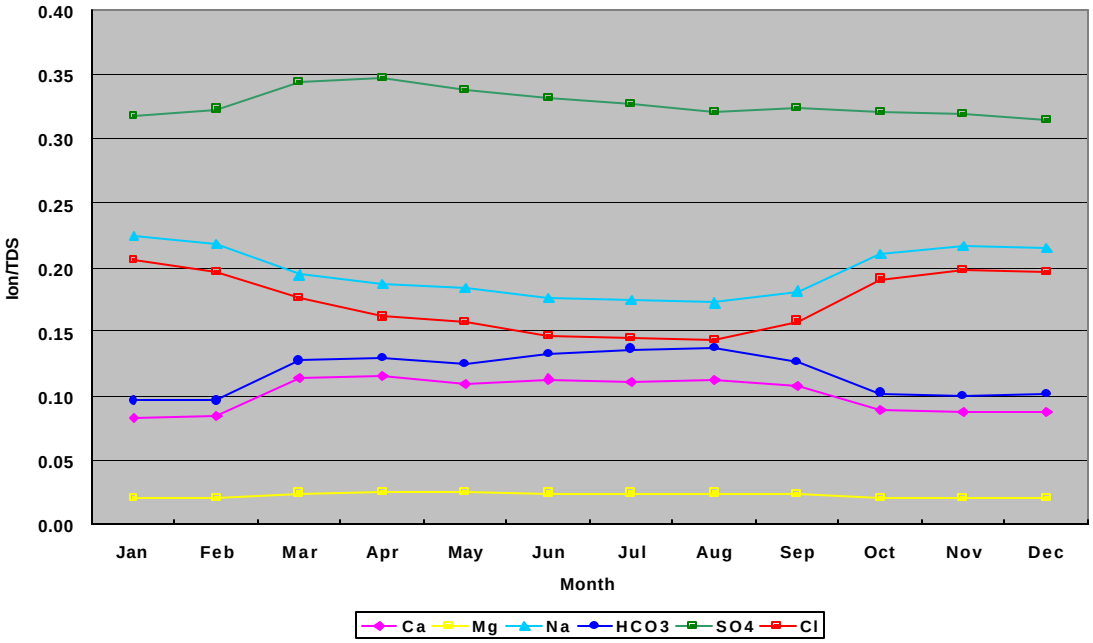

Figure 4-2. Seasonal variation of ion to TDS ratios (average, n =30) in the Rio Grande at Courchesne Bridge

The Na/TDS and Cl/TDS ratios both decrease into the peak of the irrigation season from March through September while at the same time Ca/TDS and HCO_3/TDS ratios increase. On the other hand, the ion/TDS ratios for data below Elephant Butte Dam are relatively constant through the year (Fig. 4-3). Return flows are probably responsible for the monthly changes in ion/TDS ratios at El Paso.

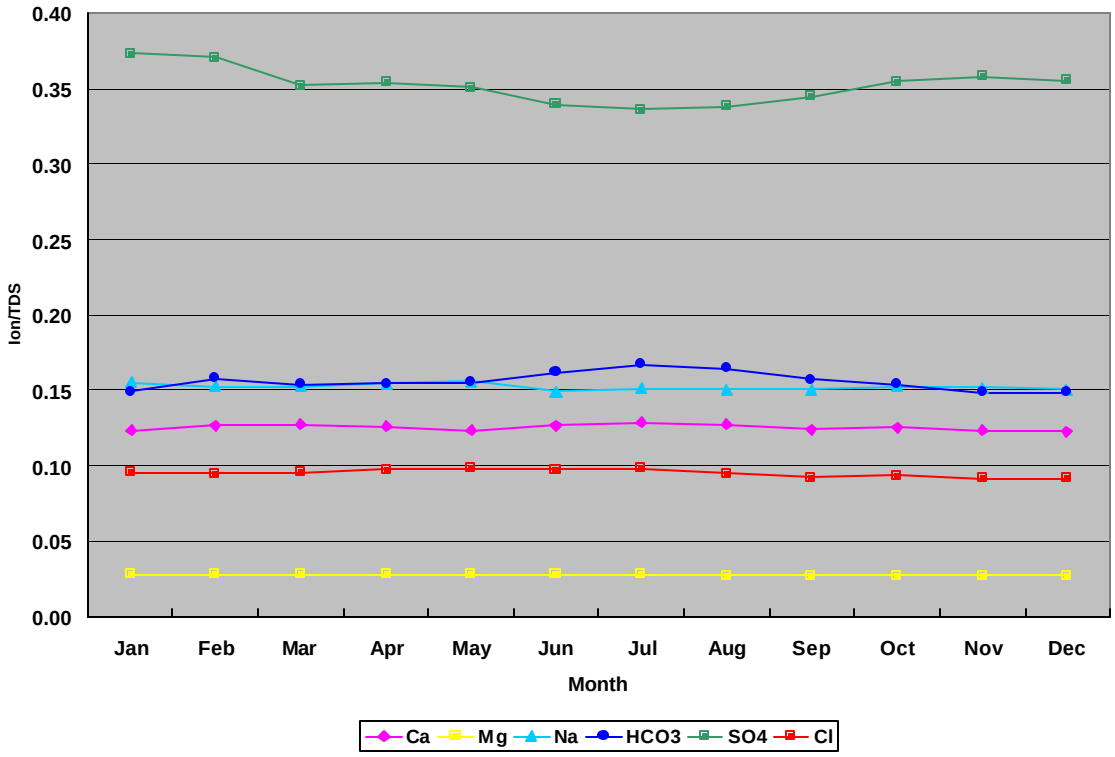

Figure 4-3. Seasonal variation of ion to TDS ratios (average, n = 30) in the Rio Grande below Elephant Butte Dam

In addition to seasonal variations, comparison of Figures 4-2 and 4-3 show differences in overall ion/TDS ratio chemistry between the EBD and ELP. Hernandez (1976) also observed that the ion/TDS ratios change downstream in the Project. These changes are best observed in Figure 4-4. Annual averages for each ion/TDS ratio show minor variability at downstream measurement sites below San Marcial until the El Paso gage station. From El Paso to Ft. Quitman, the Cl/TDS and Na/TDS ratios dramatically increase while the SO_4/TDS, HCO_3/TDS, and Ca/TDS ratios decrease. Because the exact ion/TDS ratios are site-specific, the average monthly ratios for all the gage stations used in this study are shown below in Tables 4-3 to 4-8.

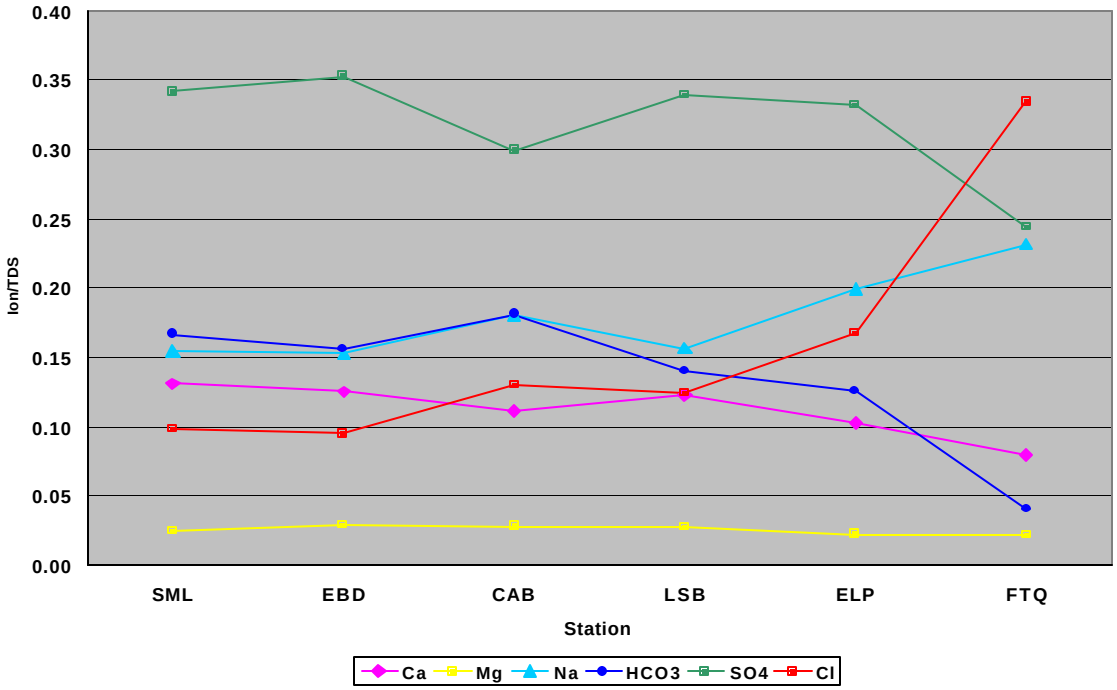

Figure 4-4. Annual average ion to TDS ratios in the Project (1934-1963). Stations are Rio Grande at San Marcial; Rio Grande below Elephant Butte Dam; Rio Grande below Caballo Dam; Rio Grande above Leasburg Dam; Rio Grande at Courchesne Bridge, Rio Grande at Ft. Quitman.

.

Table 4-3. Ion/TDS ratios of Rio Grande at San Marcial

Month/Ion	Ca	Mg	Na	HCO_3	SO_4	Cl
Jan	0.1324	0.0252	0.1546	0.1812	0.3107	0.1129
Feb	0.1317	0.0250	0.1557	0.1804	0.3210	0.1066
Mar	0.1299	0.0260	0.1573	0.1774	0.3257	0.1019
Apr	0.1310	0.0259	0.1546	0.1829	0.3157	0.1045
May	0.1354	0.0250	0.1430	0.1957	0.2869	0.0961
Jun	0.1311	0.0255	0.1502	0.1828	0.3117	0.0994
Jul	0.1321	0.0255	0.1543	0.1807	0.3204	0.1048
Aug	0.1329	0.0251	0.1475	0.1187	0.4242	0.0780
Sep	0.1285	0.0250	0.1567	0.1287	0.4225	0.0815
Oct	0.1279	0.0263	0.1747	0.1489	0.4105	0.0993
Nov	0.1332	0.0254	0.1566	0.1807	0.3297	0.1037
Dec	0.1383	0.0261	0.1489	0.1866	0.3167	0.1035

Table 4-4. Ion/TDS ratios Rio Grande below Elephant Butte Dam

Month/Ion	Ca	Mg	Na	HCO_3	SO_4	Cl
Jan	0.1233	0.0276	0.1550	0.1489	0.3730	0.0958
Feb	0.1263	0.0277	0.1527	0.1579	0.3709	0.0944
Mar	0.1273	0.0276	0.1525	0.1534	0.3525	0.0958
Apr	0.1255	0.0277	0.1540	0.1541	0.3535	0.0969
May	0.1236	0.0278	0.1558	0.1552	0.3506	0.0981
Jun	0.1266	0.0281	0.1496	0.1620	0.3396	0.0974
Jul	0.1285	0.0277	0.1509	0.1669	0.3365	0.0981
Aug	0.1272	0.0270	0.1502	0.1640	0.3382	0.0951
Sep	0.1242	0.0270	0.1503	0.1572	0.3448	0.0926
Oct	0.1247	0.0271	0.1527	0.1531	0.3544	0.0932
Nov	0.1233	0.0266	0.1516	0.1487	0.3583	0.0916
Dec	0.1226	0.0269	0.1502	0.1484	0.3558	0.0917

Table 4-5. Ion/TDS ratios in the Rio Grande below Caballo Dam

Month/Ion	Ca	Mg	Na	HCO_3	SO_4	Cl
Jan	0.0859	0.0306	0.2228	0.2154	0.2528	0.1501
Feb	0.0909	0.0301	0.2109	0.2027	0.2663	0.1444
Mar	0.1264	0.0269	0.1580	0.1539	0.3210	0.1333
Apr	0.1269	0.0273	0.1534	0.1579	0.3362	0.1139
May	0.1238	0.0277	0.1563	0.1587	0.3330	0.1132
Jun	0.1248	0.0275	0.1548	0.1620	0.3320	0.1108
Jul	0.1244	0.0276	0.1560	0.1666	0.3284	0.1100
Aug	0.1279	0.0270	0.1533	0.1715	0.3144	0.1122
Sep	0.1264	0.0271	0.1579	0.1695	0.3165	0.1195
Oct	0.0922	0.0287	0.2100	0.1925	0.2714	0.1497
Nov	0.0904	0.0295	0.2177	0.2060	0.2598	0.1533
Dec	0.0902	0.0302	0.2180	0.2138	0.2539	0.1503

Table 4-6. Ion/TDS ratios in the Rio Grande above Leasburg Dam

Month/Ion	Ca	Mg	Na	HCO_3	SO_4	Cl
Jan	0.1216	0.0254	0.1596	0.1156	0.3551	0.1424
Feb	0.1232	0.0265	0.1586	0.1313	0.3554	0.1287
Mar	0.1283	0.0257	0.1537	0.1504	0.3234	0.1221
Apr	0.1273	0.0263	0.1548	0.1424	0.3278	0.1154
May	0.1239	0.0262	0.1573	0.1449	0.3331	0.1157
Jun	0.1239	0.0268	0.1564	0.1402	0.3379	0.1182
Jul	0.1282	0.0269	0.1542	0.1591	0.3334	0.1131
Aug	0.1297	0.0258	0.1521	0.1554	0.3220	0.1137
Sep	0.1260	0.0272	0.1550	0.1493	0.3230	0.1233
Oct	0.1220	0.0254	0.1599	0.1258	0.3440	0.1356
Nov	0.1231	0.0253	0.1614	0.1212	0.3473	0.1409
Dec	0.1256	0.0253	0.1579	0.1251	0.3501	0.1394

Table 4-7. Ion/TDS ratios in the Rio Grande at Courchesne Bridge

Month/Ion	Ca	Mg	Na	HCO_3	SO_4	Cl
Jan	0.0826	0.0201	0.2239	0.0958	0.3174	0.2052
Feb	0.0841	0.0201	0.2183	0.0964	0.3226	0.1966
Mar	0.1132	0.0246	0.1936	0.1270	0.3434	0.1754
Apr	0.1152	0.0253	0.1872	0.1293	0.3462	0.1611
May	0.1091	0.0248	0.1839	0.1244	0.3376	0.1568
Jun	0.1125	0.0243	0.1754	0.1326	0.3312	0.1463
Jul	0.1115	0.0245	0.1749	0.1360	0.3264	0.1446
Aug	0.1121	0.0239	0.1717	0.1368	0.3196	0.1440
Sep	0.1081	0.0234	0.1816	0.1258	0.3228	0.1579
Oct	0.0887	0.0210	0.2096	0.1020	0.3198	0.1907
Nov	0.0869	0.0205	0.2163	0.1006	0.3184	0.1970
Dec	0.0870	0.0205	0.2144	0.1014	0.3138	0.1960

Table 4-8. Ion/TDS ratios in the Rio Grande at Ft. Quitman

Month/Ion	Ca	Mg	Na	HCO_3	SO_4	Cl
Jan	0.0818	0.0220	0.2282	0.0422	0.2420	0.3320
Feb	0.0804	0.0223	0.2308	0.0362	0.2380	0.3419
Mar	0.0775	0.0228	0.2316	0.0313	0.2305	0.3524
Apr	0.0840	0.0224	0.2271	0.0502	0.2402	0.3492
May	0.0964	0.0230	0.2261	0.0718	0.2494	0.3508
Jun	0.0925	0.0217	0.2138	0.0661	0.2450	0.3432
Jul	0.0972	0.0216	0.2106	0.0915	0.2421	0.3335
Aug	0.0936	0.0212	0.2157	0.0987	0.2343	0.3269
Sep	0.0885	0.0226	0.2209	0.0831	0.2419	0.3332
Oct	0.0880	0.0214	0.2244	0.0675	0.2483	0.3237
Nov	0.0850	0.0214	0.2259	0.0560	0.2406	0.3224
Dec	0.0835	0.0214	0.2267	0.0486	0.2461	0.3235

4.5.3 Discussion of Salt Balances in the Rio Grande Project

The cumulative salinity balance for Project segments is shown in Figures 4-5 to 4-10. The time gap from 1964 to 1980 in the data requires resetting the cumulative salt balance at zero in 1979 or 1980 for all segments. The following equation relates major processes that influence chemical mass balance within a Project segment:

River Inflow = River Outflow - Storage - Tributary - Groundwater – Imports

Storage processes relate to chemical mass that is permanently or ephemerally held in reservoirs behind dams and in soils. Storage of chemical mass can have either net positive or negative affect on chemical balance, depending upon storage release relative to river inflow. Tributary processes relate to minor amounts of dissolved solids introduced by ephemeral drainage out of highlands adjacent to the Rio Grande. Groundwater chemical mass balance relates to discharge or recharge processes between shallow groundwater and the river and also contributions from drainage canals. Imports would relate to fertilizers, sewage, and other anthropogenic Rio Grande chemical inputs.

4.5.3.1 San Marcial to Elephant Butte Dam

The TDS salt balance of the San Marcial to Elephant Butte Dam segment exhibits an erratic behavior (Fig. 4-5). However, the individual ion salt balances generally track the trends in the TDS balance. The salt balances trend positive during periods of high flow and trend negative during periods of low flow. A positive balance indicates a mass increase of salts in Elephant Butte Reservoir, but the long-term TDS in the reservoir has not changed. No significant evidence of precipitation of minerals in the reservoir is known. Groundwater outflows could explain some of the discrepancy, but it is unlikely that long-term seepage from the reservoir is large enough to explain the strongly positive balance. On the other hand, if the amount of water held back in storage during high flow exceeds the amount released downstream, the mass salt balance would be positive.

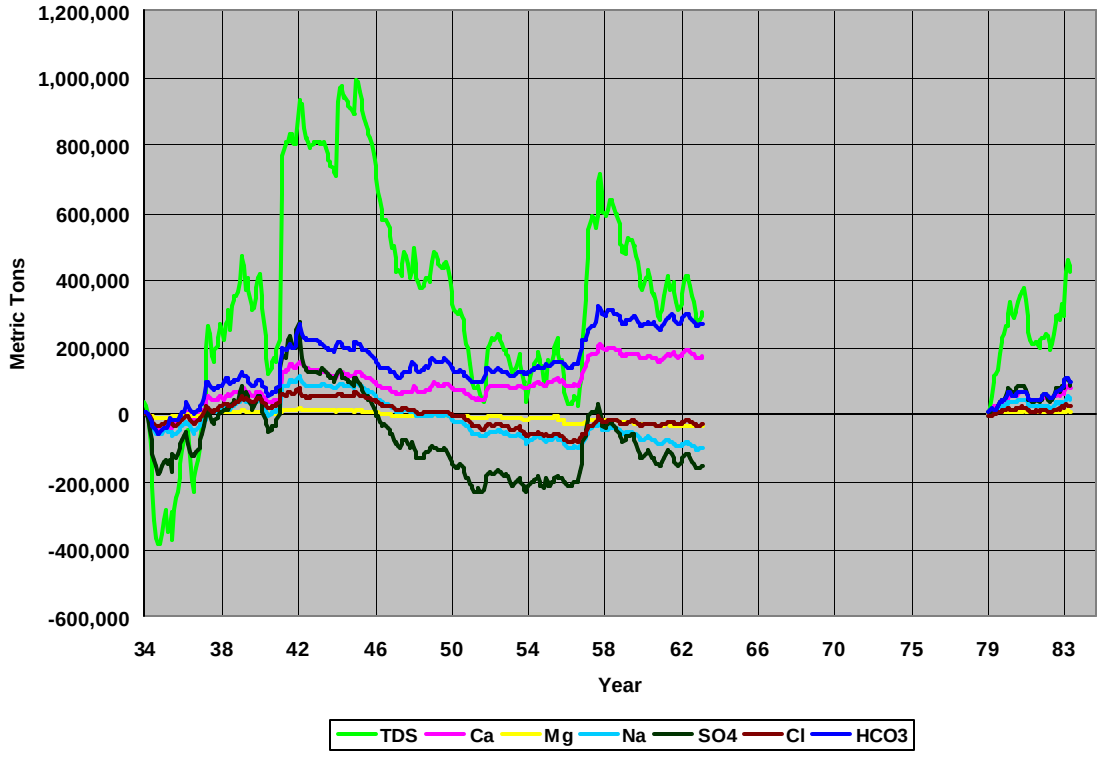

Figure 4-5. San Marcial – Elephant Butte Salt Balance

4.5.3.2 Elephant Butte Dam to Caballo Dam

Except for sulfate (SO_4), salinity balance for the early and late time frames from Elephant Butte Dam to Caballo segment show similar negative salt balance trends (Fig. 4-6). Negative balances may be due in part to tributary flows into Caballo Reservoir from storm runoff. These storm flows would bring salt into the reservoir that did not come out of Elephant Butte Reservoir. Brackish groundwater, especially geothermal, inflow to the Rio Grande at Truth or Consequences between Elephant Butte Dam and Caballo is a possible major contributor to salinity in this stretch. However, a relatively neutral TDS balance coincides with the early to mid-1950s drought. Because of very low flow of the Rio Grande and subsequent low storage in the reservoirs, the system essentially became supported by the local base flow contributed by groundwater and by through flow of the Rio Grande without important reservoir storage fluctuations.

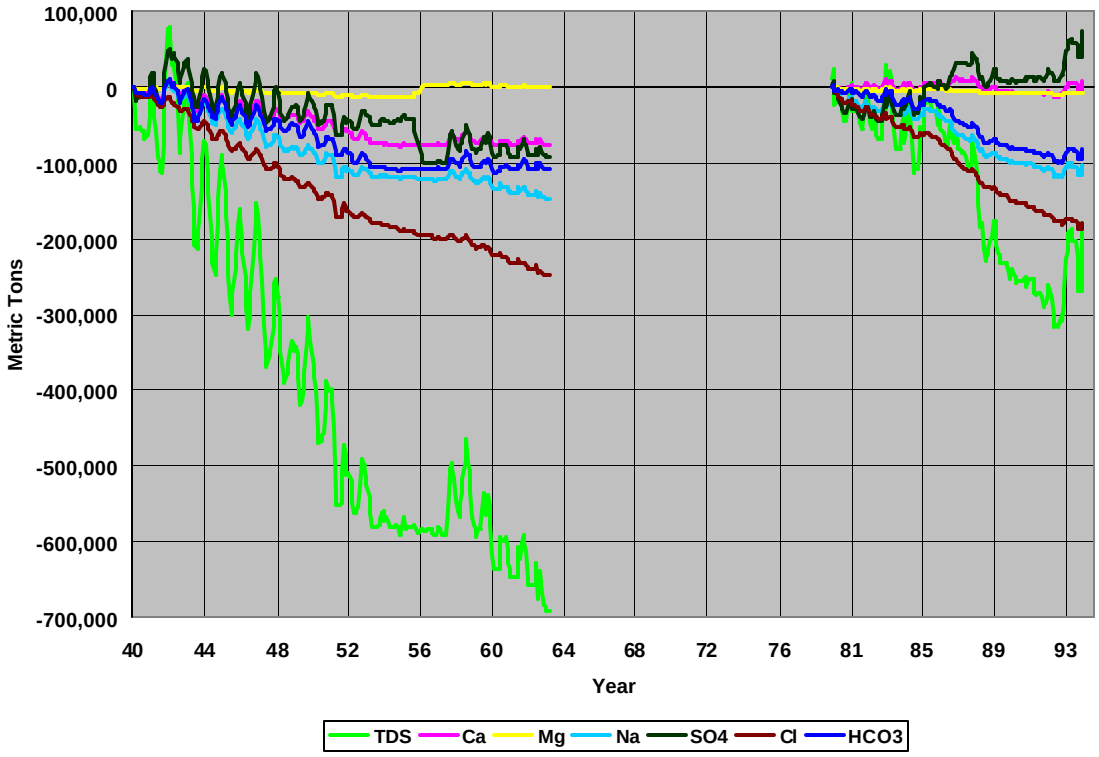

Figure 4-6. Elephant Butte – Caballo Salt Balance

4.5.3.3 Caballo Dam to Leasburg Dam

With the exception of bicarbonate, the salt balances in the Caballo to Leasburg segment follow a negative trend for both time periods (Fig. 4-7). The negative balance indicates flushing of salts out of the valley soils and transport of salts by the Rio Grande downstream. However, the bicarbonate (HCO_3) balance is slightly positive, possibly indicating carbonate mineral precipitation in local soils.

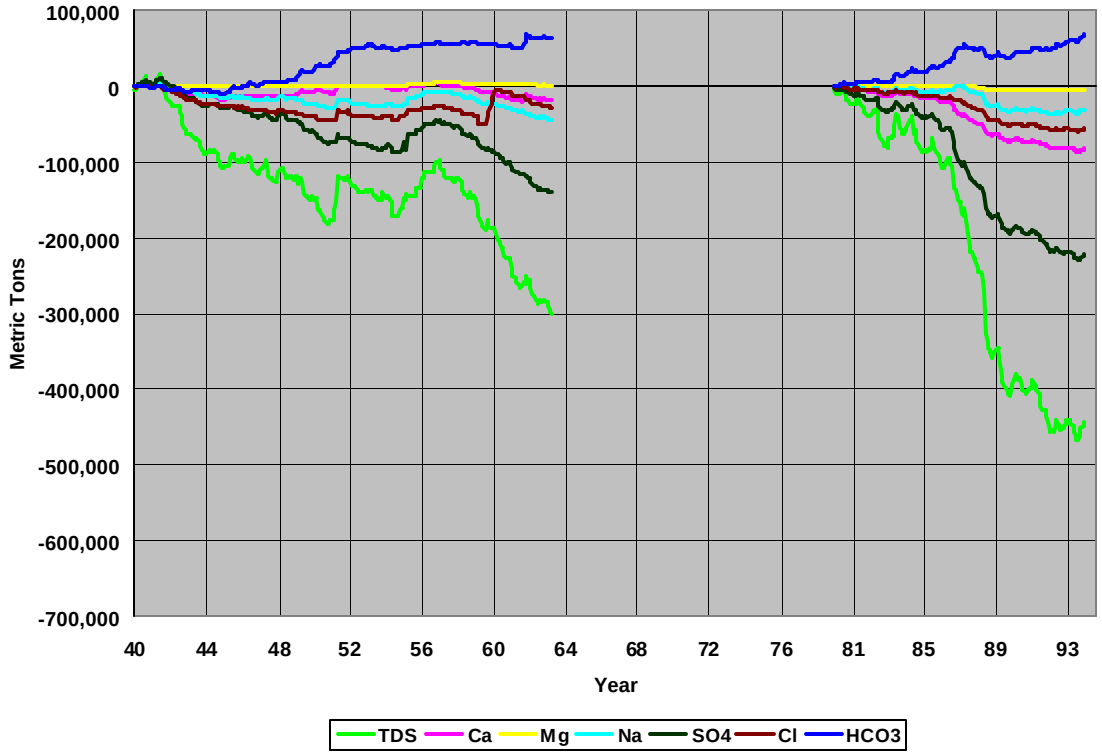

Figure 4-7. Caballo – Leasburg Salt Balance

4.5.3.4 Leasburg to Courchesne Bridge at El Paso

In the Mesilla Valley, there are significant salt balance changes beginning with a severe drought of the 1950s. During this time, local farmers began drilling wells with 1,682 wells in production by 1955. The lack of surface water for aquifer recharge, coupled with pumping of groundwater, produced a drop in groundwater levels that reduced or even eliminated flows from the drains. The TDS salt balance reversed drastically from negative to positive in a relatively short period of time. An average net salt balance increase of approximately 100,000 metric

tons a year is shown in Figure 4-8. Calcium (Ca), sulfate (SO_4), and bicarbonate (HCO_3) show the greatest increase. As a result of continued reliance on groundwater for irrigation and municipal supply, the salt balance since 1980 continues to show a strong positive trend.

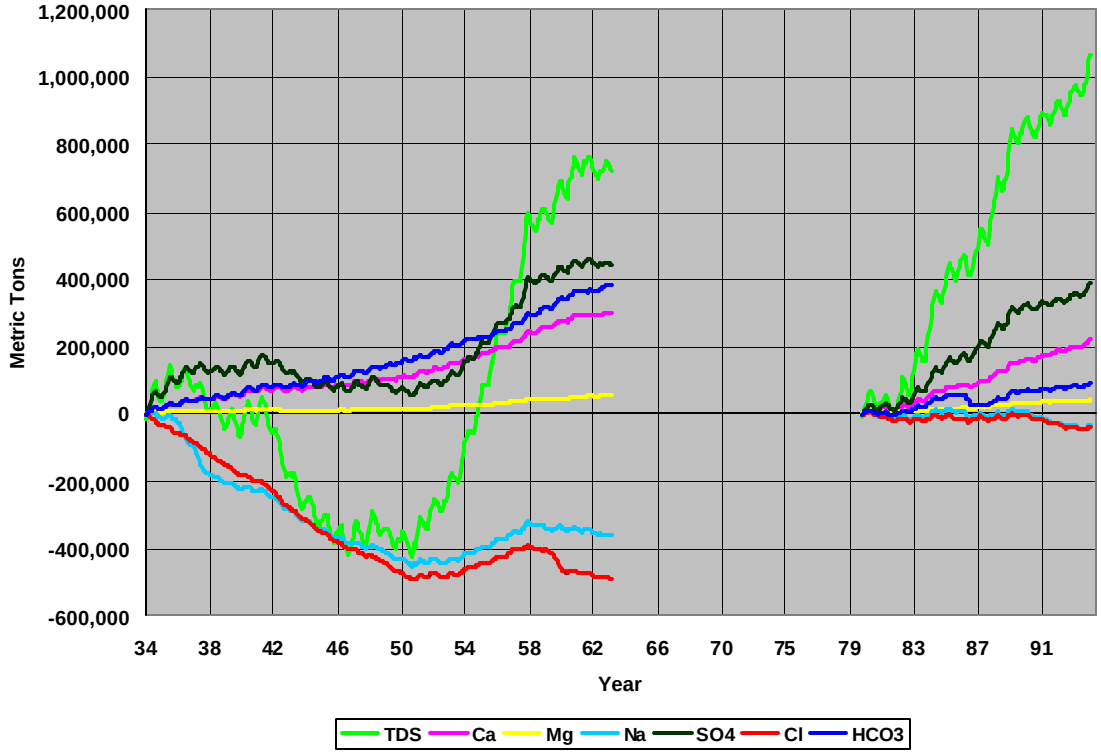

Figure 4-8. Leasburg – Courchesne Bridge at El Paso Salt Balance

4.5.3.5 Elephant Butte to Courchesne Bridge

The salt balance between New Mexico and Texas is presented in Figure 4-9. The New Mexico portion of the Project includes 10,880 acres of water-righted Texas land in the Mesilla Valley. The drought of the 1950s prominently reversed the TDS salt balance from a negative to positive trend. The TDS balance continues to trend positive into the 1990s, indicating salt build up in soils and/or groundwater in the EBID. The individual ion balances follow the same general trends for both time periods. Sodium (Na) and chloride (Cl) exhibit negative balances; while sulfate (SO_4), calcium (Ca) and bicarbonate (HCO_3) show positive balances.

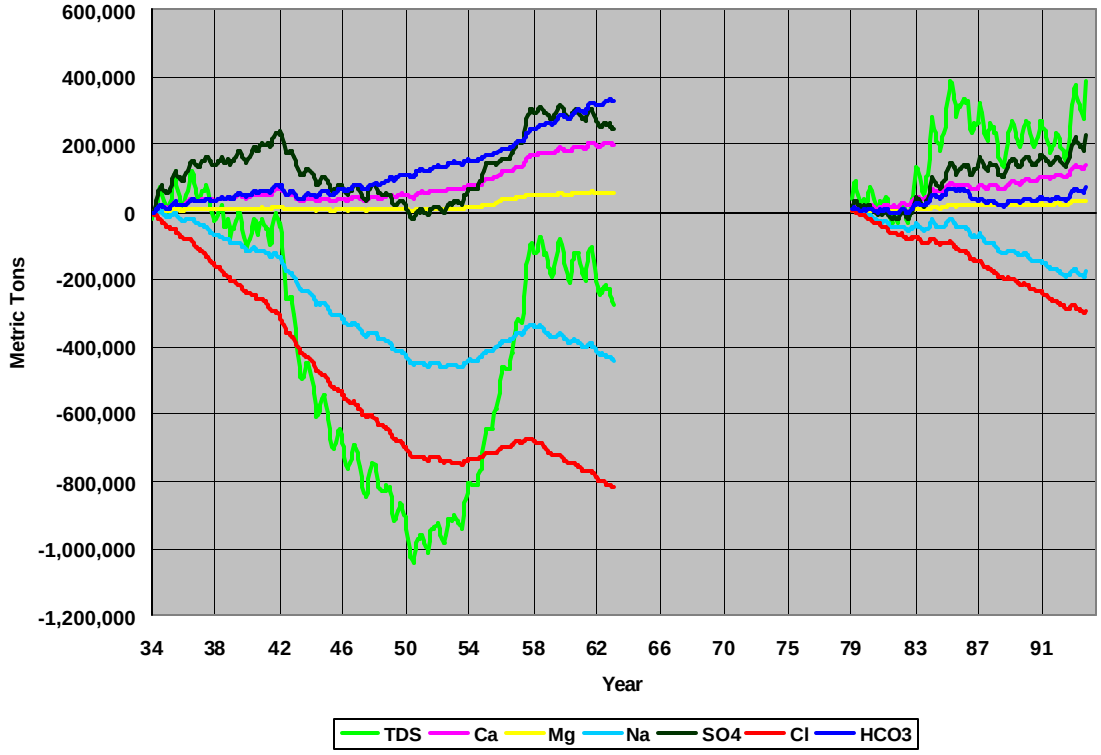

Figure 4-9. Elephant Butte – Courchesne Bridge at El Paso Salt Balance

4.5.3.6 Courchesne Bridge to Fort Quitman

The salt balances from El Paso to Ft. Quitman are shown in Figure 4-10. From 1934 to about 1986, the 50-year salt balances for TDS, sulfate (SO_4), bicarbonate (HCO_3), calcium (Ca), and sodium (Na) show a positive salinity balance trend. The rate of increase is relatively uniform except for sodium. Chloride (Cl) is a notable exception and shows a strong negative balance. In the summer of 1986, TDS shows a strong trend reversal from positive to negative. In 1986, high flows occurred in the Project as a result of spillway over flow and high releases at Elephant Butte Dam. Miyamoto (1995) discusses the effect of this large outflow of salt on the downstream reach of the Rio Grande in detail. Sulfate (SO_4), sodium (Na), and chloride (Cl) ions show major negative salt balance trends. Calcium (Ca), magnesium (Mg), and bicarbonate (HCO_3) ion balance exhibit little mass change. The large flow of fresh water in 1986 flushed out a mass of salt equivalent to the previous 30-year salt accumulation in the El Paso Valley.

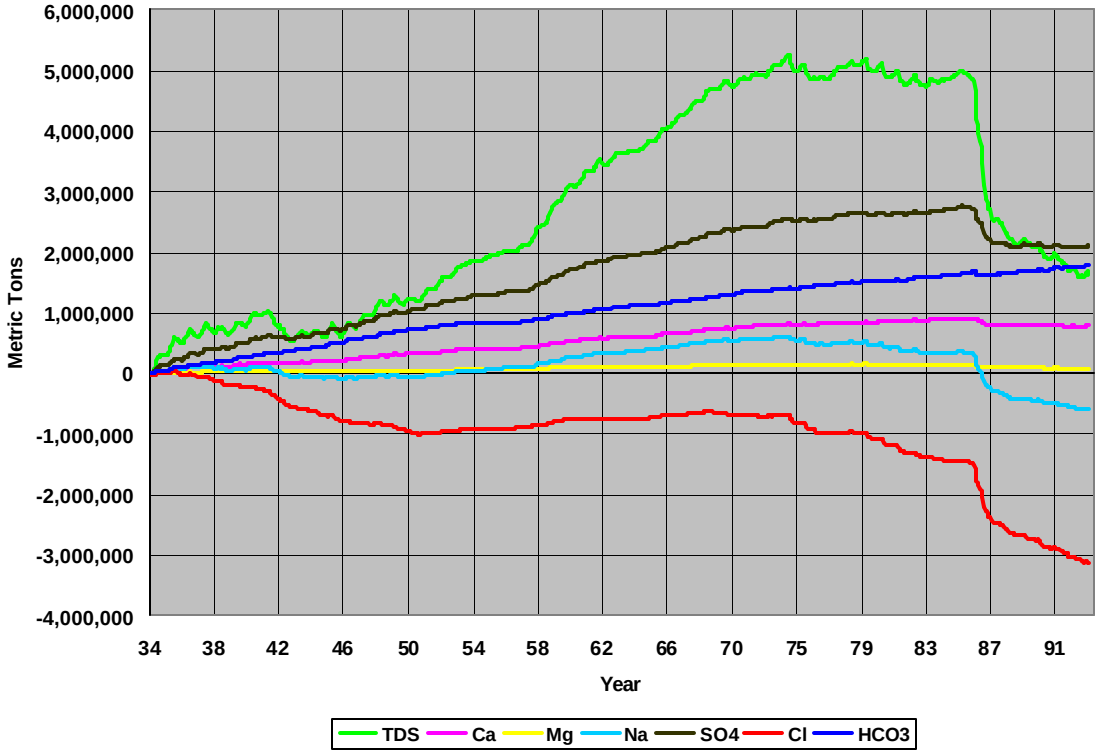

Figure 4-10. Courchesne Bridge at El Paso– Ft. Quitman Salt Balance

4.6 DISCUSSION

A compilation and analysis of all available monthly flow and water quality data from 1934 to the present time at six gage stations along the Rio Grande from San Marcial, New Mexico to Fort Quitman, Texas is presented by this surface water quality study.

A conversion coefficient for relating conductivity EC_{25} (µS/cm) to TDS (mg/L) was developed for the surface waters where TDS (mg/) equals 0.66 times EC_{25} (µS/cm). Gage station specific monthly ratios (ion/TDS) are used to estimate major ion concentrations when only conductivity is reported in the compiled data. This approach allowed for a complete record of ion/TDS for analysis of long-term cumulative salt balance estimates for the major divisions or valleys of the Project. The most dramatic differences in overall ion/TDS ratios occur at El Paso and Ft. Quitman for annual averages between 1934 and 1963.

Cl/TDS and Na/TDS ratios increase while SO_4/TDS, HCO_3/TDS, and Ca/TDS ratios decrease.

Cumulative salt balance for the major divisions represents the mass inflow of salts (ions and TDS) minus the mass outflow of salts. A positive value indicates a build up of salts in the soils and shallow groundwater, while a negative value indicates a flushing of salts in the soils and groundwater from the valley segment. The groundwater component observed is considered to represent the shallow flood plain aquifers that interact with the river and irrigation through canals and drains. No doubt some anthropogenic sources other than irrigation play a role in the ion balance, but the sources are not identified.

The New Mexico portion of the Project (including 10,880 acres of water-righted land in the Texas portion of the Mesilla Valley) had a negative (good) salt balance before 1963. After 1980, it shows a positive (bad) balance. On the other hand, the Texas portion of the Project had a positive balance before the mid 1980s. Excess flow in 1986 removed significant salt from this section, and the balance has been more favorable since.

Continuing data collection is needed to avoid gaps in data such as that occurring from 1964-1980. Salt management planning is needed throughout the Project, both for long-term agricultural sustainability and for managing instantaneous quality for municipal users.

5.0 CONCLUSIONS AND RECOMMENDATIONS

5.1 Summary

The concept of topographically driven groundwater flow as described by Toth (1963) and elaborated upon by Freeze and Witherspoon (1966 and 1967) provides a simple first order and very enlightening view of how salinity evolves in the Mesilla Basin. Local flow systems of Toth (1963) found in the Mesilla Basin interact with the Rio Grande canals and drains on an annual or certainly seasonal basis. The intermediate groundwater flow systems are contained in the aquifers tapped by most deeper and intermediate depth irrigation and municipal water supply wells. Regional groundwater flow is characterized by flow paths of great length and depth. Geothermal water in the area represents a regional groundwater flow system in bedrock that may in fact be intrabasinal in character and also represents a net recharge to the Mesilla Basin. Other thermal water may be interbasinal and be contained in deep, largely confined basin-fill sediments and aquifers. Groundwater flow theory predicts that deep regional flow systems will seep upward and tend to intermingle with local and intermediate groundwater and surface water in the topographically lowest area or discharge region of a groundwater basin. Upward leakage along vertical permeable conduits or hydrogeologic windows into the regional groundwater flow systems may allow intermingling and mixing along the margins of central basin areas. These upflows from regional flow provide major salinity sources to the Mesilla Basin. Salinity from present day evaporation will be largely confined to the shallow local flow systems.

Mixing between thermal and non-thermal groundwater and surface water, dissolution reactions, and ion exchange are major contributors to the Mesilla Basin chemistry. While evaporative concentration of salts is important in surface and very shallow groundwater, mixing with deeper groundwater and geothermal waters is occurring and probably becomes dominant as the southern end of the Mesilla Basin is approached and along the eastern margin of the Mesilla Basin

where known geothermal system outflow is entering shallow aquifers. Further study is required to fully quantify salinity processes.

5.2 Recommendations

Because non-thermal processes are dominant in controlling K and SiO_2 concentrations, mapping of K and SiO_2 concentrations may be very useful to characterize the extent of regions underlain by highly productive arkosic sands in the basin. A comparison of K and SiO_2, with available transmissivity information, would confirm the utility of this hypothesized geochemical approach to blocking out aquifer zones for refined modeling.

Definitive separation and quantification of the evaporative (evapo-transpiration) processes from mixing with geothermal waters for non-thermal groundwater and surface water salinity will require geochemical modeling and additional isotopic study.

Finally, routine water chemistry analysis of the Rio Grande, drains, canals, and groundwater should include the stable isotopes of hydrogen and oxygen, Cl, and Br. Analyses of stable isotopes of hydrogen and oxygen are not expensive. While high precision strontium isotope ratios are expensive to obtain, their value to understanding salinity processes and sources is enormous and should be obtained on selected water samples when budgets allow.

6.0 REFERENCES

Ackerly, N.W. 1998. The evolution of the Rio Grande. In *Proceedings of the 43rd Annual New Mexico Water Conference: Water Challenges on the Lower Rio Grande*. Edited by C.T. Ortega Klett. New Mexico Water Resources Research Institute, Report No. 310, New Mexico State University, Las Cruces, NM. pp. 26-32.

Ackerly, N.W. 2000. Paleohydrology of the Rio Grande: A first approximation. In *Proceedings of the 44th Annual New Mexico Water Conference: The Rio Grande Compact: It's the Law*. Edited by C.T. Ortega Klett. New Mexico Water Resources Research Institute, Report No. 310, New Mexico State University, Las Cruces, NM. pp. 113-123.

Ackerly, N.W., M. Behr, T.L. Powell and P. Bruckhart. 1992. *Irrigation Systems in the Mesilla Valley- An Historical Overview.* Center for Anthropological Research, Report No. 710.

Akermann, H. 1982. Unpublished interpretations of Geophysical Service Inc., Western Division-Midland, TX. Refractions with Vibroseis. U.S. Geological Survey.

Algeo, T.J. 1996. Meteoric water/rock ratios and the significance of sequence and parasequence boundaries in the Gobbler Formation (Middle Pennsylvanian) of south-central New Mexico, in Witzke, B. J., Ludvigson, G. A., and Daly, J., eds., Paleozoic Sequence Stratigraphy: Views from the North American Craton: Geological Society of America Special Paper 306, p. 359-371.

Allen, B.D., S.D. Connell, J.W. Hawley and B.D. Stone. 1998. Core drilling provides information about Santa Fe Group aquifer beneath Albuquerque's West Mesa. *New Mexico Geology*. 20:8-13.

Anderholm, S.K. 1985. *Clay-size fraction and powdered whole-rock X-ray analyses of alluvial basin deposits in central and southern New Mexico*. U.S. Geological Survey Open-File Report 85-163. 18 p.

Anderholm, S.K. 1994. *Ground-water recharge near Santa Fe, north-central New Mexico*. U.S. Geological Survey Water-Resources Investigations Report 94-4078. 68 p.

Anderholm, S.K. 2000. *Mountain-front recharge along the eastern side of the Middle Rio Grande basin, central New Mexico*. U.S. Geological Survey Water-Resources Investigations Report 00-4010. 36 p.

Anderholm, S.K., M.J. Radell and S.F. Richey. 1995. *Water-quality assessment of the Rio Grande Valley study unit, Colorado, New Mexico, and Texas—Analyses of selected nutrient, suspended-sediment, and pesticide data*. U.S. Geological Survey Water-Resources Investigations Report 94-4061. 203 p.

Anthony, E.Y., J.M. Hoffer, W.K. Waggoner and W. Chen. 1992. Compositional diversity in Late Cenozoic mafic lavas in the Rio Grande Rift and Basin and Range Province, southern New Mexico. *Geologic Society of America Bulletin*.104:973-979.

Anthony, E.Y. and J. Poths. 1992. The surface exposure dating and magma dynamics, the Potrillo Volcanic Field, Rio Grande Rift, New Mexico. *Geochimica et Cosmochimica Acta*. 56:4105-4108.

Ashworth, J.B. 1990. *Evaluation of ground-water resources in El Paso County, Texas*. Texas Water Development Board Report 324. 25p.

Balleau, W.P. 1999. Groundwater modeling in the lower Rio Grande. In *Proceedings of the 43rd Annual New Mexico Water Conference: Water Challenges on the Lower Rio Grande*. Edited by C.T. Ortega Klett. New Mexico Water Resources Research Institute, Report No.310, New Mexico State University, Las Cruces, NM. pp.46-38.

Banner, J.L. G.J. Wasserburg, P.F. Dobson, A.B. Carpenter and C.H. Moore. 1989. Isotopic and trace element constraints on the origin and evolution of saline groundwaters from central Missouri. *Geochimica et Cosmochimica Acta*. 53:383-398.

Banner, J.L. G.J. Wasserburg, J.H. Chen and C.H Moore. 1990. ^{234}U-^{238}U-^{230}Th-^{232}Th systematics in saline groundwaters from central Missouri. *Earth and Planetary Science Letters*. 101:296-312.

Beck, M.B., and G. van Straten. 1983. *Uncertainty and Forecasting of Water Quality.* Berlin, Germany: Springer-Verlag.

Bedinger, M.S., K.A. Sargent, and W.H. Langer. 1989. *Studies of geology and hydrology in the basin and range province, Southwestern United States, for isolation of high-level radioactive waste: Characterization of the Rio Grande Region, New Mexico and Texas.* U.S. Geological Survey Professional Paper 1370-C. 42 p.

Betancourt, J.L., T.R. Van Devender, and P.S. Martin. 1990. *Packrat Middens: The last 400,000 Years of Biologic Change*. Tucson, AZ: The University of Arizona Press. 467 p.

Bethke, C.M. 1996. *Geochemical Reaction Modeling*. New York: Oxford University Press. 397 p.

Bexfield, L.M. and S.K. Anderholm. 1997. *Water-quality assessment of the Rio Grande Valley, Colorado, New Mexico, and Texas - ground-water quality in the Rio Grande flood plain, Cochiti Lake, New Mexico, to El Paso, Texas, 1995*. U.S. Geological Survey Water-Resources Investigations Report 96-4249. 93 p.

Birch, F.S. 1980. *Three-dimensional gravity model of basin hydrologic parameters in New Mexico*. Unpublished report prepared for the U.S. Geological Survey by the University of New Mexico under contract 14-08-001-17899. 27 p.

Blackwell, D.D. 1978. Heat flow and energy loss in the Western United States. In *Cenozoic Tectonics and Regional Geophysics of the Western Cordillera: Geological Society of America Memoir 152*. Edited by R.B. Smith and G.P. Eaton. pp. 175-208.

Bothern, L. R. 2003. Geothermal salt intrusion into Mesilla basin aquifers and the Rio Grande, Dona Ana County, New Mexico, USA: Unpub. M. S. Thesis, New Mexico State University, Las Cruces, 127 p.

Bowie, M.W. and V.T. McLemore. 1987. Clay mineralogy of selected sedimentary and volcanic rocks, Socorro County, New Mexico. In *Guidebook to the Socorro area, NewMexico*. Compiled by V.T. McLemore and M.W. Bowie. New Mexico Bureau of Mines & Mineral Resources Guidebook. pp. 46-54.

Box, G.E.P. and G.M. Jenkins. 1976. *Time Series Analysis: Forecasting and Control*. Oakland, CA: Holden-Day.

Bras, R.L. and I. Rodriguez-Iturbe. 1985. *Random Functions and Hydrology*. Reading, MA: Addison-Wesley.

Bryan, K. 1938. Geology and ground-water conditions of the Rio Grande depression in Colorado and New Mexico. In *Rio Grande Joint Investigation in the Upper Rio Grande Basin in Colorado, New Mexico, and Texas*. National Resources Committee, Regional Planning, Part VI. Washington, D.C., U.S. Government Printing Office. 1:part 2:196-225.

Burke, W. H., R.E. Denison, E.A. Hetherington, R.B. Koepnick, H.F. Nelson, and J.B. Otto. 1982. Variation of seawater $^{87}Sr/^{86}Sr$ throughout Phanerozoic time: Geology, v. 10, p. 516-519.

Butcher, D.P. 1990. Geochemistry and Nd-Sr systematics of selected lithologic units of the Oligocene Organ cauldron and batholith, south central New Mexico: unpub. M.S. Thesis, New Mexico State University, Las Cruces, 145 p.

Capo, R.C., B.W. Stewart and O.A. Chadwick. 1998. Strontium isotopes as tracers of ecosystem processes theory and methods: Geoderma, v. 82, p. 197-225.

Castiglia, P.J. and P.J. Fawcett. 2001. Shoreline and lacustrine records of late Quaternary climate change in the Chihuahuan Desert, Mexico. *Eos, Transactions of the American Geophysical Union.* 82:47 [AGU Fall Meeting Supplement, Abstract PP22A-0507. F757].

Chapin, C.E. and S.M. Cather. 1994. Tectonic setting of the axial basins of the northern and central Rio Grande Basin, New Mexico. In *Basins of the Rio Grande Rift—Structure, stratigraphy, and tectonic setting*. Edited by G.R. Keller and S.M. Cather. Geological Society of America Special Paper 291. pp. 5-25.

Chapin, C.E. and W.R. Seager. 1975. Evolution of the Rio Grande rift in the Socorro and Las Cruces areas. *New Mexico Geological Society, 26th Annual Field Conference Guidebook*. pp. 297-321.

Clark, I. and P. Fritz. 1997. *Environmental Isotopes in Hydrogeology*. New York: Lewis Publishers. 328 p.

Cliett, T. 1969. Groundwater occurrence of the El Paso area and its related geology. *New Mexico Geological Society, 20th Annual Field Conference Guidebook*. pp. 209-214.

Cliett, T. and J.W. Hawley. 1996. General geology and groundwater occurrence of the El Paso area. In *Proceedings of the 40th Annual New Mexico Water Conference, "Reaching the Limits: Stretching the Resources of the Lower Rio Grande*." Edited by C.T. Ortega Klett. New Mexico Water Resources Research Institute, Report No. 297, New Mexico State University, Las Cruces, NM. pp. 51-56.

Collins, E.W. and J.A. Raney. 2000. *Geologic map of west Hueco Bolson, El Paso region, Texas*. The University of Texas at Austin, Bureau of Economic Geology, Miscellaneous Map No. 40, scale 1:100,000.

Condie, K.C. and A.J. Budding. 1979. Geology and geochemistry of Precambrian rocks, central and south-central New Mexico: New Mexico Bureau of Mines and Mineral Resources Memoir 35, p. 58.

Connell, S.D., B.D. Allen and J.W. Hawley. 1998. Subsurface stratigraphy of the Santa Fe Group from borehole geophysical logs, Albuquerque area, New Mexico. *New Mexico Geology*. 20:2-7.

Connin, S.L., J. Betancourt and J. Quade. 1998. Late Pleistocene C4 plant dominance and summer rainfall in the southwestern United States from isotopic study of herbivore teeth. *Quaternary Research*. 50:179-193.

Conover, C.S. 1954. *Ground-water conditions in the Rincon and Mesilla Valleys and adjacent areas in New Mexico*. U.S. Geological Survey Water-Supply Paper 1230. 200 p.

Córdoba, D.A., S.A. Wengerd and J.W. Shomaker (editors). 1969. The Border Region (Chihuahua, Mexico, and the United States). *New Mexico Geological Society, 20th Annual Field Conference Guidebook*. 228 p.

Craig, H. 1961. Isotopic variations in meteoric waters: Science, v. 133, p. 1702-1703.

Crumpler, L.S. 2001. Volcanism in New Mexico: An overview. In *Volcanology in New Mexico*. Edited by L.S. Crumpler and S.G. Lucas. New Mexico Museum of Natural History and Science Bulletin. 18:17-29.

Crumpler, L.S. and J.C. Aubele. 2001. Volcanoes of New Mexico: An abbreviated guide for non-specialists. In *Volcanology in New Mexico*. Edited by L.S. Crumpler and S.G. Lucas. New Mexico Museum of Natural History and Science Bulletin. 18: 5-15.

Cuniff, R.A. 1986. *New Mexico State University Geothermal Exploratory Well, DT-3*. Final completion report. Physical Science Laboratory, New Mexico State University, Las Cruces, NM. 151 p.

D'Arrigo, R.D. and G.C. Jacoby. 1992. A tree-ring reconstruction of New Mexico winter precipitation and its relation to El Niño/southern oscillation events. In *El Niño: Historical and paleoclimatic aspects of the Southern Oscillation*. Edited by H.F. Diaz and V. Markgraf. New York: Cambridge University Press. 476 p.

Dansgaard, W. 1964. Stable isotopes in precipitation: Tellus, v. 16, p. 461-469.

Darton, N.H. 1916. *Geology and Undergroundwater of Luna County, New Mexico*. U.S. Geological Survey Bulletin 618. 188 p.

Davis, S.N., D.O. Whittemore and J. Fabyka-Martin. 1998. Uses of chloride/ bromide ratios in studies of potable water: Groundwater, v. 36, no. 2, p. 338-350.

DeAngelo, M.V. and G.R. Keller. 1988. Geophysical anomalies in southwestern New Mexico. *New Mexico Geological Society, 49th Annual Field Conference Guidebook*. pp. 71-75.

Dethier, D.P. 2001. Pleistocene incision rates in the western United States calibrated using Lava Creek B tephra. *Geology*. 29:9:783-786.

Dickinson, W.R. 1970. Interpreting detrital modes of graywacke and arkose. *Journal of Sedimentary Petrology*. 40: 695-707.

Dunham, K.C. 1935. *The geology of the Organ Mountains*. New Mexico Bureau of Mines and Mineral Resources Bulletin 11. 272 p.

Eakin, T.E., D. Price and J.R. Harill. 1976. *Summary appraisals of the nation's groundwater resources - Great Basin region*. U.S. Geological Survey Professional Paper 813-G. 37 p.

Ellis, S.R., G.W. Levings, L.F. Carter, S.F. Richey and M.J. Radell. 1993. Rio Grande Valley, Colorado, New Mexico, and Texas. *Water Resources Bulletin*. 29:4:617-646.

Elston, W. E. 1976. Tectonic significance of mid-Tertiary volcanism in the Basin and Range Province a critical review with special reference to New Mexico, in W.E. Elston and S.A. Northrop, eds., Cenozoic Volcanism in Southwestern New Mexico: New Mexico Geological Society Special Publication 5, p. 93-102.

Elephant Butte Irrigation District (EBID). 1998. General data and information.

Faulds, J.E. and R.J. Varga. 1998. The role of accommodation zones and transfer zones in the regional segmentation of extended terranes. In *Accommodation Zones and Transfer Zones: The Regional Segmentation of the Basin and Range Province*. Edited by J.E. Faulds and J.H. Stewart. Boulder, Colorado. Geological Society of America Special Paper. 323:1-45.

Faure, G. 1986. Principles of Isotope Geology: John Wiley and Sons, Inc., New York, 589 p.

Fenneman, N.M. 1931. *Physiography of the Western United States*. New York: McGraw-Hill Book Co. 534 p.

Feth, J.H. 1964. Hidden recharge. *Groundwater*. 2:4:14-17.

Fisher, R. S. and W.F. Mullican. 1997. Hydrochemical evolution of sodium-sulfate and sodium-chloride groundwater beneath the northern Chihuahuan, Trans-Pecos, Texas, USA. *Hydrogeology Journal*. 5:2:4-16.

Fontes, J. –Ch. 1980. Environmental isotopes in groundwater hydrology, in Fritz, P. and Fontes, J. –Ch., eds, Handbook of Environmental Isotope Geochemistry, Volume 1, The Terrestrial Environment: Elsevier, New York, p. 75-140.

Fournier, R.O. 1960. Solubility of quartz in water in the temperature interval from 25 ^{o}C to 300 ^{o}C: Geological Society of America Bulletin, v. 71, p. 1867-1868.

Fournier, R.O. 1977. Chemical geothermometers and mixing models for geothermal systems: Geothermics, v. 5, p. 41-50.

Fournier, R.O. and R.W. Potter. 1979. Magnesium correction to the Na-K-Ca chemical geothermometer: Geochim et Cosmochim Acta, v. 43, p. 1543-1550.

Fournier, R.O. and A.H. Truesdell. 1973. An empirical Na-K-Ca geothermometer fro natural waters: geochim et Cosmochim Acta, v. 37, p. 1255-1275.

Fournier, R.O., D.E. White and A.H. Truesdell. 1974. Geochemical indicators of subsurface temperature, 1. Basic assumptions: Journal of Research, U. S. Geological Survey, v. 2, no. 3, p. 259-262.

Franson, M.A. (ed.). 1985. *Standard Methods for the Examination of Water and Wastewater, Sixteenth Edition*. Washington DC: American Public Health Association with the American Water Works Association and the Water Pollution Control Federation.

Freeze, R.A. and P.A. Witherspoon. 1966. Therorical analyis of regional groundwater flow. I. Analytical and numerical solutions to the mathematical model: Water Resources Research, v. 2, p. 641-656.

Freeze, R.A. and P.A. Witherspoon. 1967. Theoretical analysis of regional groundwater flow. II. Effect of water table configuration and subsurface permeability variations: Water Resources Research, v. 3, p. 623-634.

Frenzel, P.F. and C.A. Kaehler. 1992. *Geohydrology and simulation of ground-water flow in the Mesilla Basin, Doña Ana County, New Mexico and El Paso County, Texas; with a section on water quality and geochemistry by S. K. Anderholm*. U.S. Geological Survey Professional Paper 1407-C. 105 p.

Gat, J. R. 1996. Oxygen and hydrogen isotopes in the hydrologic cycle: Annual Review of Earth and Planetary Sciences, v. 24, p. 225-262.

Gates, J.S., D.E. White, W.D. Stanley and H.D. Ackerman. 1978. *Availability of fresh and slightly saline groundwater in the basins of westernmost Texas*. U.S. Geological Survey Open-File Report 78-663. 115 p.

Giggenbach, W.F. 1988. Geothermal solute equilibria. Derivation of Na-K-Mg-Ca geoindicators: Geochim et Cosmochim Acta, v. 52, p. 2749-2765.

Gile, L.H. 1987. A pedologic chronology of Kilbourne Hole, southern New Mexico: I. Soils in tuff; II. Time of the explosions. *Soil Science Society of America Journal*. 51:746-760.

Gile, L.H. and R.B. Grossman. 1979. *The Desert Project Soil Monograph*. U.S. Department of Agriculture, Springfield, VA. National Technical Information Service, Document No. PB80-13534. 984 p.

Gile, L.H., R.P. Gibbens and J.M. Lenz. 1995. Soils and sediments associated with remarkable, deeply penetrating roots of crucifixion thorn (Koeberlinia spinosa Zucc*.). Journal of Arid Environments*. 35:137-151.

Gile, L.H., R.P. Gibbens and J.M. Lenz. 1998. Soil-induced variability in root systems of creosotebush (Larrea tridentata) and tarbush (Flourensia cernua). *Journal of Arid Environments*. 39:57-78.

Gile, L.H., J.W. Hawley and R.B. Grossman. 1981. *Soils and geomorphology in a Basin and Range area of southern New Mexico–Guidebook to the Desert Project.* New Mexico Bureau of Mines and Mineral Resources Memoir 39. 222 p.

Gile, L.H., F.F. Peterson and R.B. Grossman. 1966. Morphological and genetic sequences of carbonate accumulation in desert soils. *Soil Science*. 101:5:347-360.

Gile, L.H., J.W. Hawley, R.B. Grossman, H.C. Monger, C.E. Montoya and G.H. Mack. 1995. *Supplement to the Desert Project Guidebook, with emphasis on soil micromorphology*. New Mexico Bureau of Mines and Mineral Resources Bulletin 142. 96 p.

Goff, F., B.F. Kues, M.A. Rogers, L.D. McFadden, and J.N. Gardner (editors). 1996. The Jemez Mountain region. *New Mexico Geological Society, 47th Annual Field Conference Guidebook*. 484 p.

Grauch, V.J.S. 1999. Principal features of high-resolution aeromagnetic data collected near Albuquerque, New Mexico. *New Mexico Geological Society, 50th Annual Field Conference Guidebook.* pp. 115-118.

Grauch, V.J.S., C.L. Gillespie and G.R. Keller. 1999. Discussion of new gravity maps for the Albuquerque basin area*. New Mexico Geological Society, 50th Annual Field Conference Guidebook*. pp. 119-124.

Grauch, V.J.S., D.A. Sawyer, G.R. Keller and C.L. Gillespie. 2000. Geologic and hydrologic framework: A. Contributions of gravity and aeromagnetic studies to improving the understanding of subsurface hydrogeology, Middle Rio Grande Basin, New Mexico. In *U.S. Geological Survey Middle Rio Grande Basin Study - Proceedings of the Fourth Annual Workshop*. Albuquerque, New Mexico. February 15-16, 2000. Edited by J.C. Cole. U.S. Geological Survey Open File Report 00-488. pp. 3-4.

Gross, J. 1988. *A hydrogeological investigation of the Las Cruces geothermal field*. M.S. Thesis, New Mexico State University. 212 p.

Gross, J. and J. Cochran. 1984. *Uranium disequilibrium investigation of the Las Cruces East Mesa geothermal field.* New Mexico Energy Research and Development Institute, Report NMERDI 2-67-2238 (3). 50 p.

Gross, J. and L. Icerman. 1983. *Subsurface investigations for the area surrounding Tortugas Mountain, Doña Ana County, New Mexico*. New Mexico Energy Research and Development Institute, Interim Report NMERDI 2-67-2238 (2). 70 p.

Gustavson, T.C. 1991. *Arid basin depositional systems and paleosols: Fort Hancock and Camp Rice Formations (Pliocene-Pleistocene) Hueco Bolson, West Texas and adjacent Mexico*. The University of Texas at Austin, Bureau of Economic Geology Report of Investigations No. 198. 49 p.

Haan, C.T. 1977. *Statistical methods in hydrology*. Ames, IA: Iowa State University Press.

Haase, C.S. and R.P. Lozinsky. 1992. Estimation of hydrologic parameters. In *Hydrogeologic Framework of the Northern Albuquerque Basin*. Compiled by J.W. Hawley and C.S. Haase. New Mexico Bureau of Mines and Mineral Resources Open File Report 387. pp. VI-1 - VI-3.

Hamilton, S.L. and T. Maddock III. 1993. *Application of a groundwater flow model to the Mesilla Basin, New Mexico and Texas*. University of Arizona, Department of Hydrology and Water Resources Document Number 93-020.

Hanor, J.S. 1988. Origin and migration of subsurface sedimentary brines: Society of Economic Paleontologists and Mineralogists Short Course 21.

Hanor, J.S. 1994. Origin of saline fluids in sedimentary basins, in Parnell, J. ed., Geofluids: Origin, Migration and Evolution of Fluids in Sedimentary Basins: Geological Society Special Publication 78, p. 151-174.

Hanson, R.T., J.S. McLean and R.S. Miller. 1994. *Hydrogeologic framework and preliminary simulation of ground-water flow in the Mimbres Basin, southwestern New Mexico*. U.S. Geological Survey Water-Resources Investigations Report 94-4011. 118 p.

Harbour, R.L. 1972. *Geology of the northern Franklin Mountains, Texas and New Mexico*. U.S. Geological Survey Bulletin 1298. 129 p.

Harris, A.H. 1997. Geographic and chronologic patterns in Late Pleistocene vertebrate faunas, southern New Mexico. In *New Mexico's Fossil Record 1*. Edited by S.G. Lucas, J.W. Estep, T.E. Williamson and G.S. Morgan. New Mexico Museum of Natural History and Science Bulletin No. 11:129-134.

Hawley, J.W. 1969. Notes on the geomorphology and late Cenozoic geology of northwestern Chihuahua. *New Mexico Geological Society, 20th Annual Field Conference Guidebook*. pp. 131-142.

Hawley, J.W. 1975. Quaternary history of Doña Ana county regions south-central New Mexico. *New Mexico Geological Society, 26th Annual Field Conference Guidebook.* pp. 138-150.

Hawley, J.W. (compiler). 1978. *Guidebook to the Rio Grande Rift in New Mexico and Colorado*. New Mexico Bureau of Mines and Mineral Resources Circular 163. 241 p.

Hawley, J.W. 1984. *Hydrogeologic cross sections of the Mesilla Bolson, New Mexico and Texas*. New Mexico Bureau of Mines and Mineral Resources Open-File Report 190. 10 p. [Appendix B in Hawley and Lozinsky 1992].

Hawley, J.W. 1986. Physiographic provinces (and) landforms of New Mexico. In *New Mexico in Maps*. Edited by J.L. Williams. Albuquerque, NM: University of New Mexico Press. pp. 28-31.

Hawley, J.W. 1993. *Geomorphologic setting and Late Quaternary history of Pluvial-lake Basins in the Southwestern New Mexico Region*. New Mexico Bureau of Mines and Mineral Resources Open File Report 391. 28 p.

Hawley, J.W. 1996. Hydrogeologic framework of potential recharge areas in the Albuquerque Basin, central New Mexico. In *Hydrogeology of Potential Recharge Areas and Hydrogeochemical Modeling of Proposed Artificial Recharge Methods in Basin- and Valley-fill Aquifer Systems, Albuquerque Basin, New Mexico*. Edited by J.W. Hawley and T.M. Whitworth. New Mexico Bureau of Mines and Mineral Resources Open File Report 402-D. pp. 1-70.

Hawley, J.W. 1998. Hydrogeologic mapping in the Basin and Range province, progress since 1900, and future prospects. In *U.S. Geological Survey Middle Rio Grande Basin Study--Proceedings of the Second Annual Workshop.* Albuquerque, New Mexico. February 10-11, 1998. Edited by J.L. Slate. U.S. Geological Survey Open File Report 98-337, pp. 3-7.

Hawley, J.W. and C.S. Haase. 1992. *Hydrogeologic framework of the northern Albuquerque Basin*. New Mexico Bureau of Mines and Mineral Resources Open File Report 387. Variously paged.

Hawley, J.W. and J.M. Kernodle. 2000. Overview of the hydrogeology and geohydrology of the northern Rio Grande basin – Colorado, New Mexico, and Texas. In *Proceedings of the 44th Annual New Mexico Water Conference "The Rio Grande Compact: It's the Law."* Edited by C.T. Ortega Klett. New Mexico Water Resources Research Institute, Report No. 312, New Mexico State University, Las Cruces, NM. pp. 46-38.

Hawley, J.W. and F.E. Kottlowski. 1969. Quaternary geology of the south-central New Mexico border region. In *Border Stratigraphy Symposium*. New Mexico Bureau of Mines and Mineral Resources Circular 104. pp. 89-115.

Hawley, J.W. and R.P. Lozinsky. 1992. *Hydrogeologic Framework of the Mesilla Basin in New Mexico and Western Texas*. New Mexico Bureau of Mines and Mineral Resources Open File Report 323. 55 p.

Hawley, J.W., C.S. Haase and R.P. Lozinsky. 1995. Hydrogeologic framework of the northern Albuquerque Basin. In *Proceedings of the 39th Annual New Mexico Water Conference: The Water Future of Albuquerque and Middle Rio Grande Basin*. Edited by C. Ortega Klett. New Mexico Water Resources Research Institute, Technical Report No. 290, New Mexico State University, Las Cruces, NM. pp. 37-55.

Hawley, J.W., J.F. Kennedy and B.J. Creel. 2001. The Mesilla Basin aquifer system of New Mexico, West Texas and Chihuahua—an overview of its hydrogeologic framework and related aspects of groundwater flow and chemistry. In *Aquifers of West Texas*. Edited by R.E. Mace, W.F. Mullican III and E.S. Angle. Austin, Texas Water Development Board Report 356: 76-99.

Hawley, J.W., F.E. Kottlowski, W.S. Strain, W.R. Seager, W.E. King and D.V. LeMone. 1969. The Santa Fe Group in the south-central New Mexico border region. In *Border Stratigraphy Symposium*. New Mexico Bureau of Mines and Mineral Resources Circular 104. pp. 52-76.

Hawley, J.W., B.J. Hibbs, J.F. Kennedy, B.J. Creel, M.D. Remmenga, M. Johnson, M. Lee and P. Dinterman. 2000. *Trans-International Boundary aquifers in southwestern New Mexico*. New Mexico Water Resources Research Institute, New Mexico State University, prepared for U.S. Environmental Protection Agency-Region 6 and International Boundary and Water Commission; Technical Completion Report - Interagency Contract X-996350-01-3. 126 p.

Healy, D.F. 1996. *Water-quality assessment of the Rio Grande Valley study unit, Colorado, New Mexico, and Texas—Occurrence and distribution of selected pesticides and nutrients at selected surface-water sites in the Mesilla Valley, 1994-1995*. U.S. Geological Survey Water-Resources Investigations Report 96-4069. 85 p.

Hearne, G.A. and J.D. Dewey. 1988. *Hydrologic Analysis of the Rio Grande Basin North of Embudo, New Mexico, Colorado and New Mexico*. U.S. Geological Survey Water-Resources Investigations Report 86-4113. 244 p.

Hem, J.D. 1985. *Study and interpretation of the chemical characteristics of natural water*. U.S. Geological Survey Water-Supply Paper 2254. 263 p.

Hernandez, J.W. 1976. *Rio Grande water quality baseline study for the Rio Grande, canals and associated drains from San Marcial, New Mexico to Fort Quitman, Texas*. New Mexico Water Resources Research Institute, Technical Completion Report No. 064, New Mexico State University, Las Cruces, NM. 17 p. and appendices.

Heywood, C.E. 1995. Investigation of aquifer-system compaction in the Hueco Basin, Texas, USA. In *5th International Symposium on Land Subsidence.* Delft, Netherlands. International Association of Hydrological Sciences Publication. 234:35-45.

Hibbs, B. 1999. Hydrogeologic and water quality issues along the El Paso/Juarez corridor: An international case study. *Environmental and Engineering Geoscience*. 5:27-39.

Hibbs, B., B.K. Darling and I.C. Jones. 1998. Hydrogeologic regimes of arid-zone aquifers beneath low-level radioactive waste and other waste repositories in Trans-Pecos, Texas and northern Chihuahua, Mexico. In *Gambling with Groundwater–Physical, Chemical, and Biological Aspects of Aquifer-*

stream Relationships. Edited by J. Van Brahana and others. St. Paul, Minnesota: American Institute of Hydrology. pp. 311-322.

Hibbs, B.J., M.M. Lee and J.W. Hawley. 1999. Evolution of hydrochemical facies in the Mimbres Basin aquifer system: A transboundary resource. In *Hydrological issues of the 21st Century: Ecology, Environment, and Human Health*. American Institute of Hydrology, Hydrological Science and Technology. 15:1-4:52-65.

Hibbs, B. J., M.M. Lee, J.W. Hawley and J.F. Kennedy. 2000. Some notes on the hydrogeology and ground-water quality of the Animas Basin system. *Southwestern New Mexico: New Mexico Geological Society, 51st Annual Field Conference Guidebook*. pp. 227-234.

Hibbs, B.J., R.N. Boghici, M.E. Hayes, J.B. Ashworth, A.T. Hanson, Z.A. Samani, J.F. Kennedy and B.J. Creel. 1997. *Transboundary Aquifers of the El Paso/Ciudad Juarez/Las Cruces Region*. Texas Water Development Board and New Mexico Water Resources Research Institute. Special Report for U.S. Environmental Protection Agency, Region 6, Dallas, Texas. 155 p.

Hibbs, B., R. Boghici, J. Ashworth, M. Hayes, D. Peckham, R. Guillen, O. Fuentes, N. Laloth, M. Morales, A. Maldonado, B. Creel, J. Kennedy, A. Hanson, Z. Samani, F. Nuñez, R. Lemus, G. Moreno, E. Rascon, R. Kuo, S. Waggoner, C. Ito, J. Robinson, J. Valdez, D. Little, A. Rascon, A. Reyes, K. Williams, M. Vaughan, O. Cabra, T. Kelly and C. King. 1998. *Transboundary aquifers and binational ground-water data base, City of El Paso/Ciudad Juarez area: International Boundary and Water Commission*, U.S. Environmental Protection Agency, Texas Water Development Board, New Mexico Water Resources Research Institute, Comision Internacional de Limites y Aguas, Comision Nacional del Agua, Junta Municipal de Agua y Saneamiento de Ciudad Juarez. 47 p. plus CD ROM.

Hill, C. A. 1996. Geology of the Delaware basin, Guadalupe, Apache, and Glass Mountains, New Mexico and West Texas: Permian Basin Section, Society of Economic Paleontologists and Mineralogists Publication 96-39, 480 p.

Hill, R.T. 1896. Descriptive topographic terms of Spanish America. *National Geographic*. 7:291-302.

Hill, R.T. 1900. Physical geography of the Texas region. *U.S. Geological Survey Topographical Atlas.* Folio *3*. 12 p.

Hoefs, J. 1997. Stable Isotope Geochemistry: Springer-Verlag, Berlin, p. 308.

Hoffer, J.M. 2001. Geology of the West Potrillo Mountains. In *Volcanology in New Mexico*. Edited by L.S. Crumpler and S.G. Lucas. New Mexico Museum of Natural History and Science Bulletin 18:141-145.

Hounslow, A.W. 1995. Water quality data analysis and interpretation: Lewis Publishers, Boca Raton, 397 p.

International Boundary and Water Commission (IBWC). 1939—2000. Flow of the Rio Grande and related data from Elephant Butte Dam, New Mexico, to the Gulf of Mexico*. International Boundary and Water Commission, Water Bulletin*. Nos. 9 to 70.

Icerman, L. and R.L. Lohse. 1983. *Geothermal low temperature reservoir assessment in Doña Ana County, New Mexico*. New Mexico Energy Research and Development Institute, Report NMERDI 2-69-2202. 188 p.

Izett, G.A. and R.E. Wilcox. 1982. *Map Showing Localities and Inferred Distributions of the Huckleberry Ridge, Mesa Falls, and Lava Creek Ash Beds (Pearlette Family Ash Beds) of Pliocene and Pleistocene Age in the Western United States and Southern Canada*. U.S. Geological Survey Miscellaneous Investigations Map I-1325, scale 1:4,000,000.

Johnson, T.M. and D.J. Depaolo. 1994. Interpretation of isotopic data in groundwater-rock systems, model development and application to Sr isotope data from Yucca Mountain. *Water Resources Research*. 30:5: 1571-1587.

Keller, G.R. and S.M. Cather (eds.). 1994. *Basins of the Rio Grande rift: Structure, stratigraphy and tectonic setting*. Geological Society of America Special Paper 291. 304 p.

Keller, G.R., B.S. Penn and S.H. Harder. 1998. Las Cruces country: A geophysical and remote sensing perspective. *New Mexico Geological Society, 49th Annual Field Conference Guidebook*. pp. 87-91.

Kelley, S.A. and J.P. Matheny. 1983. *Geology of Anthony quadrangle, Doña Ana County, New Mexico*. New Mexico Bureau of Mines and Mineral Resources Geologic Map 54, scale 1:24,000.

Kennedy, J.F. 1998. Aquifer sensitivity assessment for the Mesilla Valley. In *Proceedings of the 43rd Annual New Mexico Water Conference: Water Challenges on the Lower Rio Grande*. Edited by C.T. Ortega Klett. New Mexico Water Resources Research Institute, Report No. 310, New Mexico State University, Las Cruces, NM. pp. 84-104.

Kennedy, J.F., J.W. Hawley and M. Johnson. 2000. The hydrogeologic framework of basin-fill aquifers and associated ground-water-flow systems in southwestern New Mexico—an overview. *New Mexico Geological Society, 51st Annual Field Conference Guidebook*. pp. 235-244.

Kernodle, J.M. 1992a. *Summary of U.S. Geological Survey ground-water-flow models of basin-fill aquifers in the Southwestern Alluvial Basins region, Colorado, New Mexico, and Texas*. U.S. Geological Survey Open File Report 90-361. 81 p.

Kernodle, J.M. 1992b. *Results of Simulations by a Preliminary Numerical Model of Land Subsidence in the El Paso, Texas Area*. U.S. Geological Survey Water-Resources Investigations Report 92-4037. 35 p.

Kernodle, J.M., D.P. McAda and C.R. Thorn. 1995. *Simulation of Ground-water Flow in the Albuquerque Basin, Central New Mexico*. U.S. Geological Survey Water-Resources Investigations Report 94-4251. 114 p.

King, W.E. and J.W. Hawley. 1975. Geology and ground-water resources of the Las Cruces area. *New Mexico Geological Society, 26th Annual Field Conference Guidebook*. pp. 195-201.

King, W.E., J.W. Hawley, A.M. Taylor and R.P. Wilson. 1971. *Geology and Ground-water Resources of Central and Western Doña Ana County, New Mexico*. New Mexico Bureau of Mines and Mineral Resources Hydrologic Report 1. 64 p.

Knowles, D.B. and R.A. Kennedy. 1958. *Ground-water resources of the Hueco Bolson northeast of El Paso, Texas*. U.S. Geological Survey Water-Supply Paper 1426. 186 p.

Kottlowski, F.E. 1958. Geologic history of the Rio Grande near El Paso. *West Texas Geological Society, Guidebook 1958 Field Trip*. pp. 46-54.

Kottlowski, F.E. 1960. *Reconnaissance geologic map of Las Cruces 30-minute quadrangle.* New Mexico Bureau of Mines and Mineral Resources Geologic Map 14.

Krider, P.R. 1998. Paleoclimatic significance of late Quaternary lacustrine and alluvial stratigraphy, Animas Valley, New Mexico. *Quaternary Research*. 50:283-289.

Kucks, R.P., P.L. Hill and C.E. Heywood. 2001. *New Mexico aeromagnetic and gravity maps and data: A web site for distribution of data*. U.S. Geological Survey Open-File Report 01-0061.

Land, L.F. and C.A. Armstrong. 1985. *A preliminary assessment of land-surface subsidence in the El Paso area, Texas*. U.S. Geological Survey Water-Resources Investigations Report 85-4155. 96 p.

Lee, W.T. 1907. *Water resources of the Rio Grande Valley in New Mexico*. U.S. Geological Survey Water-Supply Paper 188. 59 p.

Leeder, M.R., G.H. Mack and S.L. Salyards. 1996. Axial—transverse fluvial interactions in half-graben: Plio-Pleistocene Palomas Basin, southern Rio Grande Rift, New Mexico, USA. *Basin Research*. 12:225-241.

Leeder, M.R., G.H. Mack, J. Peakall and S.L. Salyards. 1996. First quantitative test of alluvial stratigraphic models: Southern Rio Grande rift, New Mexico. *Geology*. 24:1:87-90.

Leggat, E.R., M.E. Lowry and J.W. Hood. 1962. *Ground-water resources of the lower Mesilla Valley, Texas and New Mexico*. Texas Water Commission Bulletin 6203. 191 p.

Love, D.W. and W.R. Seager. 1996. Fluvial fans and related basin deposits of the Mimbres drainage. *New Mexico Geology*. 18:4:81-92.

Lovejoy, E.M.P. 1976. *Geology of Cerro de Cristo Rey uplift, Chihuahua and New Mexico.* New Mexico Bureau of Mines and Mineral Resources Memoir 31. 84 p.

Lozinsky, R.P. and J.W. Hawley. 1986. The Palomas Formation of south-central New Mexico - a formal definition. *New Mexico Geology*. 8:4:73-82.

Lucas, S.G. and J.W. Hawley. 2002. The Otero Formation, Pleistocene lacustrine strata in the Tularosa Basin, southern New Mexico. *New Mexico Geological Society, 53rd Annual Field Conference Guidebook*. pp. 277-283.

Machette, M.N., T. Long, G.O. Bachman and N.R. Trimbel. 1997. *Laboratory data for Calcic soils in central New Mexico: Background information for mapping Quaternary deposits in the Albuquerque Basin.* New Mexico Bureau of Mines and Mineral Resources Circular 205. 63 p.

Mack, G.H. and W.R. Seager. 1990. Tectonic controls on facies distribution of the Camp Rice and Palomas Formations (Pliocene-Pleistocene) in the southern Rio Grande rift. *Geological Society of America Bulletin*. 102:45-53.

Mack, G.H., D.W. Love and W.R. Seager. 1997. Spillover models for axial rivers in regions of continental extension: The Rio Mimbres and Rio Grande in the southern Rio Grande rift, USA. *Sedimentology*. 44:637-652.

Mack, G.H., F.E. Kottlowski and W.R. Seager. 1998. The stratigraphy of south-central New Mexico. *New Mexico Geological Society, 49th Annual Field Conference Guidebook*. pp. 135-153.

Mack, G.H., S.L. Salyards and W.C. James. 1993. Magnetostratigraphy of the Plio-Pleistocene Camp Rice and Palomas formations in the Rio Grande rift of southern New Mexico. *American Journal of Science*. 293:49-77.

Mack, G. H., D.R. Cole, W.C. James, T.H. Giordano and S.L. Salyards. 1994. Stable oxygen and carbon isotopes of pedogenic carbonate as indicators of Plio-Pleistocene paleoclimate in the southern Rio Grande rift, south-central New Mexico: American Journal of Science, v. 284, p. 621-640.

Mack, G.H., W.C. McIntosh, M.R. Leeder, M.R. and H.C. Monger. 1996. Plio-Pleistocene pumice floods in the ancestral Rio Grande, southern Rio Grande rift, USA. *Sedimentary Geology*. 103:1-8.

Mack, G.H., S.L. Salyards, W.C. McIntosh and M.R. Leeder. 1998. Reversal magnetostratigraphy and radioisotopic geochronology of the Plio-Pleistocene Camp Rice and Palomas Formations, southern Rio Grande rift. *New Mexico Geological Society, 49th Annual Field Conference Guidebook*. pp. 229-236.

Mack, G.H., D.R. Cole, and L. Trevino. 2000. The distribution and discrimination of shallow, authigenic carbonate in the Pliocene-Pleistocene Palomas Basin, southern Rio Grande rift: Geological Society of America Bulletin, v. 112, no. 5, p. 643-656.

Mack, P.D.C. 1985. *Correlation and provenance of facies within the upper Santa Fe Group in the subsurface of the Mesilla Valley, southern New Mexico*. M.S. Thesis, New Mexico State University. 137 p.

Makridakis, S. and S.C. Wheelwright. 1978. *Interactive forecasting*. San Francisco, CA : Holden-Day.

Maxey, G.B. 1968. Hydrogeology of desert basins. *Groundwater*. 6:1-22.

Mazor, E. 1997. *Chemical and Isotopic Groundwater Hydrology*. New York: Marcel Dekker, Inc. 413 p.

McArthur, J.M., R.J. Howarth and T.R. Bailey. 2001. Strontium isotope stratigraphy: LOWESS version 3: best fit to the marine Sr-isotope curve for 0-509 Ma and accompanying look-up table for deriving numerical age: The Journal of Geology, v.109, p. 155-170.

McGrath, D.B. and J.W. Hawley. 1987. Geomorphic evolution and soil-geomorphic relationships in the Socorro area, central New Mexico. In *Guidebook to the Socorro area, New Mexico*. Compiled by V.T. McLemore and M.W. Bowie. New Mexico Bureau of Mines & Mineral Resources Guidebook. pp. 55-67.

Meinzer, O.E. and R.E. Hare. 1915. *Geology and Water Resources of Tularosa Basin, New Mexico*. U.S. Geological Survey Water-Supply Paper 343. 317 p.

Metcalf, A.L. 1967*. Late Quaternary mollusks of the Rio Grande Valley, Caballo Dam to El Paso, Texas*. Texas Western Press, University of Texas at El Paso, Science Series No. 1. 62 p.

Metcalf, A.L. 1969. Quaternary surface sediments and mollusks - southern Mesilla Valley, New Mexico and Texas. *New Mexico Geological Society, 20th Annual Field Conference Guidebook*. pp. 158-164.

Metcalfe, S., A. Say, S. Black, R. McCullock and S. O'Hara. 2002. Wet conditions during the last glaciation in the Chihuahuan Desert, Alta Babicora basin, Mexico. *Quaternary Research*. 57:91-101.

Mifflin, M.D. 1968. *Delineation of Groundwater Flow Systems in Nevada*. Desert Research Institute, Technical Report Series H-W, Hydrology and Water Resources Publication 4, University of Nevada/Reno. 109 p.

Mifflin, M.D. 1988. Region 5, Great Basin. In *Hydrogeology–The Geology of North America*. Edited by W. Back, J.S. Rosenshein, and P.R. Seaber. Geological Society of America DNAG. O-2. pp. 69-78.

Miyamoto, S., L.B. Fenn and D. Swietlik. 1995. *Flow, salts, and trace elements in the Rio Grande: A review.* Texas A&M, College Station, TX. Texas Agricultural Experiment Station Technical Report 169. 34 p.

Monger, H.C. and W.C. Lynn. 1996. Clay mineralogy of the Desert Project and Rincon Surface study area. In *Studies of soil and landscape evolution in southern New Mexico: Supplement to the Desert Project Soil Monograph, v. II*. Edited by L.H. Gile and R.J. Ahrens. Lincoln, NB. Soil Survey Investigations (NRCS) Report. 44:111-155.

Monger, H. C., D.R. Cole, J.W. Gish and T.H. Giordano. 1998. Stable carbon and oxygen isotopes in Quaternary soil carbonates as indicators of ecogeomorphic changes in the northern Chihuahuan Desert, USA: Geoderma, v. 82, p. 137-172.

Morrison, R.B. 1969. Photointerpretive mapping from space photographs of Quaternary geomorphic features and soil associates in northern

Chihuahua and adjoining New Mexico and Texas. *New Mexico Geological Society, 20th Field Conference Guidebook.* pp. 116-129.

Myers, R. G. and B.R. Orr. 1986. *Geohydrology of the aquifer in the Santa Fe Group, northern West Mesa of the Mesilla Basin near Las Cruces, New Mexico.* U.S. Geological Survey, Water-Resources Investigations Report 84-4190. 37 p.

Nicholson, K. 1993. Geothermal Fluids Chemistry and Exploration Techniques: Springer-Verlag, Berlin, p. 263.

Nickerson, E.L. 1987. *Selected geohydrologic data for the Mesilla Basin, Doña Ana County, New Mexico and El Paso County, Texas*. U.S. Geological Survey Open-File Report 87-75. 59 p.

Nickerson, E.L. 1989. *Aquifer tests in the flood-plain alluvium and Santa Fe Group at the Rio Grande near Canutillo, El Paso County, Texas*. U.S. Geological Survey Water-Resources Investigations Report 89-4011. 29 p.

Nickerson, E.L. 1995. *Selected geohydrologic data for the Mesilla ground-water basin, 1987 through 1992 water years, Doña Ana County, New Mexico and El Paso County, Texas*. U.S. Geological Survey Open-File Report 95-111. 123 p.

Nickerson, E.L. 1998. U.S. Geological Survey seepage investigations of the Lower Rio Grande in the Mesilla Valley. In *Proceedings of the 43rd Annual New Mexico Water Conference: Water Challenges on the Lower Rio Grande*. Edited by C.T. Ortega Klett. New Mexico Water Resources Research Institute, Report No. 310, New Mexico State University, Las Cruces, NM. pp. 59-68.

Nickerson, E.L. and R.G. Myers. 1993. *Geohydrology of the Mesilla ground-water basin, Doña Ana county, New Mexico, and El Paso County, Texas*. U.S. Geological Survey Water-Resources Investigations Report 92-4156. 89 p.

Orr, B.R. and R.G. Myers. 1986. *Water resources in basin-fill deposits in the Tularosa Basin, New Mexico.* U.S. Geological Survey Water-Resources Investigations Report 85-4219. 94 p.

Orr, B.R. and D.W. Risser. 1992. *Geohydrology and potential effects of development of freshwater resources in the northern part of the Hueco Bolson, Doña Ana and Otero Counties, New Mexico, and El Paso County, Texas.* U.S. Geological Survey Water-Resources Investigations Report 91-4082. 92 p.

Orr, B.R. and R.R. White. 1985. *Selected hydrologic data from the northern part of the Hueco Bolson, New Mexico and Texas*. U.S. Geological Survey Open-File Report 85-696. 88 p.

Ortiz, D., K.M. Lange and L.V. Beal. 2001. *Water resources data, New Mexico, Water Year 2000, volume 1: the Rio Grande Basin, the Mimbres River Basin, and the Tularosa Valley Basin*. U.S. Geological Survey Water-Data Report NM-00-1. 411 p.

Osmond, J.K. and J.B. Cowart. 1976. The theory and uses of natural uranium isotopic variations in hydrology. *Atomic Energy Review*. 14:621-679.

Rimstidt, J.D. and H.L. Barnes. 1980. The kinetics of silica-water reactions: Geochimica et Cosmochimica Acta, v. 44, p. 1683-1700.

Patterson, J.L. 1965. *Magnitude and frequency of floods in the United States—Part 8, Western Gulf of Mexico basins*. U.S. Geological Survey Water-Supply Paper 1682. pp. 418-419.

Peterson, D.M., R. Khaleel and J.W. Hawley. 1984. *Quasi Three-dimensional Modeling of Groundwater Flow in the Mesilla Bolson New Mexico*. New Mexico Water Resources Research Institute, Technical Completion Report No. 178, New Mexico State University, Las Cruces, NM. 185 p.

Piper, A.M. 1944. A graphic procedure in the geochemical interpretation of water-analyses: Transactions, American Geophysical Union, v. 25, p. 914-923.

Phillips, F.M. J.F. Hogan, S.K. Mills and J.M.H. Hendrickx. 2002. Environmental tracers applied to quantifying causes of salinity in arid-region rivers: Preliminary results from the Rio Grande, southwestern USA, in A.S. Alsharhan, W.W. Wood, eds., Water Resources Perspectives: Evaluation, Management and Policy: Elsevier, Amsterdam.

Plummer, L.N., L.M. Bexfield, S.K. Anderholm, W.E. Sanford and E. Busenberg. 2000. Geologic and hydrologic framework: C. Geochemical characterization of groundwater flow paths in parts of the Santa Fe Group aquifer system, Middle Rio Grande Basin, New Mexico. In *U.S. Geological Survey Middle Rio Grande Basin Study—Proceedings of the Fourth Annual Workshop.* Albuquerque, New Mexico. February 15-16, 2000. Edited by J.C. Cole. U.S. Geological Survey Open File Report 00-488. pp. 7-12.

Postel, S. 1993. Water and Agriculture. In *Water in Crisis: Pacific Institute for Studies in Development, Environment, and Security*. Edited by P. Gleick. Stockholm Environment Institute: Oxford Press.

Postel, S. 1999. *Pillar of Sand*. New York, NY: Worldwatch Institute & W.W. Norton.

Reed, M.J. and R.H. Mariner. 1991. Quality control of chemical and isotopic analyses of geothermal water samples In *Proceedings, Sixteenth Workshop on Geothermal Reservoir Engineering*. Stanford Geothermal Program Workshop Report SGP-TR-134. pp. 9-13.

Reeves, C.C., Jr. 1969. Pluvial Lake Palomas, northwestern Chihuahua, Mexico. *New Mexico Geological Society, 20th Annual Field Conference Guidebook*. pp. 143-154.

Reiter, M. 1999. Hydrogeothermal studies in the southern part of Sandia National Laboratories/Kirtland Air Force Base: Data regarding ground-water flow across the boundary of an intermontane basin. In *Faults and Subsurface Fluid Flow in the Shallow Crust*. Edited by W.C. Haneberg and others. American Geophysical Union, Washington, D.C. Geophysical Monograph Series.113:207-222.

Reiter, M. 2001. Using precision temperature logs to estimate horizontal and vertical groundwater flow components. *Water Resources Research*. 37:3:663-674.

Reiter, M. and S.C. Wade. 1994*. A hydrothermal study to estimate vertical groundwater flow in the Canutillo Well Field, between Las Cruces and El Paso*. New Mexico Water Resources Research Institute, Technical Completion Report No. 282, New Mexico State University, Las Cruces, NM. 71 p.

Reiter, M., R.E. Eggleston, B.R. Broadwell and J. Minier. 1986. Estimates of terrestrial heat flow from deep petroleum tests along the Rio Grande rift in central and southern New Mexico. *Journal of Geophysical Research*. 91: B6:6225-6245.

Reynolds, C.B. & Associates. 1986. *Shallow seismic reflection survey, Canutillo area, Texas and New Mexico*. Unpublished consultant's report for U.S. Geological Society by Charles B. Reynolds & Associates, 4409 San Andres Ave., NE, Albuquerque, NM 87110. 8 p., 2 figs., 12 enclosed seismic profiles.

Reynolds, C.B. & Associates. 1987. *Shallow seismic reflection line CA-1, Doña Ana County, New Mexico and El Paso County, Texas*. Unpublished consultant's report for U.S. Geological Society by Charles B. Reynolds & Associates, 4409 San Andres Ave., NE, Albuquerque, NM 87110. 4 p., 1 fig., 2 enclosed seismic profiles.

Richardson, G.B. 1909. *Description of the El Paso quadrangle, Texas*. U.S. Geological Survey Geological Atlas, El Paso folio, series 116. 11 p.

Richardson, G.L., T.G. Gebbard, Jr. and W.F. Brutsaert. 1972. *Water-table investigation in the Mesilla Valley*. Engineering Experiment Station, Technical Report 76, New Mexico State University. 206 p.

Rimstidt, J.D. and H.L. Barnes. 1980. The kinetics of silica-water reactions: Geochimica et Cosmochimica Acta, v. 44, p. 1683-1700.

Ross, H.P. and J.C. Witcher. 1998. Self-potential surveys of three geothermal areas in the southern Rio Grande rift, New Mexico. *New Mexico Geological Society, 49th Annual Field Conference Guidebook*. pp. 93-100.

Sanford, W.E., L.N. Plummer, D.P. McAda, L.M. Bexfield and S.K. Anderholm. 2000. Geologic and hydrologic framework: B. Estimation of hydrologic parameters for the ground-water model of the Middle Rio Grande Basin using Carbon 14 and water-level data. In *U.S. Geological Survey Middle Rio Grande Basin Study—Proceedings of the Fourth Annual Workshop.* Albuquerque, New Mexico. February 15-16, 2000. Edited by J.C. Cole. U.S. Geological Survey Open File Report 00-488. pp. 4-6.

Sawyer, D.A. and J.S. Pallister. 1989. Geologic Framework of the southern Basin and Range. In *Field Excursions to Volcanic Terranes in the Western United States, Vol. I: Southern Rocky Mountain Region*. Edited by C.E. Chapin and J. Zidek. New Mexico Bureau of Mines and Mineral Resources Memoir 46. pp. 121-126.

Sayre, A.N. and P. Livingston. 1945. *Ground-water resources of the El Paso area, Texas*. U.S. Geological Survey Water-Supply Paper 919. 190 p.

Scanlon, B.R., B.K. Darling and W.F. Mullican III. 2001. Evaluation of groundwater recharge in basins of Trans-Pecos Texas. *In Aquifers of West Texas*. Edited by R.E. Mace, W.F. Mullican III and E.S. Angle. Austin, Texas Water Development Board Report 356: pp. 26-40.

Schmidt, R.H. Jr. 1986. Chihuahuan climate. In *Invited Papers from the Second Symposium on Resources of the Chihuahuan Desert Region—United States and Mexico, II.* Alpine, Texas. October, 1983. Chihuahuan Desert Research Institute. pp. 40-63.

Schmidt, R.H., Jr. and R.A. Marston. 1981. Los Medanos de Samalayuca, Chihuahua, Mexico. *New Mexico Journal of Science*. 21:2:21-27.

Scofield, C.S. 1940. Salt balance in irrigated areas. *Journal Agricultural Research*. 61:17-39, illus.

Scurlock, D. 1998. *From the Rio to the Sierra: An environmental history of the Middle Rio Grande basin*. U.S. Department of Agriculture, Rocky Mountain Research Station. Forest Service General Technical Report, RMRS-GTR-5. 440 p.

Seager, W.R. 1981. *Geology of the Organ Mountains and southern San Andres Mountains, New Mexico*. New Mexico Bureau of Mines and Mineral Resources Memoir 36. 97 p.

Seager, W.R. 1983. Laramide wrench faults, basement-cored uplifts and complementary basins in southern New Mexico. *New Mexico Geology*. 5: 69-76.

Seager. W.R. 1987. Caldera-like collapse at Kilbourne Hole Maar, New Mexico. *New Mexico Geology*. 9:4:69-73.

Seager, W.R. 1989. Geology beneath and around the West Potrillo Basalts, Doña Ana and Luna Counties, New Mexico. *New Mexico Geology*. 11:3:53-58.

Seager, W.R. 1995. *Geologic map of the southwest part of Las Cruces and northwest part of El Paso*. 1x2 degree sheets, New Mexico. New Mexico Bureau of Mines and Mineral Resources Geologic Map GM-60, scale 1:125,000.

Seager, W.R. and J.W. Hawley. 1973. *Geology of Rincon quadrangle, New Mexico*. New Mexico Bureau of Mines and Mineral Resources Bulletin 102. 56 p.

Seager, W.R. and G.H. Mack. 1986. Laramide paleotectonics of southern New Mexico. *American Association of Petroleum Geologists*. Memoir 41. pp. 660-685.

Seager, W.R. and G.H. Mack. 1994. *Geology of the East Potrillo Mountains and vicinity, Doña Ana County, New Mexico*. New Mexico Bureau of Mines and Mineral Resources Bulletin 113. 27 p.

Seager, W.R. and P. Morgan. 1979. Rio Grande rift in southern New Mexico, west Texas, and northern Chihuahua. In *Rio Grande Rift: Tectonics and Magnetism*. Edited by R.E. Riecker. American Geophysical Union, Washington, D.C. pp. 87-106.

Seager, W.R., R.E. Clemons and J.W. Hawley. 1975. *Geology of Sierra Alta Quadrangle, Doña Ana County, New Mexico.* New Mexico Bureau of Mines and Mineral Resources Bulletin 102. 56 p.

Seager, W.R., J.W. Hawley and R.E. Clemons. 1971. *Geology of San Diego Mountain area, Doña Ana County, New Mexico.* New Mexico Bureau of Mines and Mineral Resources Bulletin 97. 38 p.

Seager, W.R., F.E. Kottlowski and J.W. Hawley. 1976. *Geology of Doña Ana Mountains, New Mexico*. New Mexico Bureau of Mines and Mineral Resources Circular 147. 36 p., 2 tables, 13 figs., 3 sheets.

Seager, W. R., R.E. Clemons, J.W. Hawley and R.E. Kelley. 1982. *Geology of northwest part of Las Cruces.* 1x2 degree sheet, New Mexico. New Mexico Bureau of Mines and Mineral Resources Geological Map 53, scale 1:125,000.

Seager, W.R., G.H. Mack, M.S. Raimonde and R.G. Ryan. 1986. Laramide basement-cored uplift and basins in south-central New Mexico. *New Mexico Geological Society, 37th Annual Field Conference Guidebook.* pp. 123-130.

Seager, W.R., J.W. Hawley, F.E. Kottlowski and S.A. Kelley. 1987. *Geology of the east half of Las Cruces and northeast El Paso.* 1x2 degree sheets, New Mexico. New Mexico Bureau of Mines and Mineral Resources Geologic Map GM-57, scale 1:125,000.

Seager, W.R., M. Shafiqullah, J.W. Hawley and R.F. Marvin. 1984. New K-Ar dates from basalts and evolution of the southern Rio Grande Rift. *Geological Society of America Bulletin*. 95:87-99.

Sharp, J.M., Jr. 2001. Regional groundwater flow systems in basins in Trans-Pecos Texas. In *Aquifers of West Texas*. Edited by R.E. Mace, W.F. Mullican III and E.S. Angle. Austin, Texas, Water Development Board Report 356. pp. 41-55.

Sheng, Z., R.E. Mace and M.P. Fahey. 2001. The Hueco Bolson: an aquifer at the crossroads. In *Aquifers of West Texas*. Edited by R.E. Mace, W.F. Mullican III and E.S. Angle. Austin, Texas, Texas Water Development Board Report 356. pp. 66-75.

Shomaker, J.W. and S.R. Finch, Jr. 1996. *Multilayer ground-water flow model of southern Jornada del Muerto Basin, Doña Ana County, New Mexico, and predicted effects of pumping wells LRG-430-S-29 and -S-30*. John Shomaker & Associates, Inc., Albuquerque, NM. 26 p.

Slichter, C.S. 1905. *Observations on groundwaters of the Rio Grande valley*. U.S. Geological Survey Water-Supply Paper 141. 83 p.

Smith, G.A. 1994. Climatic influences on continental deposition during late-stage filling of an extensional basin, southeastern Arizona. *Geological Society of America Bulletin*. 106:1212-1228.

Snyder, J.T. 1986. *Heat flow in the southern Mesilla Basin, with an analysis of East Potrillo geothermal system, Doña Ana County, New Mexico*. M.S. Thesis, New Mexico State University. 252 p.

Spalding, R.F., A.D. Druliner, L.S. Whiteside and A.W. Struempler. 1984. Uranium geochemistry in groundwater from Tertiary sediments. *Geochimica et Cosmochimica Acta.* 48:2679-2692.

Spiegel, Z. and B. Baldwin. 1963. *Geology and water resources of the Santa Fe area, New Mexico.* U.S. Geological Survey Water-Supply Paper 1525. 258 p.

Stanton, R. J., D.L. Jeffery and W.M. Ahr. 2002. Early Mississippian climate based on oxygen isotope compositions of brachiopods, Alamogordo Member of the Lake Valley Formation, south-central New Mexico: Geological Society of America Bulletin, v. 114, no. 1, p. 4-11.

Stewart, B. W., R.C. Capo and O.A. Chadwick. 1998. Quantitative strontium isotope models for weathering, pedogenesis and biochemical cycling: Geoderma, v. 82, p. 173-195.

Stickel, R. 1991. The effect of groundwater flow on the hydrochemical variability of groundwater in the southern Jornada del Muerto basin, Dona Ana and Sierra counties, New Mexico: Unpub. M. S. Thesis, New Mexico State University, Las Cruces, 111 p.

Strain, W.S. 1966. *Blancan mammalian fauna and Pleistocene formations, Hudspeth County, Texas*. Austin, Texas, Texas Memorial Museum Bulletin 10. 55 p.

Strain, W.S. 1971. Late Cenozoic bolson integration in the Chihuahua tectonic belt. In *The Geologic Framework of the Chihuahua Tectonic Belt.* West Texas Geological Society Publication No. 71-59. pp. 167-173.

Stuyfrzand, P.J. 1999. Patterns in groundwater chemistry resulting from groundwater flow. *Hydrogeology Journal.* 7:1:15-27.

Swanberg, C.A. 1975. Detection of geothermal components in groundwaters of Doña Ana County, southern Rio Grande rift, New Mexico. *New Mexico Geological Society, 26th Annual Field Conference Guidebook.* pp. 175-180.

Thode, H.G., and J. Monster. 1965. Sulfur-isotope geochemistry of petroleum, evaporites, and ancient seas, in A. Young and J.E. Galley, eds., Fluids in the Subsurface Environment: American Association of Petroleum Geologists Memoir 4, p. 367-377.

Thomas, H.E. 1962. *The meteorologic phenomenon of drought in the Southwest-Drought in the Southwest, 1942-56*. U.S. Geological Survey Professional Paper 372-A. A1-A43.

Thomas, H.E. 1963. *Effects of drought in the Rio Grande basin--Drought in the Southwest, 1942-56*. U.S. Geological Survey Professional Paper 372-D. D1-D59.

Thorn, C.R., D.P. McAda and J.M. Kernodle. 1993. *Geohydrologic Framework and Hydrologic Conditions of the Albuquerque Basin, Central New Mexico*. U.S. Geological Survey Water-Resources Investigations Report 93-4149. 106 p.

Tolman, C.F. 1909. Erosion and deposition in southern Arizona bolson region. *Journal of Geology*. XVII:II:136-163.

Tolman, C.F. 1937. *Groundwater*. New York: McGraw-Hill Book Co. 593 p.

Toth, J. 1963. A theoretical analysis of groundwater flow in small drainage basins. *Journal of Geophysical Research*. 68:4795-4812.

Toth, J. 1999. Groundwater as a geologic agent: an overview of the causes, processes and manifestations: Hydrogeology Journal, v. 7, p. 1-14.

Uphoff, T.L. 1978. *Subsurface stratigraphy and structure of the Mesilla and Hueco Bolsons, El Paso region, Texas and New Mexico*. M.S. Thesis, The University of Texas at El Paso. 66 p.

U.S. Department of Commerce. 1999. *Cooperative Weather Station Data Files*. National Climate Data Center. National Oceanic and Atmospheric Administration.

U.S. Reclamation Service. 1914. *Maps of the Mesilla Valley showing various known river channels.* U.S. Department of the Interior, Bureau of Reclamation, Rio Grande Project.

USGS. nd. *Water Resources Data, Calendar Year Streamflow Statistics*. U.S. Geological Survey. Online data retrieval system: URLhttp://water.usgs.gov/nm/nwis/sw.

USGS, 2000. Water Quality Data, URL http://waterdata.usgs.gov/nwis/qwdata

Vandaele, W. 1983. Applied time series and Box-Jenkins models. San Diego, CA: Academic Press.

Vanderhill, J.B. 1986. *Lithostratigraphy, vertebrate paleontology, and magneto-stratigraphy of Plio-Pleistocene sediments in the Mesilla Basin, New Mexico.* Doctoral dissertation, The University of Texas, Austin, TX. 311 p.

Van der Hoven, S.J. 1994. Strontium isotopes as an indicator of the sources of calcium in secondary carbonates in an arid environment: Unpub. M.S. Thesis, University of Arizona, Tucson, 51 p.

Van Devender, T.R. 1990. Late Quaternary vegetation and climate of the Chihuahuan Desert, United States and Mexico. In *Packrat Middens*. Edited by J.L. Betancourt, T.R. Van Devender and P.S. Martin. Tucson, AZ: University of Arizona Press. pp. 104-133.

Veizer, J., D. Ala, K. Azmy, P. Bruckshen, D. Buhl, F. Bruhn, G.A.F. Carden, A. Diener, S. Enbeth, Y. Godderis, T. Jasper, C. Korte, F. Pawellek, O.G. Podlaha and H. Strauss. 1999. $^{87}Sr/^{86}Sr$, $\delta^{13}C$, and $\delta^{18}O$ evolution of Phanerozoic seawater: Chemical Geology, v. 161, p. 59-88.

Vuataz, F. D., and F. Goff. 1986. Isotope geochemistry of thermal and thermal waters in the Valles Caldera, Jemez Mountains, northern New Mexico: Journal of Geophysical Research, v. 91, no. B2, p. 1835-1853.

Wade, S.C. and M. Reiter. 1994a. Hydrothermal estimation of vertical ground-water flow, Cañutillo, Texas. *Groundwater*: 32:5:735-742.

Wade. S.C. and M. Reiter. 1994b. *A hydrothermal study to estimate vertical groundwater flow in the Cañutillo Well Field, between Las Cruces and El Paso*. New Mexico Water Resources Research Institute, Technical Completion Report No. 282, New Mexico State University, Las Cruces, NM. 71 p.

Walton, J., G. Ohlmacher, D. Utz and M. Kutinawala. 1999. Response of the Rio Grande and shallow groundwater in the Mesilla Bolson to irrigation, climate stress, and pumping. *Environmental and Engineering Geoscience*. 5:1:41-50.

Wasiolek, M. 1995. *Subsurface Recharge to the Tesuque Aquifer System from Selected Drainage Basins along the Western Side of the Sangre de Cristo Mountains near Santa Fe, New Mexico*. U.S. Geological Survey Water-Resources Investigations Report 94-4072. 43 p.

Wen, C-L. 1983. *A study of bolson-fill thickness in the southern Rio Grande rift, southern New Mexico, west Texas and northern Chihuahua*. M.S. Thesis, The University of Texas at El Paso. 74 p.

West, F. 1996. The Mesilla Valley: A century of water resources investigations. In *Proceedings of the 40th Annual New Mexico Water Conference, "Reaching the Limits: Stretching the Resources of the Lower Rio Grande*." Edited by C.T. Ortega Klett. New Mexico Water Resources Research Institute, Report No. 297, New Mexico State University, Las Cruces, NM. pp. 21-28.

Wilcox, L.V. 1968. *Discharge and salt burden of the Rio Grande above Ft. Quitman, Texas and salt-balance conditions on the Rio Grande Project. Summary Report for the 30-year Period 1934-1963*. Soil and Water Research Division, Agricultural Research Service, USDA. Riverside, CA. U.S. Salinity Laboratory Research Report No. 113.

Wilkins, D.E. and D.R. Currey. 1997. Timing and extent of Late Quaternary paleolakes in the Trans-Pecos closed basin, west Texas and south-central New Mexico. *Quaternary Research*. 47:306-315.

Wilkins, D.W. 1986. *Geohydrology of the Southwest Alluvial Basins, Regional Aquifer-systems analysis in parts of Colorado, New Mexico, and Texas*. U.S. Geological Survey Water-Resources Investigations Report 84-4224. 61 p., plates.

Wilkins, D.W. 1998. *Summary of the Southwest Alluvial Basins, Regional Aquifer-systems Analysis in Parts of Colorado, New Mexico, and Texas*. U.S. Geological Survey Professional Paper 1407-A. 49 p.

Williams, W.J.W. 1999. *Evolution of Quaternary intraplate mafic lavas using ^{3}He surface exposure and ^{40}Ar/^{39}Ar dating, and detailed elemental He, Sr, Nd, and Pb isotopic signatures: Potrillo Volcanic Field, New Mexico, U.S.A., and San Quintín Volcanic Field, Baja California Norte, México*. Doctoral dissertation, The University of Texas at El Paso. 195 p.

Williams, J.H. 2001. Salt Balance in the Rio Grande Project from San Marcial, New Mexico to Fort Quitman, Texas: unpublished M.S. Thesis, New Mexico State University, Las Cruces, 42 p.

Williams, W.J.W., E.Y. Anthony, M. Whitelaw, J. Poths, H. Healey and J. Geissman. 1993. ^{3}He surface exposure dates and chemistry of the Potrillo volcanic field, Rio Grande rift, and magmatic ^{3}He/^{4}He signatures of Quaternary lavas of the southwestern United States. In *International Association of Volcanology and Chemistry of the Earth's Interior (IAVCEI).* 1993 General Assembly in Canberra, Australia. Abstract Volume 123.

Wilson, C.A., R.R. White, R.B. Orr and R.G. Roybal. 1981. *Water Resources of the Rincon and Mesilla Valleys and Adjacent Areas*. New Mexico State Engineer Technical Report 43. 514 p.

Wilson, C.A. and R.R. White. 1984. *Geohydrology of the central Mesilla Valley, Doña Ana County, New Mexico*. U.S. Geological Survey Water-Resources Investigations Report 82-444. 144 p.

Winograd, I.J. and W. Thordarson. 1975. *Hydrogeologic and Hydrogeochemical Framework, South-central Great Basin, Nevada-California, with Special Reference to the Nevada Test Site*. U.S. Geological Survey Professional Paper 712-C. 126 p.

Witcher, J.C. 1988. Geothermal resources of southwestern New Mexico. *New Mexico Geological Society, 39th Annual Field Conference Guidebook*. pp. 191-197.

Woodward, D.G. and R.G. Myers. 1997. *Seismic investigation of the Buried Horst between the Jornada del Muerto and Mesilla Ground-Water Basins near Las Cruces/Doña Ana County, New Mexico*. U.S. Geological Survey Water-Resources Investigations Report 97-4147. 45 p.

Yeamans, F. 1983. Basin and Range geothermal hydrology: An empirical approach. In *The Role of Heat in the Development of Energy and Mineral Resources in the northern Basin and Range Province*. Geothermal Resources Council Special Report 13. pp. 159-175.

Zohdy, A.A.R. 1969. The use of Schlumberger and equatorial soundings in groundwater investigations near El Paso, Texas. *Geophysics*. 4:713-728.

Zohdy, A.A.R., R.J. Bisdorf and J.S. Gates. 1976. *Schlumberger soundings in the lower Mesilla Valley in the Rio Grande, Texas and New Mexico*. U.S. Geological Survey Open-File Report 76-324. 77 p.